The Function of *Bre* Gene in Embryonic Interdigital Tissues

WONG, Wan Man

A Thesis Submitted in Partial Fulfillment
of the Requirements for the Degree of
Master of Philosophy

in

Anatomy

December 2006

Supervisor: Professor Kenneth Lee


香港中文大學
大學
圖書館系統
15 JUL 2008
UNIVERSITY
LIBRARY SYSTEM
THE CHINESE UNIVERSITY OF HONG KONG

Thesis/ Assessment Committee

Professor Hector S.O. Chan (Chair)

Professor Kenneth K.H. Lee (Thesis Supervisor)

Professor Patricia P.H. Chow (Committee Member)

Professor W.S. O (External Examiner)

Abstract of thesis entitled:

The Function of *Bre* Gene in Embryonic Interdigital Tissues

Submitted by Wong Wan Man

for the degree of Master of Philosophy

at The Chinese University of Hong Kong in December, 2006

Abstract

In multicellular organisms, programmed cell death (PCD) is one of the most important processes that occur during development. It helps to determine the definitive morphology of organs and tissues. A good example of how PCD helps to sculpture the overall shape of an organ is the developing limbs –where cell death in the interdigital tissues of the hand- and foot-plates shapes the contour of the hands and feet. Consequently, the limb has been popularly adopted by developmental biologists as a model for studying PCD. Furthermore, it is easy to experimentally manipulate the hand- and foot-plate and the spatial-temporal expression pattern of PCD in the interdigital tissues is highly predictable.

In this study, I have used the limb model to elucidate the function of a gene called Brain and Reproductive organ-Expressed *(Bre)*. *Bre* was originally discovered when fibroblasts were treated with UV and DNA-damaging agents. These agents inhibited *Bre* expression and consequently *Bre* was proposed as a stress-modulating gene. I have investigated the involvement of *Bre* in the regulation of apoptosis in the interdigital tissues. I began with micro-dissecting and isolating the interdigital tissues from the

footplate of E12.5 and E13.5 hindlimbs. Using semi-quantitative RT-PCR, it was determined that *Bre* isoform 5 but not *Bre* isoforms 1, 2, 3 and 4 was expressed by interdigital tissues. In addition, E12.5 interdigital tissues expressed a higher level of *Bre* isoform 5 mRNA than E13.5 interdigital tissues. It has already been reported that hindlimb interdigital tissues are committed to PCD at E13.5 but not E12.5. Therefore, it appears that *Bre* expression is high when the interdigital cells are not committed to PCD and down-regulated when the cells are committed. I have established a primary interdigital cell culture system so that the effects of loss of function of *Bre* could be tested. *Bre* expression in interdigital cells was silenced using *Bre*-specific small interference RNA and the viability of these cells was compared with that of control culture by MTT assay. The result showed that the number of viable cells in the *Bre*-siRNA-treated culture was significantly lower than that in the control culture. The preliminary result of the reduction in cell viability by suppressing *Bre* expression suggests that BRE may play an anti-apoptotic role in interdigital cultured cells. In order to further investigate the downstream effect of *Bre* silencing, protein profiles of *Bre*-silenced culture and control culture were analyzed using two-dimensional electrophoresis and MALDI-TOF analysis. The comparative proteomic analysis revealed that several proteins were affected by *Bre* silencing. These include PDIA6 and vimentin which were suppressed. The effects of suppressing *Bre* expression were also profiled transcriptionally. The result revealed that the regulation of *Pdia6* and *vimentin* expression by *Bre* silencing was on transcriptional and post-transcriptional level respectively. These observations provide some preliminary insights into the function of *Bre* gene in the interdigital tissues.

題目名稱:

腦和生殖器官表達基因在胚胎趾間組織中的功能

黃韻雯於 2006 年 12 月在香港中文大學呈交碩士論文

摘要

對於多細胞生物來說，程序性細胞死亡是其發育過程中最重要的進程之一。程序性細胞死亡有助於器官和組織外觀的建立。四肢發育就是程序性細胞死亡有助於塑造器官形態的最好例証－手腳的形態由指(趾)間組織細胞發生程序性細胞死亡而形成。因此，許多發育生物學家選擇四肢的發育作爲研究程序性細胞死亡的模型。並且，在實驗方面，處理手腳掌較爲容易，而程序性細胞死亡在指(趾)間組織的時空表達模式亦較容易預測。

在本研究中，我們用四肢模型來闡明腦和生殖器官表達 (*Bre*) 基因的功能。*Bre* 基因最先是於成纖維細胞在紫外線和去氧核糖核酸損傷劑處理的過程中被發現出來。由於這些處理可以抑制 *Bre* 基因的表達，因此 *Bre* 基因被看作一種應激調節基因。我已經發現 *Bre* 基因參與了趾間組織的凋亡調節。我首先用顯微解剖的方法分離 12.5 天和 13.5 天胚胎的肢趾間組織，隨後用半定量逆轉錄聚合酶鏈式反應的方法，檢測到趾間組織所表達的是 *Bre* 5 亞型而非 1, 2, 3 和 4 亞型。此外，*Bre* 在 12.5 天胚胎趾間組織的表達高於 13.5 天胚胎趾間組織的表達。曾有報道說，胚胎肢趾間組織的凋亡主要發生於第 13.5 天，而並非 12.5 天。即是說，當趾間細胞在未曾發生程序性細胞死亡時，*Bre* 基因的表達就會較高; 反之，其表達就會下

調。爲了檢測 *Bre* 基因功能的變化，我建立了趾間細胞的原代培養系統。我用基因幹擾的方法沉默了 *Bre* 在趾間細胞的表達，並且用 MTT 細胞活性測驗去比較有 *Bre* 表達的原代培養細胞和沒有 *Bre* 表達的原代培養細胞的生存率。結果顯示，前者的生存率明顯地低於後者。這個初步的結果提出了 *Bre* 可能在原代培養趾間細胞中扮演抗凋亡的角色。爲了進一步探究 *Bre* 基因沉默的下游反應，我們用了二維電泳和基質輔助雷射脫附游離飛行質譜儀來分析其蛋白質組學的情況。對比蛋白質組學顯示，*Bre* 基因沉默可以抑制蛋白二硫化物異構家族 A，成員 6 蛋白 (PDIA6)和波型蛋白 (vimentin) 的表達。我們也研究了 *Bre* 基因沉默對這些蛋白轉錄水平的影響。結果發現，*Bre* 基因沉默分別在轉錄水平和轉錄後水平上對 *Pdia6* 和 *vimentin* 的表達有所調節。這些數據初步闡明了 *Bre* 基因在趾間組織中的功能。

Acknowledgements

It is my pleasure to thank every person who made this thesis possible. Firstly, I would like to gratefully acknowledge the enthusiastic supervision of Professor Kenneth Lee. With his inspiration and his great effort to hold numerous stimulating discussions, he provided me a lot of good ideas during the course of study. I would also like to express my deep and sincere gratitude to Professor Patricia Chow for her encouragement, sound advice and care during these years.

My sincere thanks are due to my colleagues for providing a stimulating and fun environment in which to learn and grow. I am especially grateful to Dr M.K. Tang and Dr S.W. Shan for their essential assistance throughout the study. I warmly thank Ms L.S. Kung, Ms H.J. Hou, Ms Y.W. Au and Mr Y.T. Wong for their technical assistance and support and Miss Y.Y. Chong for the preparation of TESPA coated slides.

I would like to express my deep gratitude to my friends and colleagues for their support, concern and care. They helped me to get through the difficult times. I am especially gratefully to Professor David Yew and Ms Y. Liu for their medical support and advices.

Lastly, and the most importantly, I am forever indebted to my parents and brother who provided me with their unconditional care, endless support and continuous encouragement.

Lists of Figures and Tables

Table of Abbreviations

a.a.	Amino acid
AER	Apical ectodermal ridge
AIF	Apoptosis-inducing Factor
ANZ	Anterior necrotic zone
Apaf-1	Apoptotic Protease Activating Factor-1
Bmp	Bone Morphogenetic Protein
bp	Base pairs
Bre	Brain and Reproductive Organ Expressed protein
BSA	Bovine serum albumin
Caspase	Cysteinyl Aspartate-specific Protease
cDNA	Complementary DNA
CHAPS	3-[(3-cholamidopropyl)dimethylammonio]-1-propane sulfonate
DD	Death domain
DEPC	Diethypyrocarbonate
DIABLO	Direct inhibitor of apoptosis protein-binding protein with low pI
DIG	Digoxigenin
DISC	Death-inducing signaling complex
DMEM	Dulbecco's modified eagle's medium
DMSO	Dimethyl sulfoxide
dNTP	Deoxyribonucleotide triphosphate

DPBS	Dulbecco's phosphate buffered saline
DR	Death Receptor
DTT	Dichlorodiphenyltrichloroethane
E	Embryonic
EDTA	Ethylenediaminetetraacetic acid
FADD	Fas-associated Death Domain protein
FBS	Fetal bovine serum
Fgf	Fibroblast Growth Factor
GFP	Green Fluorescent Protein
HEK293	Human embryonic kidney epithelial cell line
IAA	Iodoacetamide
IEF	Isoelectric focusing
INZ	Interdigital necrotic zone
IPG	Immobiline pH gradient
kb	Kilobase
kDa	Kilodalton
LPM	Lateral plate mesoderm
mA	Milliampere
MALDI-TOF	Matrix-assisted laser desorption/ ionization time-of-flight
MAPK	Mitogen Activated Protein Kinase
MCF7	Human breast adenocarcinoma cell line
ml	Milliliter
mm	Millimeter

mM	Millimolar
mRNA	Messenger RNA
MTT	3-(4,5-dimethylthiazol-2-yl)-2,5-diphenyltetrazolium bromide
nm	Nanometer
NBT/BCIP	Nitroblue tetrazolium salt and 5-bromo-4-chloro-3-indolylphosphate
NFκB	Nuclear Factor kappa B
NP-40	Nonidet P40
PARP	Poly-ADP-ribose Polymerase
PBS	Phosphate buffered saline
PCD	Programmed cell death
PCR	Polymerase chain reaction
pI	Isoelectric point
PMSF	Phenylmethylsulfonyl fluoride
PNZ	Posterior necrotic zone
RIP	Receptor Interacting Protein
ROS	Reactive oxygen species
rpm	Revolutions per minute
RT	Reverse transcription
siRNA	Small interfering RNA
SDS	Sodium dodecyl sulfate
SDS-PAGE	SDS-Polyacrylamide gel electrophoresis

Shh	Sonic Hedgehog
Smac	Second Mitochondrial Activator of Caspase
SODD	Suppressor of Death Domain protein
SP	Stretomycin sulphate/ Penicillin
tBID	Truncated BID
TESPA	Aminopropyltriethoxysilane
TBST	Tris buffer saline tween-20
TFA	Trifluoroacetic acid
TGF-β	Transforming Growth Factor-beta
TNF	Tumor Necrosis Factor
TRADD	TNF Receptor-associated Death Domain Protein
TRAF	TNFR-associated Factor
UV	Ultraviolet
ZPA	Zone of polarizing activity
2D	Two-dimensional
2D-PAGE	Two-dimensional polyacrylamide gel electrophoresis
3β-HSD	3 beta-hydroxysteroid dehydrogenase
β-actin	Beta-actin
μA	Micro-ampere
μl	Microliter
μg	Microgram

Table of Contents

Chapter I

Introduction

1.1 Brain and Reproductive Organ Expressed Gene

Li et al., 1995 identified a stress-responsive gene that was highly expressed in brain, ovary and testis. Hence, the gene was named brain and reproductive organs (*Bre*) gene. It was discovered that *Bre* expression was significantly decreased after UV irradiation, DNA damaging agent and retinoic acid treatment. The human *Bre* gene encodes an mRNA that is 1.9kb long and in turn translates a protein with 383 amino acids. The BRE protein weighs 44 kilodaltons and has an acidic isoelectric point (Li et al., 1995; Gu et al., 1998).

Bre gene does not share any significant homology with other known genes (Gu et al., 1998). However, the human *Bre* gene is highly conserved with its mouse and hamster counterparts. It shares 98% and 99% homology with those of mouse and hamster, respectively (Ching et al., 2001; Poon et al., 2004). Although *Bre* was originally reported to express mainly in the brain and reproductive organs, it is also strongly expressed in the adrenal gland, heart, pituitary gland and the spleen in human tissues (Miao et al., 2001). Moreover, *Bre* was expressed in the digestive and respiratory organs (Poon et al., 2004). *Bre* has since been shown to have multiple isoforms, in both human and mouse, formed

from alternative spicing. Human and their mouse counterparts have alternative splicing sites at both ends and 5'end, respectively (Ching et al., 2001, 2003).

The function of the *Bre* gene has been investigated in various biological models but the detailed function and the physiological role of BRE has still not been clarified. Gu et al., 1998 demonstrated that BRE specifically interacted with the juxtamembrane domain of p55 Tumor Necrosis Factor (TNF) receptor by yeast-two-hybrid screening and *in vitro* biochemical assays. Furthermore, it was suggested that BRE had a role in modulation of TNF-α-specific Nuclear Factor kappa B (NFκB) activation because overexpression of BRE in HEK293 and MCF7 cells resulted in an inhibition of TNF-induced NFκB activation (Gu et al., 1998). Beside TNF p55 receptor, BRE was also shown to bind to Fas which is another death-associated receptor (Li et al., 2004). The same authors, also suggested that BRE participated in the apoptotic pathway and have a role inhibiting, by ubiquitination-like activity, components in/or proximal to the Death-inducing signaling complexes (DISC) that are required for mitochondria activation. This idea is supported by the fact that BRE inhibited the mitochondrial apoptotic machinery during apoptotic induction and an increased association of BRE with ubiquitinated proteins after death-receptor stimulation was also detected (Li et al., 2004). Since failure of apoptotic induction is one of the key factors in cancer development, the same workers investigated the role of BRE in tumorogenesis. They demonstrated that the mouse Lewis lung carcinoma D122, stably transfected with the *Bre* gene, developed into local tumor significantly faster than D122 cells stably transfected with the empty vector and parental D122, in both the syngeneic C57BL/6 host and nude mice. Hence, BRE was proposed to enhance tumor growth through its antiapoptotic activity (Chan et al., 2005). In addition,

Bre was also reported to be related to cell proliferation and DNA repair. In 2006, Tang et al. demonstrated that BRE could directly or indirectly modulate cell proliferation, since suppression in *Bre* expression by specific small-interfering RNA (siRNA) resulted in an increased in cell proliferation while overexpression of *Bre* led to a decreased in cell proliferation (Tang et al., 2006). In addition, BRE was initially found to be suppressed following treatment by UV-radiation and DNA damaging agent and so it has long been considered to play a role in DNA repair. In 2003, Shiekhattar and co-workers found out that BRE, also named as BRCC45, together with BRCA1, BARD1 and BRCC36 formed a complex which revealed an enhanced E3 ligase activity. They suggested that this haloenzyme BRE-containing complex could enhance cellular survival following DNA damage because suppression of BRCC45 and BRCC36 expression *in vivo* by specific siRNAs led to an increased sensitivity to ionizing radiation and a defect in G2/M check point progression (Dong et al., 2003). Apart from acting as a biological-response modifier, BRE was also shown to play a role in the generation of a chemical component of the cell. Miao et al., 2001 was first to report *Bre* was expressed at high levels in the adrenal cortex, glial and neuronal cells of the brain and in the round spermatids, Sertoli cells and Ledig cells of testis. All of these tissues are associated with steroid hormones and/or TNF synthesis. Moreover, an alternation of *Bre* expression was observed in the adrenal glands under pathological conditions. Therefore, it was proposed that *Bre* expression was associated with steroids and/or TNF production and the regulation of endocrine functions (Miao et al., 2001). This argument was further supported by the same group in 2005. They suggested that BRE influences steroidogenesis through its effects on 3β-hydroxysteroid dehydrogenase action (3β-HSD), probably affecting the transcription

of 3β-HSD because impairment of pregnenolone-to-progesterone conversion and reduced expression of 3β-HSD type I mRNA were observed in *Bre*-antisense-transfected cells compared with control (Miao et al., 2005).

In sum, *Bre* is a stress-responsive gene with high homology across all species. It is highly expressed in the brain, adrenal cortex and gonads. The reported functions of BRE are very diverse and include TNF-α signaling, regulation of apoptosis, tumorogensis, cell proliferation, DNA repair and steriodogenesis.

1.2 Programmed cell death

The total number of cells in an organism is determined and tightly controlled by a balance between cell proliferation and PCD, which also known as apoptosis. Cell undergoing apoptosis is characterized by cell shrinkage, condensation and also by collapsed of the cytoskeleton, disassembled nuclear envelope and fragmented nuclear DNA (Wyllie et al., 1980; Patel et al., 1996; Dynlacht et al., 2000). The machinery of apoptosis depends on a group of proteases called Cysteinyl Aspartate-specific Proteases (Caspases). Caspases is a family of cysteine proteases that cleave substrates specifically after a conserved aspartate residue (Alnemri et al., 1996; Hu et al., 1998a). These enzymes exist as pro-caspases and can be cleaved and activated by other caspases. Caspase-8 and Caspase-9 act as initiators while Caspase-3, Caspase-6 and Caspase-7 act as executioners or effectors of apoptosis (Cohen, 1997). Activated effector-Caspases can in turn cleave key substrates for cell survival such as Poly-ADP-ribose polymerase

(PARP) (Tewari et al., 1995), which is necessary for DNA repair (Lindahl et al., 1995). Since Caspase-3 is an executioner during apoptosis, its importance on programmed cell death has long been a subject of study. To evaluate the physiological role of Caspase-3, null mice were generated and analyzed. A considerable number of Caspases-3 knockout mice die *in utero* at embryonic day E12.5. Also, some of neonates die with brain defects. These defective brains contain extra tissue masses because apoptosis, which is essential for brain development, is inhibited (Kuida et al., 1996; Woo et al., 1998).

Apoptosis can be activated in two ways, either by internal stimuli or by external signal received by the death receptors locating on the cell membrane. The former, which is also called intrinsic apoptotic pathway, is mediated through the mitochondria (Zamzami et al., 1996). It can be stimulated by accumulation of reactive oxygen intermediates (Ratan et al., 1994; Quillet-Mary et al., 1997), Apoptosis-inducing Factor (AIF) (Susin et al., 1997) and other death stimuli such as growth-factor deprivation. The early phases of mitochondrial apoptosis are characterized by a change in permeability of mitochondrial membrane (Zamzami et al., 1995) and a release of Cytochrome c from the intermembrane space of the mitochondrion into the cytosol (Kluck et al., 1997; Yang et al., 1997a). Beside Cytochrome c, other pro-apoptotic factors such as Caspase-9 (Susin et al., 1999), the protein named Second Mitochondrial Activator of Caspase (Smac) and Direct inhibitor of apoptosis protein-binding protein with low pI (DIABLO) are also released from mitochondria during apoptosis (Du et al., 2000; Verhagen et al., 2000).

The intrinsic apoptotic pathway is mainly regulated by various proteins from the Bcl-2 family (Knudson and Korsmeyer, 1997). The Bcl-2 family members are categorized into anti-apoptotic and pro-apoptotic. The anti-apoptotic proteins include

BCL-2 (Hockenbery et al., 1990; Sentman et al., 1991; Strasser et al., 1991) and BCL-X_L (Cheng et al., 1996) while pro-apoptotic proteins include BAX (Hunter and Parslow, 1996), BAK (Chittenden et al., 1995), BAD (Yang et al., 1995). BCL-2 and BCL-X_L inhibit apoptosis by preventing the release Cytochrome c from mitochondria (Kluck et al., 1997; Yang et al., 1997a) and activation of Caspase-9 (Hu et al., 1998b). On the contrary, BAK and BAX are responsible for promoting the release of Cytochrome c (Jurgensmeier et al., 1998; Rosse et al., 1998; Shimizu et al., 1999) while BAD binds to anti-apoptotic members and prevent their activation (Letai et al., 2002). Another candidate, Apoptotic Protease Activating Factor-1 (Apaf-1) plays a vital role in mitochondrial apoptotic event (Zou et al., 1997). When an internal death stimulus is received, Cytochrome c is released from mitochondria into cytosol (Kluck et al., 1997; Yang et al., 1997a). In the presence of Cytochrome c and dATP, APAF-1 interacts with pro-caspase-9 through a mutual domain (Liu et al., 1996) to form an apoptosome. This interaction results in an activation of pro-caspase-9 (Zou, et al., 1999). Activated Caspase-9 in turn cleaves pro-caspase-3, pro-caspase-6 and pro-caspase-7 leading to cell death (Srinivasula et al., 1998).

Apoptosis that results from binding death factors to corresponding death receptors extracellularly is known as extrinsic apoptotic pathway. The death receptors include TNF p55 receptor (Tartaglia et al., 1993), Fas (Dhein et al., 1995) and Death Receptor (DR) 3 (Chinnaiyan et al., 1996a), DR4 (Pan et al., 1997), DR5 (Chaudhary et al., 1997) and DR6 (Pan et al., 1998). All of them belong to the TNF receptor superfamily and contain a homologous death domain (DD) in their cytoplasmic regions. Stimulation of the death receptors results in recruitment of adaptor proteins to the cytoplasmic domain of the death receptors. These adaptor proteins can be divided into two categories. The first class

includes DD-containing adaptor proteins (Chinnaiyan et al., 1996b) while the second class includes the family of TNFR-associated Factors (TRAFs) and other proteins without death domains (Rothe et al., 1994). TNF Receptor-associated DD protein (TRADD) (Hsu et al., 1995), Fas-associated DD protein (FADD) (Chinnaiyan et al., 1995) and Receptor Interacting Protein (RIP) (Stanger et al., 1995) are examples of DD-containing adaptor proteins. When TNF binds to TNF p55 receptor, TRADD interacts with the receptor and mediates either apoptosis or activation of NFκB (Hsu et al., 1995) which depends on the type of adaptor proteins recruited by TRADD. If FADD is recruited, apoptosis is induced (Hsu et al., 1996b). In case of the recruitment of TRAF-2 and/or RIP, activation of NFκB results (Hsu et al., 1996a). However, when Fas is stimulated, unlike TNF p55 receptor, only FADD is recruited to the receptor (Chinnaiyan et al., 1995). Convergence of Fas and TNF p55 receptor signaling pathways signals through adaptor protein FADD (Chinnaiyan et al., 1996b) which in turn recruits procaspase-8 to the DISC (Medema et al., 1997). The autocatalytic activity of DISC generates active Caspase-8 which in turn cleaves pro-caspase-3 into mature Caspase-3 (Boldin et al., 1996; Muzio et al., 1996). Activation of Caspase-3 results in the execution of programmed cell death. In addition, it has been reported that Fas could mediate apoptosis through JNK activation (Yang et al., 1997b; Villunger et al., 2000).

The intrinsic apoptotic pathway has always been reported to be interconnected with the extrinsic apoptotic pathway and vice versa. For example, protection from Fas-induced apoptosis by overexpression of BCL-2 *in vivo* has been observed (Lacronique et al., 1996). Furthermore, BID, which is a pro-apoptotic member of Bcl-2 family (Wang et al., 1996), has been verified to be cleaved by active Caspase-8 (Li et al., 1998). The

truncated BID (tBID) translocates into mitochondria and stimulates the release of Cytochrome c (Luo et al., 1998) which relays the apoptotic signal to mitochondria.

In conclusion, cell number is tightly regulated not only through cell proliferation but also programmed cell death, which is mainly relayed by an intrinsic and extrinsic apoptotic pathway. The intrinsic pathway is stimulated by internal apoptotic signals while the extrinsic pathway is stimulated by the binding of death factors to corresponding death receptors extracellulary. These two pathways not only work dependently but also crosstalk with each other very closely.

1.3 Limb development in mouse

For a long time, the vertebrate limb has been used as a model for studying the cellular and molecular mechanisms that regulate pattern formation and development of tissues during embryogenesis (Johnson and Tabin, 1997; Capdevila and Izpisua Belmonte, 2001). Chicken and mouse embryos have been used extensively in these studies (Capdevila and Izpisua Belmonte, 2001) (For simplicity, limb formation in mouse embryo will be focused in the following paragraphs which are starting with limb initiation, followed by outgrowth and then patterning.).

In mouse embryo, the forelimbs begin to develop at Embryonic day 9.5 (E9.5) while the hindlimbs start to form at E10. Therefore, the hindlimbs develop with an E0.5 time-lag compared with the forelimb (Wanek et al., 1989). At the beginning of limb formation, undifferentiated mesenchymal cells, locating in lateral plate mesoderm (LPM)

aggregate together and then proliferate to give rise to the limb buds which are located between C5-C8 and L3-L5 in the flank of the embryo (Solursh et al., 1987; Hayashi and Ozawa, 1995). These cells are encased in the ectoderm jacket and informed about their positions in limb development. These positional values are then acquired by the mesenchymal cells and interpreted for development in the later stages (Tickle, 2006).

The limb has three primary axes. They are proximo-distal axis (extending from the shoulder to fingers), antero-posterior axis (from the thumb to little finger) and dorso-ventral axis (from the back of hand to palm) (Figure 1). The initiation of limb formation is regulated by proteins from Fibroblast Growth Factor (FGF) family (Cohn et al., 1995; Ohuchi et al., 1995; Tickle and Münsterberg, 2001). *Fgf-10* is expressed in undifferentiated mesenchymal cells within the limb field and induces the expression of *Fgf-8* in the overlying ectoderm which forms the apical ectodermal ridge (AER) at later stage of development (Ohuchi et al., 1997; Xu et al., 1998; Yonei-Tamura et al., 1999; Kawakami et al., 2001). The elongation of the proximal-distal axis is controlled by the AER which keeps on producing FGFs and secretes them to the underlying mesenchyme (Saunders, 1948; Capdevila and Izpisua Belmonte, 2001; Lee, 2002; Logan, 2003).

The antero-posterior axis is regulated by a collection of cells located at the posterior region of the limb bud which is called zone of polarizing activity (ZPA) (Saunders and Gasseling, 1968; Tickle et al., 1975; Sanz-Ezquerro and Tickle, 2001; Logan, 2003; Sanz-Ezquerro and Tickle, 2003; Tickle, 2006). When ZPA is transplanted to a position on an anterior margin of the limb bud, an extra set of mirror-imaged digits is produced along the antero-posterior axis (Saunders and Gasseling, 1968; Tickle et al.,

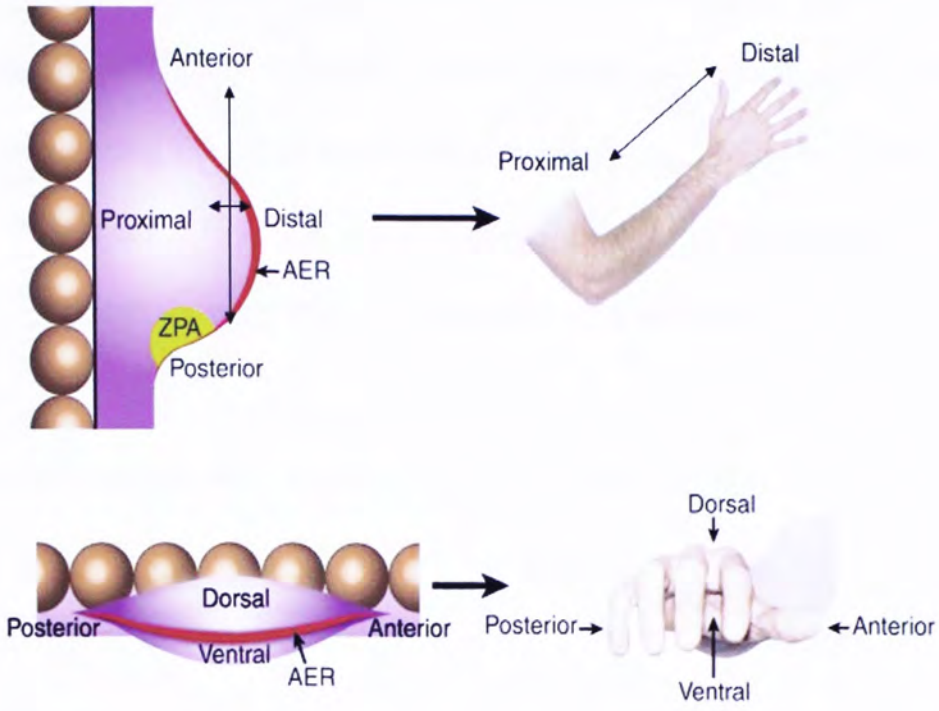

Figure 1.

Representation of the antero-posterior, proximo-distal and dorso-ventral axes in the developing limb and the corresponding structures of mature limb formed in human. AER, apical ectodermal ridge (Adopted from Logan, 2003).

1975; Tickle, 1995; Sanz-Ezquerro and Tickle, 2001; Sanz-Ezquerro and Tickle, 2003; Tickle, 2006). The morphogens responsible for this polarizing activity are *Sonic Hedgehog* (*Shh*) proteins (Riddle et al., 1993). *In-situ* hybridization study revealed that *Shh* was expressed specifically in the ZPA and exogenous application of the SHH protein was capable of inducing the same mirror-image digit duplication at the anterior side of the limb bud (Riddle et al., 1993). In addition to establishing the antero-posterior axis, the ZPA is also responsible for controlling both digit number and digit identity (Panman and Zeller, 2003).

The dorsal-ventral axis is determined by ectoderm once the limb bud forms (MacCabe et al., 1974; Pautou, 1977; Geduspan and MacCabe, 1987; Tickle, 1995; Capdevila and Izpisua Belmonte, 2001; Lee, 2002). The molecules those are important for dorsal-ventral axis specification and development are *Wnt-7a* and *Engrailed 1*. *Wnt-7a* is expressed in the dorsal ectoderm of limb bud (Dealy et al., 1993; Parr et al., 1993). A transgenic mouse with functionally inactivated *Wnt-7a* was produced by Parr and McMahon in 1995. This mouse had footpads on both the ventral and dorsal surfaces of the hindlimbs (Parr and McMahon, 1995). On the contrary, *Engrailed 1* which is normally only expressed at the ventral side of the limb and loss of its function in mutant mice results in double dorsal phenotype (Loomis et al., 1996; Logan et al., 1997).

Besides the establishment of three primary axes, formations of the digits and joints also play important roles in limb development. Separation of the digits is achieved by cell death and results in sculpting the limb into its final shape. The apoptotic regions of the limb include the interdigital necrotic zone (INZ), interior necrotic zone, anterior necrotic zone (ANZ) and posterior necrotic zone (PNZ) (Saunders, 1966; Saunders and

Fallon, 1967; Garcia-Martinez et al., 1993; Zuzarte-Luís and Hurlé, 2002). Mori et al., 1995 demonstrated that the cells located in these sites died by apoptosis with DNA fragmentation. The signals responsible for initiating programmed cell death in the autopod are mediated by Bone Morphogenetic Proteins (BMPs). The inhibitions of BMP-2, BMP-4, or BMP-6 expressions in the interdigital tissues result in the development of webbed feet (Yokouchi et al., 1996; Zou and Niswander; 1996). In addition to inducing apoptosis, BMP isoforms also play a major role in inducting differentiation of mesenchymal cells to become chondrocytes. Therefore, BMPs have a dual role in the developing limb. How the mesenchymal cells differentiate is dependent on the concentration of BMPs (high for inducing cell death and low for inducing chondrocytes) and also the developmental stage of the limb (Macias et al., 1997).

1.4 Role of BRE in apoptosis

Gu et al., 1998 has revealed that BRE bound specifically to the juxtamembrane of TNF p55 receptor using yeast-two-hybrid-screen and *in vitro* biochemical assays. In addition, BRE suppressed TNF-α-induced NFκB activation by gel-shift assay and luciferase assay. Therefore, BRE appears to behave like a pro-apoptotic factor through its ability to influence the TNF-mediated signaling pathway because NFκB has been reported to suppress TNF-α-induced apoptosis (Beg and Baltimore, 1996). However, it has been suggested that BRE might function like Suppressor of Death Domain protein (SODD), which blocks TNF-R1 upstream signaling resulting in the negative regulation of

NFκB activation and the apoptotic pathway (Li et al., 2004). Gu et al., 1998 reported that BRE did not interact with Fas. However, recently it has been revealed that ectopically expressed BRE protein could bind to Fas by co-immunoprecipitation (Li et al., 2004). TNF-α- and cycloheximide-induced apoptosis is inhibited by *Bre* overexpression, and the silencing of *Bre* expression using *Bre*-specific siRNA increases sensitivity to TNF-α-induced apoptosis. When anti-Fas agonist is added, overexpression of *Bre* retards the cleavages of Caspase-3, Caspase-9, and PARP and down-regulates the expression of Cytochrome c and Smac/DIABLO. When ectoposide or TNF-α is added, the same result is obtained except that the cleavages of Caspase-8 and t-bid are also retarded. BRE binds phosphorylated, sumoylated and ubiquitinated proteins in overexpressing cell line upon TNF-α or anti-Fas agonist addition. Two minutes after TNF receptor stimulation, BRE dissociates from TNF p55 receptor, but not from Fas. Furthermore, BRE has been shown to localize in cytosol and to a less extent, in the nuclei. No transportation to mitochondria has been observed upon death-receptor stimulation and etoposide addition (Li et al., 2004). Li et al., 2004 concluded that BRE had an anti-apoptotic function that targeted to death-receptor-mediated apoptosis. In addition, they proposed that components which were upstream of DISC and required for mitochondrial activation, were inhibited by BRE through ubiquitination-like activity.

1.5 Role of programmed cell death in interdigital tissue regression

Classically, the vertebrate limb has been used as a model of studying programmed cell death because PCD occurs in specific areas and at a specific time (Zuzarte-Luís and Hurlé, 2005). There are several areas in the vertebrate limb that undergo apoptosis during development and these include the anterior necrotic zone (ANZ), the posterior necrotic zone (PNZ), the opaque patch (OP) and the interdigital necrotic zone (INZ) (Saunders, 1966; Saunders and Fallon, 1967; Dawd and Hinchliffe, 1971; Alles and Sulik, 1989; Garcia-Martinez et al., 1993; Zuzarte-Luís and Hurlé, 2002). The AER, which is found on the distal margins of the limb, not only regulates the size and width of the development but also the number of digits in the developing limb (Klein et al., 1981; Todt and Fallon, 1984; Naruse and Kameyama; 1986; Capdevila and Izpisua Belmonte, 2001; Zuzarte-Luís and Hurlé, 2002; Zuzarte-Luís and Hurlé, 2005). The size and the width of AER are determined by programmed cell death and cell proliferation (Ferrari et al., 1998). Moreover, it has been proposed that apoptosis also participates in the development of the joints because cell death has been detected in the presumptive joints of the digits (Mori et al., 1995).

The interdigital tissue has been used extensively as a model for studying programmed cell death during development. Cell death occurs in the interdigital tissues in order for the digits to separate because these tissues originally link the digits together in the limb. One of the key families of protein that regulate interdigital cell death is BMPs (Zou and Niswander, 1996; Merino, et al., 1999). BMPs belong to the Transforming Growth Factor-beta (TGF-β) superfamily and has been shown to be able to

trigger apoptosis in the AER (Gañan et al., 1998; Wang et al., 2004) and the mesodermal cells (Gañan et al, 1996; Kawakami et al., 1996; Yokouchi et al., 1996; Zou and Niswander, 1996; Macias et al., 1997; Tang et al., 2000; Guha et al., 2002; Zuzarte-Luís et al., 2004). BMP-2, BMP-4, BMP-5 and BMP-7 are expressed by ectodermal cells in the AER and directly influence the development of the mesodermal cells in the digital and interdigital regions (Yokouchi et al., 1996; Laufer et al., 1997; Dupé et al, 1999; Tang et al., 2000; Zuzarte-Luís et al., 2004). Overexpression of these BMP isoforms results in premature cell death in these regions (Capdevila and Izpisua Belmonte, 2001; Zuzarte-Luís et al., 2004). Beside their abilities to induce apoptosis, BMPs at low concentration can also stimulate chondrogenesis (Macias et al., 1997) and pattern formation (Pizette et al., 2001). How the limb mesodermal cells respond to the BMPs is dependent on the developmental stage of the limb tissues, the type of modulators and BMP receptors present when the cells were exposed to the molecules (Macias et al., 1997; Grotewold and Rüther, 2002a). Until now, the pathways involved in BMP-induced apoptosis have still not been established. However, at least two apoptotic pathways have now been proposed to be BMP-related. One of them involves Smad proteins (Kimura et al., 2000; Zuzarte-Luís et al., 2004) and the other is related to a crosstalk between Wnt signal transduction and Mitogen Activated Protein Kinase (MAPK) cascade (Grotewold and Rüther, 2002b).

Although many of the features of interdigital cell death suggest it occurs via apoptosis, the main cell death machinery has still not been clarified. In order to understand the interdigital cell death mechanism, the role of Caspase-3 enzyme in interdigital cell death has been investigated (Mirkes et al., 2001; Huang and Hales, 2002).

Caspase-3 enzyme activation in response to 4-hydroxycyclophosphamide (Huang and Hales, 2002) and retinoic acid (Ali-Khan and Hales, 2003) stimuli has been investigated in the developing limb. It has been discovered that inhibition of Caspase-3 did not lead to a blockage to physiological or induced interdigital cell death – the extent of cell death was merely reduced but not eliminated (Huang and Hales, 2002). Moreover, Caspase-3-deficient mice did not show any limb phenotype (Kuida et al., 1996; Woo et al., 1998). Although many studies have shown that regression of interdigital tissues was achieved by apoptosis, interdigital cell death can also occur through a necrotic- and caspase-independent manner (Chautan et al., 1999).

In the context of interdigital programmed cell death, the evidence for the existence of an extrinsic pathway is much weaker than that for an intrinsic pathway. TNF-α-like protein has been reported to be expressed by the interdigital tissues (Wride et al., 1994). However, activation of pro-caspase-8 has not been detected during interdigital cell death (Huang and Hales, 2002). For the intrinsic pathway, the *Apaf-1*, *Bax* and *Bak* are believed to be involved in the interdigital cell death because when these genes are knockout, the animals produced show limb phenotype. The limbs are webbed (Cecconi et al., 1998; Lindsten et al., 2000). Vimentin is a substrate that has been shown to be cleaved specifically by Caspase-9 in the regressing interdigital tissues (Nakanishi et al., 2001), however, pro-caspase-8, and pro-caspase-9 activation have not been detected in the limb during apoptosis or following treatment with 4-hydroxycyclophosphamide (which normally induces programmed cell death) (Huang and Hales, 2002). Mice lacking *Caspase-9* expression also do not have any limb deformity (Kuida et al., 1998).

Beside evidences supporting the existence of an extrinsic and intrinsic pathway, other molecules have also been reported to act on the interdigital tissues. These molecules may or may not be integrated with the caspase-dependent pathway. For example, reactive oxygen species (ROS) also play a role in interdigital cell death (Salas-Vidal et al, 1998; Schnabel et al, 2006). Furthermore, not only apoptosis but also growth arrest participates in interdigital tissue regression (Lee et al, 1999; 2001).

1.6 Aim of study

In my project, I will first establish the spatial-temporal expression in the limb, as this has not been done before. Specifically, I will examine the *Bre* expression pattern in E12.5-E13.5 mouse hindlimbs using *in-situ* hybridization technique. I will correlate the expression pattern with the onset of cell death in interdigital tissues.

Secondly, using RT-PCR technique, I will determine the different *Bre* isoforms expressed by the interdigital tissues because previously it has been reported that different tissues expressed different *Bre* isoforms.

Lastly, using *Bre*-specific siRNA, I will test the effects of loss of function of *Bre* by down-regulating *Bre* expression in the interdigital cultured cells and then assay the change in cell viability in these cells. In addition, using comparative proteomics, I will compare the protein profile of *Bre*-silenced cells with that generated by control siRNA. Some of the spots with differential expression across groups will be analyzed and picked for identification. The result will be further confirmed by RT-PCR.

Chapter II

Materials and methods

2.1 Mice

ICR mice were used throughout this whole study. Pregnant ICR mice were obtained from Laboratory Animal Services Centre of The Chinese University of Hong Kong. The mice were kept at a constant temperature of 22°C and maintained on a 12-hour light/dark cycle. For mating, one male mouse was set up with four female mice in the evening hours. The mice were then checked for the presence of vaginal plugs in the following morning. If a vaginal plug was found, the mouse would be designated as half a day pregnant and the embryos inside that mouse are designated Embryonic (E) 0.5 day old.

2.2 *In-situ* hybridization

2.2.1 Histology

For histology, the E12.5 or E13.5 hindlimbs were fixed in 4% paraformaldehyde (w/v, Sigma, United States) overnight. The fixed hindlimbs were then washed in three changes of Dulbecco's Phosphate Buffered Saline (DPBS, Invitrogen Corporation,

United States) for 15 minutes. The hindlimbs were dehydrated in a graded series of ethanol (v/v, Merck, United States) from 70% to 100% (30 minutes each step). Then, the hindlimbs were cleared in xylene (Merck, United States) and embedded in paraffin wax. Finally, the specimens were sectioned at 5μm and mounted onto TESPA treated slides.

2.2.2 Preparation of riboprobe for *in-situ* hybridization

A pT-BRE plasmid containing 1,205bp encoding *Bre* isoform-five sequence was kindly provided by Professor Y.L. Chui. The plasmid cDNA was linearized by *Sal* I and *in-vitro* transcribed to generate digoxigenin (DIG)-labeled antisense riboprobe using a DIG RNA labeling kit (Roche Applied Science, United States). 1 μg purified template DNA was added with RNase-free water to make the total sample volume 13μl in a vial. 2 μl of 10X NTP labeling mixture, 2 μl of 10X transcription buffer, 1 μl of protector RNase inhibitor and 2 μl of T7 RNA polymerase were added into the vial. The mixture had been mixed gently and centrifuged briefly before it was incubated at 37°C for two hours. So as to remove template DNA, 2 μl of RNase-free DNase I had been added to the mixture which was then incubated at 37°C for 15 minutes. 2 μl of 0.2M ethylenediaminetetraacetic acid (EDTA, pH8.0) was added to the vial to stop the reaction. Afterwards, riboprobe was quantified and then stored at -80 °C for use.

2.2.3 *In-situ* hybridization

All of the procedures performed were as described by Lee et al. (1998). Briefly, paraffin sections of the specimens were dewaxed in two changes of xylene for 10 minutes. The sections were then hydrated in 100% ethanol for 10 minutes, 70% ethanol (v/v) for 5 minutes and equilibrated in DPBS for 10 minutes. The sections were digested with 10μg/ml of proteinase K (Fermentas Life Science, Canada) for 7 minutes and post-fixed in 4% paraformaldehyde for 5 minutes.

The treated specimens were washed twice in DPBS for 10 minutes and then incubated in pre-hybridization buffer containing 2X SSC (USB, United States), 1X Denhardt's reagent (refer to appendices), 5mM EDTA (Sigma, United States), 0.1% sodium dodecyl sulfate (w/v, SDS, USB, United States), 10X Dextran sulfate (Chemicon, United States), 50μg/ml salmon sperm DNA (Stratagene, United States) and 50% formamide (v/v, USB, United States) for a minimum of 2 hours. Afterwards, 0.5 μg/ml of DIG-labeled antisense riboprobe was diluted in the same buffer and added to the slides containing the specimens. The sense probe was used as a negative control. The hybridization temperature for *Bre* was 55°C. The incubation time was 16 hours.

Following hybridization, unbound riboprobe was stringently washed away in 2X SSC at 42 °C for 20 minutes (two changes), 0.1% SDS (w/v) in 0.2X SSC buffer for 15 minutes and then 0.2X SSC buffer for 10 minutes. After washing, the localization of hybridized probe in the specimens was detected using alkaline phosphatase-conjugated digoxigenin antibody (Roche Applied Science, United States). The antibody (1:50 dilution) was added to the specimens for 2 hours and washed in DPBS for 10 minutes

four changes). Nitroblue tetrazolium salt and 5-bromo-4-chloro-3-indolylphosphate (NBT/BCIP, Roche Applied Science, United States) was used as the color substrate. After color development, the sections were mounted in 50% glycerol (v/v, USB, United States).

2.3 Interdigital tissue culture

Pregnant females were sacrificed between E12.5 and E13.5. The embryos were isolated from uterus and maintained in the F-10 Ham nutrient mixture (Sigma, United States). The hindlimbs were then dissected from the trunks of the embryos. Using fine tungsten needle, the interdigital tissues between the second and the third digits, also those between the third and the forth digits, were excised and removed from the footplate. The isolated interdigital tissues were dissociated in a solution containing 0.25% trypsin (w/v, Gibco, United States), 0.03% EDTA (w/v) made up in DPBS. The tissues were incubated in the solution for 3 minutes at 37°C, with shaking. The cells were then centrifuged at 1500 revolutions per minute (rpm) for 3 minutes and then cultured in Dulbecco's Modified Eagle's Medium (DMEM, Invitrogen Corporation, United States), +10% Fetal Bovine Serum (FBS, v/v, Gibco, United States), +0.01% Stretomycin sulphate (w/v, Gibco, United States), +100u/ml penicillin (Gibco, United States) for 24 hours inside 35-mm culture dish (Corning, United States). 35-mm culture dishes were used for cell seeding in all experiments unless otherwise stated. The cells were incubated at 37°C with 5%CO_2 in the humidified chamber throughout the whole study.

2.4 Gene interference

2.4.1 Construction of *Bre*-siRNA

Gene interference study was performed by using small interfering RNA (siRNA) duplex targeting the *Bre* mRNA for degradation. siRNA targeting all *Bre* isoforms was used to silence the endogeneous *Bre* expression in the interdigital cells. The sense and antisense sequence of siRNA used for targeting *Bre* mRNA were 5'-UUC UCC GAA CGU GUC ACG UdT dT-3' and 5'-ACG UGA CAC GUU CGG AGA AdT dT-3' respectively. siRNA targeting Green Fluorescent Protein (GFP) mRNA was used as a negative control in the experiment. The sense and antisense sequence for targeting GFP were 5'-AAG CUG ACC CUG AAG UUdT dT-3' and 5'-AAC UUC AGG GUC AGC UUdG dC-3' respectively. The siRNA duplexes were synthesized, purified and annealed by Qiagen-Xeragon, (Germantown, MD, USA). For each tube of lyophilized siRNA provided by the company, 1ml of the siRNA Suspension Buffer (Qiagen-Xeragon, Germantown, MD, USA) was added. The tube was then heated at 90°C for 1 minute. This was followed by incubation at 37 °C for an hour. The reconstituted siRNA solution was ready for use. It was aliquoted and stored at -80 °C. The concentration of siRNA solution varied from tube to tube, but was stated on the data sheet provided.

2.4.2 siRNA transfection of cultured interdigital cells

The E12.5 interdigital cells were ready for siRNA transfection after they were allowed to attach to the culture plate for 24 hours. The culture medium was changed to transfecting medium that contained DMEM, +10% FBS (v/v). 1.4ml of transfecting medium was added to each 35-mm culture dish. siRNA transfection was conducted six hours after medium had been changed. 100μl of gene silencing solution containing 0.5μg of siRNA, 4μl of RNAiFect Reagent (Qiagen-Xeragon, Germantown, MD, USA) and DMEM was mixed with vortex and incubated for 40 minutes before use. 100μl of gene silencing solution was introduced into the cell culture for 24 hours at 37°C. 24 hours later, the same transfection procedure was repeated and the cells were cultured for a further 24 hours.

2.5 Semi-quantitative RT-PCR

2.5.1 Sample collection of interdigital cells and explants

Interdigital cells were harvested and washed with DPBS solution for once. 1ml of TRIzol solution (Invitrogen Corporation, United States) was added into each 35-mm culture dish containing the cell samples. The cells were then incubated for 10 minutes at 4°C and then placed into a 1.5ml RNase-free eppendorf tube. Interdigital tissues isolated from footplates were placed into a 1.5ml RNase-free eppendorf tube containing 1ml TRIzol solution. The tube was vortexed until all the explants were dissolved.

2.5.2 RNA isolation and extraction

After tissue or cell samples were dissolved in Trizol solution, 200µl of chloroform (Fisher Scientific, United States) was added into each eppendorf tube. Then the eppendorf was vortexed for 15 seconds, allowed to settle for 3 minutes at room temperature and then centrifuged at 12,000 rpm at 4°C for another 20 minutes. 500µl of supernatant was extracted from each sample and added into another 1.5ml RNase-free eppendorf tube. The remaining solution was discarded. 500µl isopropanol (BDH Chemicals Ltd., United Kingdom) was added into each sample, which was then throughoutly mixed by inverting the tube. The RNA was precipitated at -80°C for an hour. The samples were then centrifuged at 12,000 rpm at 4°C for 10 minutes. The supernatant was extracted and discarded. 1ml of 75% ethanol (v/v) made up in diethypyrocarbonate - treated water (DEPC, USB, United States) was added to each sample which was then centrifuged at 7500 rpm at 4°C for 5 minutes. After the supernatant had been discarded, the tube was dried at room temperature.

When a colorless precipitate was observed at the bottom of the tube, a suitable amount of DEPC-treated water was used for reconstitution. Then, the concentration and the purity of RNA were determined using a spectrophotometer (Biophotometer, Eppendorf, Germany) with the absorbance set at 260nm and 260/280nm.

2.5.3 Reverse-transcription and cDNA synthesis

5µl of pre-reaction mixture containing 1µg of RNA, 1µl of oligo-dT primer (Promega Corporation, United States) and DEPC-treated water was added to a microcentrifuge tube, incubated at 70 °C for five minutes and then on ice for another five minutes. 15 µl of reaction mixture containing 4 µl of ImPromII 5X Reaction Buffer (Promega Corporation, United States), 1.2µl of magnesium chloride solution (25mM, Promega Corporation, United States), 1µl of deoxyribonucleotide triphosphate (dNTP) mix (10mM, Promega Corporation, United States), 20 units ribonuclease inhibitor (Promega Corporation, United States), 1µl of ImPromII reverse transcriptase (Promega Corporation, United States) and DEPC-treated water was added to the pre-reaction mixture. A polymerase chain reaction (PCR) machine (PTC-100, MJ Research, Bio-Rad Laboratories, United States) was used for reverse-transcription and the complementary DNA (cDNA) synthesis process. The condition of the experiment was as followed:

Step	Temperature	Duration
1	25 °C	5 minutes
2	42 °C	1 hour
3	70 °C	15 minutes
4	4 °C -20 °C	For short-term storage For long-term storage

Table 1. Condition of reverse-transcription and cDNA synthesis

2.5.4 Polymerase chain reaction

cDNA obtained from reverse-transcription experiment was used as the template for PCR amplification. 20μl of PCR mixture containing 1μl of cDNA, 2.5μl of PCR 10X buffer (Bio-firm, Hong Kong), 0.75μl of magnesium chloride solution (25mM, Bio-firm, Hong Kong), 1μl of dNTP mix (10mM, Promega Corporation, United States), 1μl of forward primer, 1μl of reverse primer, 0.25μl of Taq polymerase (Bio-firm, Hong Kong) and DEPC-treated water in a microcentrifuge tube was placed into the thermal cycler for PCR amplification. All of the primers used in this study were manufactured and desalted by Invitrogen Corporation (United States). The primers' sequence and condition for semi-quantitative PCR are shown in Table 2 and Table 3 respectively. An additional 7-minute extension step at 72°C was performed at the end of the last cycle.

Primers	Primer sequence
Beta-actin (Forward)	5'-TGT TAC CAA CTG GGA CGA C-3'
Beta-actin (Reverse)	5'-AAG GAA GGC TGG AAA AGA G-3'
Bre (Forward)	5'-CAA CAT TCC CAC ATA CCT TCT C-3'
Bre (Reverse)	5'-GCC ATT TCA TTT CCA TCC CAT C-3'
Bre isoform 1 (Forward)	5'-TTC ATT CAA GTC CTG CTC T-3'
Bre isoform 1 (Reverse)	5'-ATT CAC CAG TCC AGT TGT T-3'
Bre isoform 2 (Forward)	5'-CGA TGT GTG CCT GTA CTG T-3'
Bre isoform 2 (Reverse)	5'-CAC TGG AAC TGG TGG TAC TG-3'
Bre isoform 3 (Forward)	5'-CCG ATG TGT GCC TGT AG-3'
Bre isoform 3 (Reverse)	5'-ATT CAC CAG TCC AGT TGT T-3'
Bre isoform 4 (Forward)	5'-CGG ACT TAA GTT CCA GAT CC-3'
Bre isoform 4 (Reverse)	5'-CTC CAA AGG TAC GAT GCT T-3'
Bre isoform 5 (Forward)	5'-GTG GGA CTG GAT GCT ACA AAC T-3'
Bre isoform 5 (Reverse)	5'-CGC ACT GGA ACT GGT GGT A-3'
Pdia6 (Forward)	5'-TCC TTT CCT ACC ATC ACT CC-3'
Pdia6 (Reverse)	5'-CAC AGA ACC ACA TCC TTA CC-3'
Vimentin (Forward)	5'-CAG TCC TCT GCC ACT CTT G-3'
Vimentin (Reverse)	5'-CAG TTC TAC CTT CTC GTT GG-3'

Table 2. Primers and corresponding sequences used in the study.

Primers	Annealing Temperature (Tm)	Duration of denaturing step at 95 °C in each cycle	Duration of annealing step at Tm in each cycle	Duration of extension step at 72 °C in each cycle	Number of cycles
Bre	55°C	45 seconds	30 seconds	45 seconds	30
Bre isoform 1	55°C	45 seconds	30 seconds	45 seconds	40
Bre isoform 2	55°C	45 seconds	30 seconds	45 seconds	40
Bre isoform 3	55°C	45 seconds	30 seconds	45 seconds	40
Bre isoform 4	55°C	45 seconds	30 seconds	45 seconds	40
Bre isoform 5	55°C	45 seconds	30 seconds	45 seconds	30
Pdia6	53°C	45 seconds	45 seconds	60 seconds	30
Vimentin	53°C	45 seconds	30 seconds	45 seconds	25

Table 3. Conditions of PCR for each pair of primers. An additional 7-minute extension step at 72°C was performed at the end of the last cycle.

2.6 Assay of cell viability by MTT

Interdigital cultured cells were prepared as previously described and grown in a microplate (96-well format). Four separate microplates were prepared for assay of cell viability at four different time points. Each plate contained four groups of samples including non-treatment group, control group, *Bre*-siRNA-treated group and GFP-siRNA-treated group. Each group of samples consisted of three replicates. Approximately,

2×10^3 cells per well were grown at 37°C with 5% CO_2 in the humidified chamber for 18 hours. The culture medium was then changed to transfecting medium containing DMEM, +10% FBS (v/v). 87.5μl of transfecting medium was added to each well. Transfection was conducted six hours after medium had been changed. 6.25μl of gene silencing solution containing 0.0625μg of siRNA, 0.25μl of RNAiFect Reagent and DMEM was mixed with vortex and incubated for 40 minutes before use. It was introduced into each well of *Bre*-silenced or GFP-silenced cell cultures. 6.25μl of mock transfecting solution containing 0.25μl RNAiFect Reagent and DMEM was also mixed with vortex, incubated for 40 minutes and added to the control culture. The same amount of DMEM was added to the non-treatment culture group. The viabilities of cultured cells were measured at time-point zero (just before transfection), 24 hours, 39 hours and 48 hours post transfection. At suitable time point, 9.4μl of 5mg/ml MTT solution was added to each well and the corresponding mixtures were incubated at 37°C with 5% CO_2 in the humidified chamber for four hours. After incubation, culture medium was removed and 94μl of dimethyl sulfoxide (DMSO, Sigma, United States) was added to dissolve the insoluble purple formazan product into a colored solution. The mixtures were further incubated for 15 minutes in dark at room temperature. Afterwards, the absorbance of the colored solution was quantified by measuring at 595nm by a kinetic microplate reader (Molecular Devices, United States).

2.7 Comparative proteomics

Protein changes resulted from knock-down of *Bre* were revealed by two-dimensional electrophoresis. Protein profiles were visualized by staining with silver nitrate after isoelectric point (pI) and molecular weight separation. Any proteins with differential expression between experimental and control groups were picked and identified by Matrix-Assisted Laser Desorption/ Ionization Time-of-Flight (MALDI-TOF) mass spectrometer. Two-dimensional electrophoresis was used in this study because of its unparalleled ability to separate thousands of protein simultaneously. Therefore, cluster of proteins, which is lining in the same pathway, having any differential expressions can be revealed at the same time. As a result, the role of BRE in the interdigital cells may be guessed from this piece of information. In addition, as silver staining is the most sensitive non-radioactive detection method which can detect down to one nanogram of protein, a complete set of proteins with differential expression can be visualized. Also, selected proteins can be easily identified by mass fingerprinting because well-developed mass fingerprinting databases were set up by various research institutes.

2.7.1 Collection of interdigital cells

Interdigital cells were dissociated from E12.5 and E13.5 interdigital tissues and washed with DPBS for once. 800μl of trypsin solution containing 0.25% trypsin (w/v), 0.03% EDTA (w/v) in DPBS was added to each culture dish which was then incubated at 37°C with 5% CO_2 inside a humidified chamber for 3 minutes. Afterwards, 600μl of

DPBS supplemented with 10% FBS (v/v) was added to the culture dish to terminate trypsinization process. The sample was then transferred to an eppendorf tube and centrifuged at 12,000 rpm for 3 minutes. The supernatant was discarded.

2.7.2 Preparation of cell lysate

Specifically, interdigital cells that were transfected with control and *Bre*-specific siRNA were used. The cells collected were placed in lysis buffer (8M Urea (USB, United States), 2% 3-[(3-cholamidopropyl)dimethylammonio]-1-propane sulfonate (CHAPS, w/v, Sigma-Aldrich, United States), 2M thiourea (Sigma-Aldrich, United States), 40mM dichlorodiphenyltrichloroethane (DTT, Sigma-Aldrich, United States), 1% Nonidet P40 (NP-40, v/v, USB, United States)). The samples were mixed thoroughly by pipetting up and down until the cell pellets dissolved in the lysis buffer. Then, the samples were incubated on ice for one hour followed by centrifugation at 12,000 rpm for 15 minutes at 4°C. The cell lysates were transferred to clean eppendorf tubes.

2.7.3 Assay of protein concentration in cell lysate

Bio-Rad Protein Assay (Bio-Rad Laboratories, United States) was used to measure the concentration of soluble protein in the sample. The measurement was based on the Bradford method which is a dye-binding assay. Coomassie brilliant blue G-250 dye, in the presence of phosphoric acid and ethanol forms a strong acidic solution which

has a maximum absorbance at 465nm. When the dye makes contact with the protein, the anionic form of the dye is stabilized by hydrophobic and ionic interactions with arginine residue or other basic and aromatic amino acid residues. The binding of the acidic dye solution to protein shifts the maximum absorbance to 565nm. The protein concentration of the sample can then be estimated by measuring the UV absorbance of the dye-protein mixture at 565nm.

Protein assay dye reagent concentrate and bovine serum albumin (BSA) were included in the Bio-Rad Protein Assay kit (Bio-Rad Laboratories, United States). Briefly, BSA was used as a protein standard in the assay. The linear range of the assay is 8μg/ml to 80μg/ml. Therefore, 10μg/ml, 20μg/ml, 40μg/ml, 60cg/ml and 80μg/ml of BSA protein solutions were used to create a standard curve for the assay. All samples, including the protein standards, were assayed in triplicate. 160μl of each standard solution was pipetted into separate microtiter plate well. 1μl of protein sample together with 159μl of MilliQ water were added into each well of a microtiter plate. After adding the standard protein solution and the sample solution into the wells, 40μl of dye reagent concentrate was introduced into each well. The protein solution and reagent were mixed thoroughly using a microplate mixer. The plate was then incubated at room temperature for 5 minutes. Absorbance at 595nm was measured using the kinetic microplate reader.

2.7.4 Two-dimensional gel electrophoresis

Isoelectric focusing (IEF) separates the proteins according to their pI. Proteins are amphoteric molecules. The charge that they carried depends on the pH of the surrounding. The net charge of the protein is the sum of all negative charges and positive charges of its amino acid side chains, amino- and carboxyl-terminals. Protein becomes positively charged at pH lower than its pI and negatively charged at pH higher than its pI. The net charge is zero at the pH equal to its pI value. Therefore, with the presence of electric field, proteins separate, migrate to their pI position and stop.

11-cm long IPG electrode strip with 4-7pH gradient (Amersham Biosciences, United Kingdom) and an Ettan IPGphor Strip Holder (Amersham Biosciences, United Kingdom) were used in this experiment. Before protein loading, the IPG strip holders had to be cleaned with detergent (Amersham Bioscience, United Kingdom) thoroughly and allowed to dry before assembly of the apparatus. 150μg of protein was applied for each IPG strip. The total volume of protein sample and rehydration buffer (8M Urea, 2% CHAPS (w/v), 1% IPG buffer (v/v, Amersham Biosciences, United Kingdom), 40mM DTT (Sigma-Aldrich, United States)) loaded onto the strip holder was 210μl. The maximum volume for sample loading was 50μl and the rehydration buffer made up the final volume to 210μl. The rehydration buffer was evenly introduced between the two electrodes of the strip holders. After that, different protein samples were pipetted into the central region of different strip holders. All large bubbles were removed. The protective cover foils were removed from the IPG strips. The strips were then positioned with the gel side down and the anodic end of the strip directed toward the pointed end of the strip

holders. Afterwards, the IPG strips were lowered onto the solution. 1ml of IPG Cover Fluid (Amersham Biosciences, United Kingdom) was applied to each strip so as to minimize evaporation and urea crystallization. The rehydration step was done under voltage and followed by a separation process. The electrophoresis condition for each step is listed in the Table 4. The program was stopped when the total volt-hours reached 39000.

Condition of IEF: 18°C, 50 micro-ampere (μA) per strip		
Step	Voltage	Step duration
1	30V	13 hours
2	500V	15 minutes
3	1000V	15 minutes
4	2000V	15 minutes
5	3000V	15 minutes
6	4000V	30 minutes
7	5000V	45 minutes
8	5500V	1 hour
9	5600V	20 hours

Table 4. Condition of IEF

After the first-dimensional electrophoresis was completed, the IPG strips were removed from the strip holders. Each strip was then treated with 1% DTT (w/v) in 6.5ml of equilibration buffer (50mM Tris (USB, United States), 6M of urea, 30% glycerol (v/v), 2% SDS (w/v), 0.1% bromophenol blue (w/v, Sigma-Aldrich, United States)) with shaking for 30 minutes. The medium was then changed to 1% iodoacetamide (IAA, w/v, Sigma-Aldrich, United States) dissolved in the 6.5ml of the same equilibration buffer. The strips were treated in the solution for 30 minutes with constant shaking.

The equilibrated strips were then loaded on the 12% SDS-acrylamide separating gels. Prestained protein molecular weight marker (Fermentas Life Science, Canada) with the range of 20 to 120kDa was used to determine the sizes of the proteins on the gel. 2% agarose (w/v, USB, United States) dissolved in cathode buffer was used to seal the gap between two glass plates. The apparatus was then immersed in the anode buffer with the upper chamber filling with cathode buffer. SDS-Polyacrylamide gel electrophoresis (SDS-PAGE) was performed at room temperature under constant voltage 100V, until the dye front reached the bottom of the gel.

After SDS-PAGE, the gels were released from the electrophoresis apparatus and processed separately in containers. They were fixed with shaking in fixing solution for 1 hour. After that, the gels were washed in MilliQ water for 15 minutes for 4 times and then immersed in 50% ethanol (v/v) for 20 minutes twice. The gels were then soaked in 0.02% sodium thiosulphate solution (w/v, Merck, United Kingdom) for 10 minutes with shaking, followed by 3 five-minute washes and stained by silver reaction. The silver reaction involved treating the gels in cool silver reaction solution for 1 hour at 4°C and then being rinsed twice with MilliQ water. After several brief washes, the gels were

immersed in developing solution until the desired silver staining intensity was reached. The gels were then soaked in 5% acetic acid (v/v, BDH Chemicals Ltd., United Kingdom) for 5 minutes to terminate the staining process. The medium was then poured off. The gels were scanned using a GS 800 Densitometer (Bio-Rad Laboratories, United States) and images were captured for further analysis. The protein spots on the gel were analyzed by The Discovery series, PDQuest 2D Analysis Software (Bio-Rad Laboratories, United States) version 7.13 PC.

2.7.5 Protein identification by mass fingerprinting

Any protein spots of interest that we identified were picked up from the gel and subjected to mass spectroscopy for protein identification. MALDI-TOF mass spectrometer (Voyager-DE Pro Biospectrometry Workstation, Applied Biosystems, United States) was used in this experiment.

Protein spots were isolated from the gel and processed for destaining. The gel pieces were first briefly washed in MilliQ water twice. Each gel piece was then covered with 200µl of destaining solution (15mM potassium ferricyanide (Sigma-Aldrich, United States), 50mM sodium thiosulphate) and incubated at room temperature until they turned colorless. For the best result, the destaining solution should be freshly prepared.

Each gel piece was then washed with 400µl of MilliQ water for 15 minutes for three times to remove the yellow reagent. The destained gel pieces were equilibrated in 200µl of 10mM ammonium bicarbonate (Sigma-Aldrich, United States)/50% acetonitrile

(v/v, Merck, United Kingdom) each for about 15 minutes. The equilibration step was repeated one more time. The solution was discarded and the equilibrated gel pieces were dehydrated by incubating in 200µl of acetonitrile for 15 minutes. The solution was then poured off and the spots were dried in an incubator at 30°C for 5 minutes. The gel pieces were then ready for trypsin in-gel digestion.

The trypsin (Promega, United States) was prepared by resuspension in 50mM acetic acid to form 0.1% stock solution (w/v). This solution was further diluted to 0.0015% trypsin working solution in 40mM ammonium bicarbonate /50% acetonitrile (v/v). 12µl of the working solution was added to each gel sample. The reaction mixture was then incubated at room temperature for 30 minutes to ensure complete reswelling of the gel pieces. After that, additional trypsin working solution was added to ensure the gels were totally covered by the solution. The samples were then incubated at 35°C for 16 hours. After trypsinization, 3µl of extraction solution (50% acetonitrile (v/v), 5% trifluoroacetic acid (TFA, v/v, Fluka Chemika, Switzerland)) was added to each gel piece. The mixture was then vortexed and further incubated at 35°C for 15 minutes. It was then centrifuged at 3,000 rpm for 2 minutes at room temperature.

3µl of reaction mixture from each sample was spotted onto a MALDI-TOF sample plate (Applied Biosystems, United States) which was then allowed to dry for 20 minutes at 35°C. α-cyano-4-hydroxycinnamic acid (Fluka Chemika, Switzerland) was used as matrix for the MALDI-TOF mass spectroscopy. The matrix solution (1% α-cyano-4-hydroxycinnamic acid (w/v), 50% acetonitrile (v/v), 0.1% TFA (v/v)) was first centrifuged at 3,000rpm for three minutes at room temperature. 1µl of the matrix

supernatant was spotted over each dried sample. The plate was then dried by air for 30 minutes.

The mass spectrums were analyzed using the software Data Explorer Version 4.0.0.0 (Applied Biosystems, United States). The spectrums resulted from analysis were subjected to mass fingerprinting database search. MS-Fit search from Protein prospector website, http://prospector.ucsf.edu/ucsfhtml4.0/msfit.htm was used in this experiment.

2.8 Statistical Method

If not otherwise indicated, all results are shown as mean ± standard deviation. To determine the significance of variance in the experiments, data were analyzed using the two-tailed, paired student's t-test. $P<0.05$ was considered to be statistically significant. All statistical procedures were performed using the SPSS software.

Chapter III

Results

3.1 Spatial and temporal expression of *Bre* in murine embryonic hindlimbs

E12.5 and E13.5 embryos were extracted from the pregnant ICR mice. The hindlimbs were isolated from the embryos and processed for histology. Paraffin sections of E12.5 and E13.5 hindlimb were hybridized by mouse DIG-labeled *Bre*-specific riboprobe. We established that at E12.5, *Bre* gene expression was higher in the interdigital tissues than that in digits (Figure 2). At E13.5, similar expression pattern was obtained (Figure 3). In order to quantitatively compare the expression level of *Bre* in interdigital tissues at E12.5 and E13.5, we performed semi-quantitative RT-PCR analysis. Interdigital tissues between the second and the third digits and those between the third and the forth digits were freshly excised from E12.5 and E13.5 hindlimbs. The expression level of *Bre* in the interdigital tissues was revealed using semi-quantitative RT-PCR and *Bre*-specific primers which prime the common region among all of the *Bre* isoforms (Figure 4). The result confirmed *Bre* was expressed in the interdigital tissues of E12.5 and E13.5 hindlimbs. Moreover, *Bre* was expressed at a higher level in E12.5 interdigital tissues than E13.5 interdigital tissues. The expression of *beta-actin* (*β-actin*) served as an internal control for normalization of the results. We decided to perform loss-of-function study on the interdigital tissues using *Bre*-siRNA. The experiment required primary

E12.5 and E13.5 interdigital cell culture to be established. Moreover, we needed to establish whether *Bre* expression was maintained when interdigital tissues were isolated from the hindlimbs, dissociated and maintained in culture. We performed RT-PCR on the interdigital cell culture and established that E12.5 and E13.5 interdigital cells during culture maintained *Bre* expression (Figure 5). Hence, they could be used for *Bre* gene silencing experiments.

Figure 2.

In-situ hybridization showing the expression pattern of *Bre* mRNA in E12.5 hindlimb, by using DIG-labeled *Bre* antisense riboprobe (A and B). *Bre* is expressed in the purple/blue stained cells of interdigital tissues (A, Bar =200μm; B, Bar =100μm). D, digits. INZ, interdigital necrotic zone.

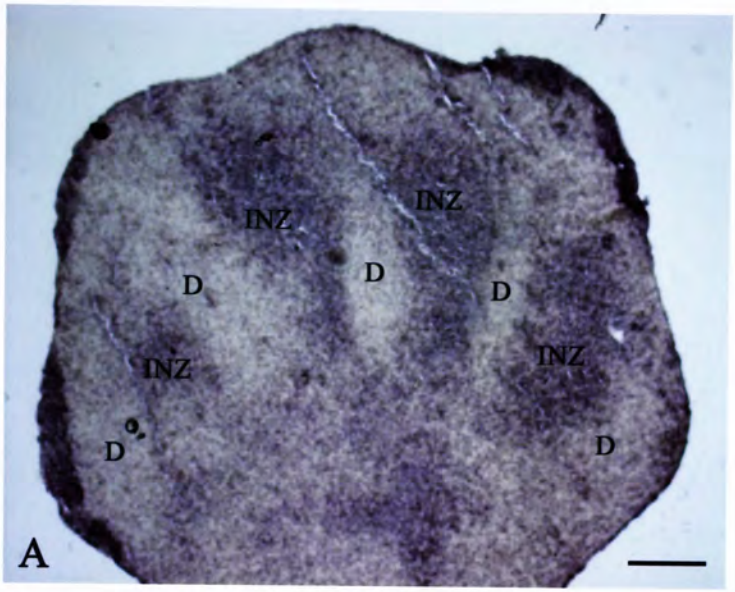
INZ
INZ
D
D
D
INZ
INZ
D
D
A

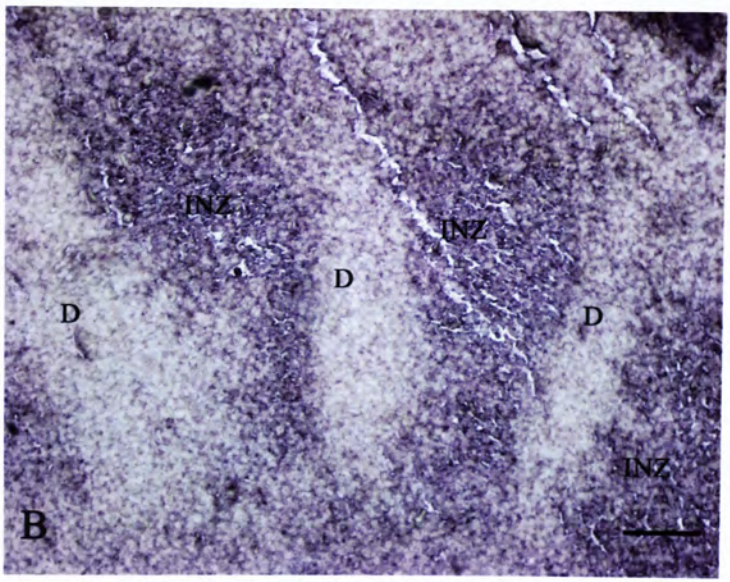
INZ
INZ
D
D
D
INZ
B

Figure 3.

In-situ hybridization showing the expression pattern of *Bre* mRNA in E13.5 hindlimb, by using DIG-labeled *Bre* antisense riboprobe (A and B). *Bre* is expressed in the purple/blue stained cells of interdigital tissues (A, Bar =200μm; B, Bar =100μm). D, digits. INZ, interdigital necrotic zone.

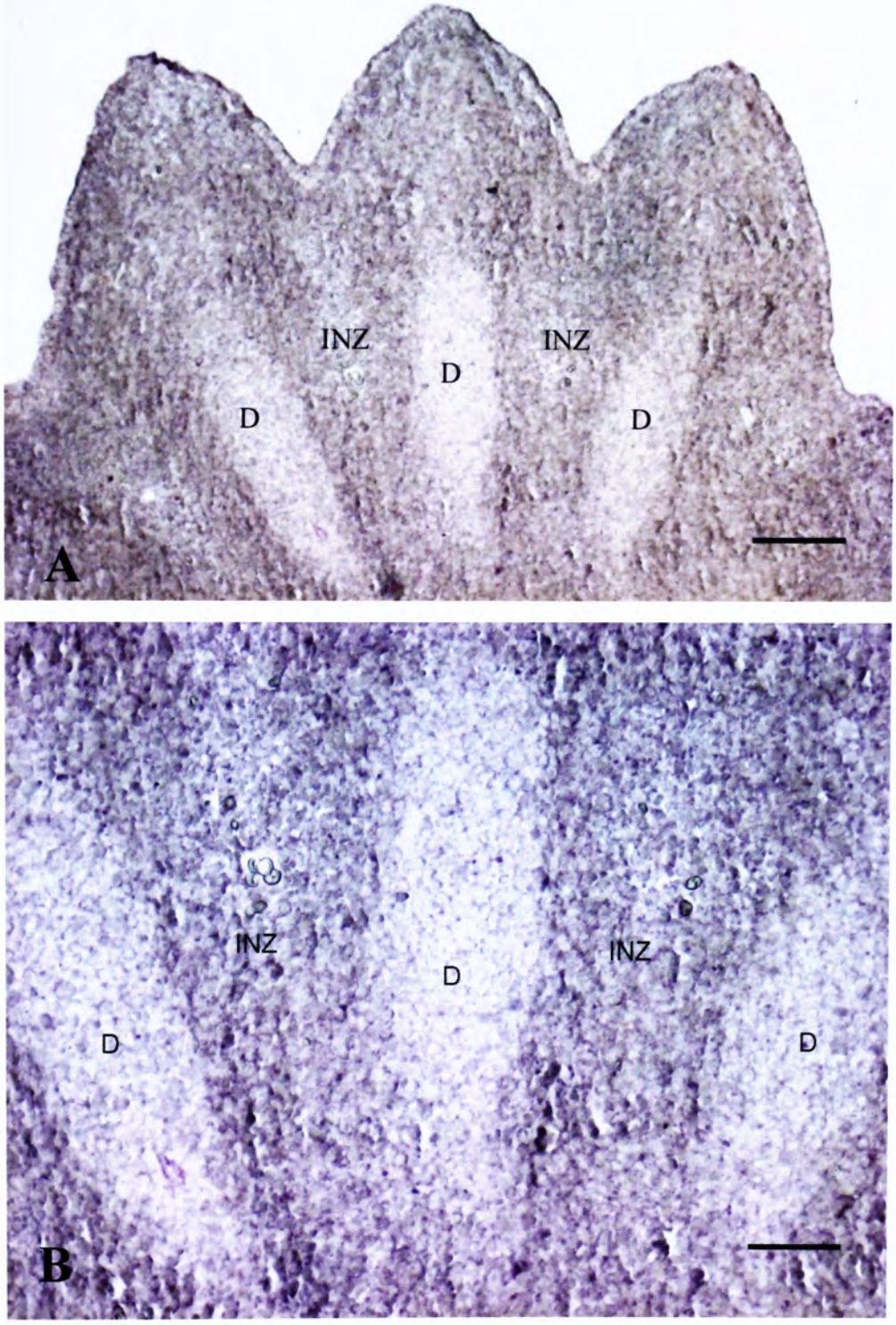
INZ
INZ
D
D
D
A
INZ
INZ
D
D
D
B

Figure 4.

Semi-quantitative RT-PCR analysis of *Bre* expression in E12.5 and E13.5 interdigital tissues. Lane A, E12.5 interdigital tissues. Lane B, E13.5 interdigital tissues. (A) The result showed that both E12.5 and E13.5 interdigital tissues expressed *Bre* mRNA. In addition, *Bre* expression was higher in E12.5 interdigital tissues than E13.5 interdigital tissues. *β-actin* was the internal control. (B) The ratio of *Bre* expression level in E12.5 interdigital tissues and E13.5 interdigital tissues. For the ease of illustration, the *Bre* expression level in E12.5 interdigital tissues was made up to 1.0. The *Bre* mRNA level in each group was normalized by its corresponding *β-actin* expression level.

A

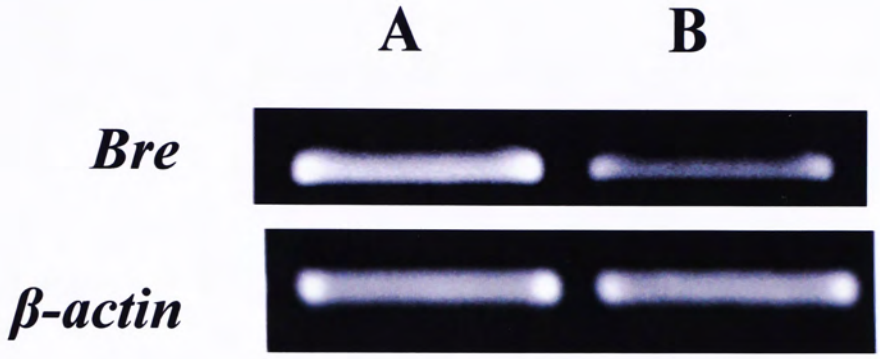
A
B
Bre
β-actin

B

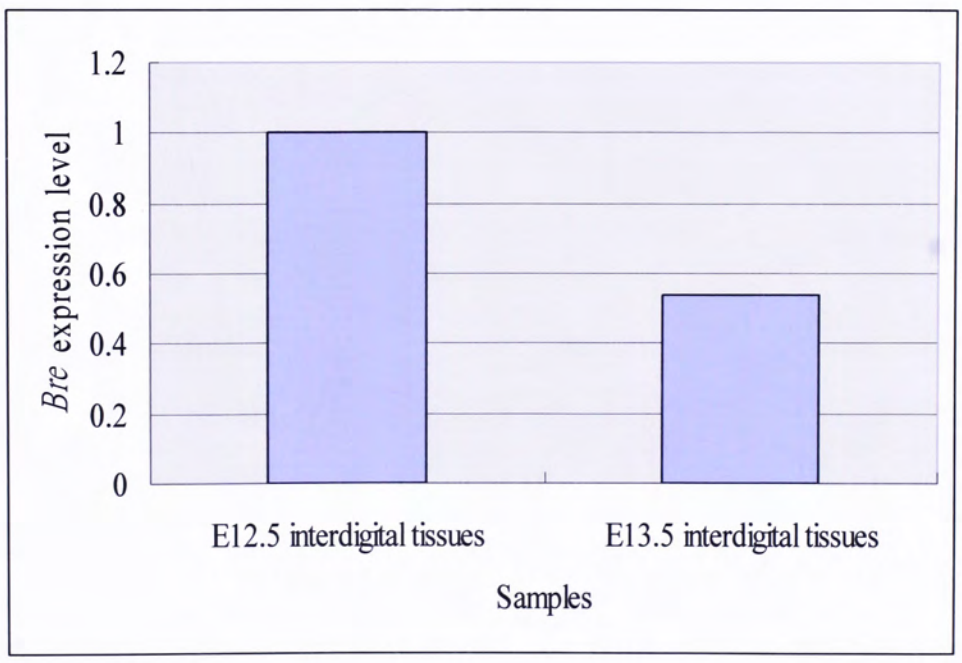
1.2
1
0.8
0.6
0.4
0.2
0
Bre expression level
E12.5 interdigital tissues
E13.5 interdigital tissues
Samples

Figure 5.

Semi-quantitative RT-PCR analysis of *Bre* expression in interdigital cells after culturing for 24 hours. Lane A, interdigital cells established from E12.5 hindlimbs. Lane B, interdigital cells established from E13.5 hindlimbs. (A) The result revealed that the interdigital cells maintained their ability to express *Bre*. Moreover, the E12.5 interdigital cells expressed a higher level of *Bre* mRNA than E13.5 interdigital cells. *β-actin* served as an internal control. (B) The ratio of *Bre* expression level in E12.5 interdigital cells and E13.5 interdigital cells. For the ease of illustration, the *Bre* expression level in E12.5 interdigital cells was made up to 1.0. The *Bre* mRNA level in each group was normalized by its corresponding *β-actin* expression level.

A

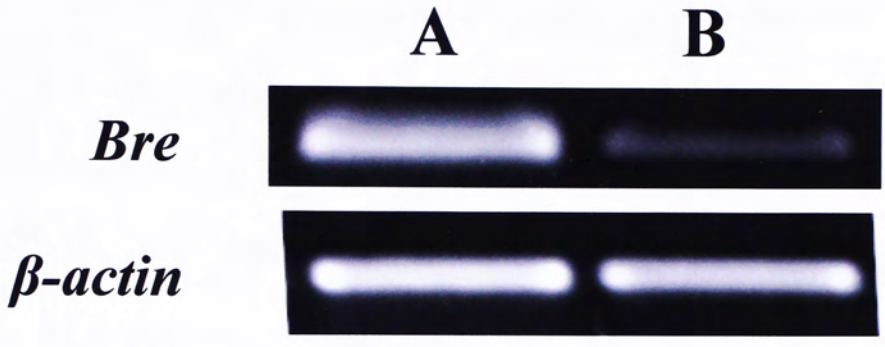
A
B
Bre
β-actin

B

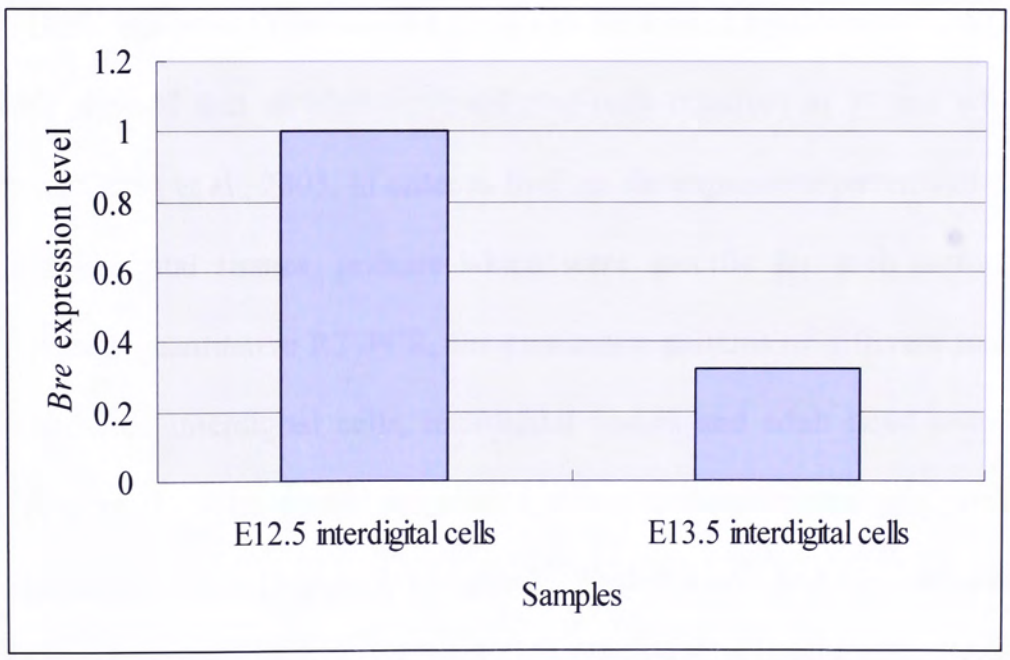
1.2
1
0.8
0.6
0.4
0.2
0
Bre expression level
E12.5 interdigital cells
E13.5 interdigital cells
Samples

3.2 Expressions of *Bre* isoforms in interdigital tissues

Previously, human *Bre* was reported to have different isoforms expressed in various human cell lines. Six isoforms, resulted from alternatively splicing either at 5' end or 3'end, were shown to be expressed in human cell lines by RT-PCR (Ching et al., 2001). In its mouse counterpart, *Bre* was also reported to have five isoforms expressed in the heart tissues as determined in NCBI database. However, unlike its human counterpart, these isoforms were only resulted from alternatively splicing at 5'end. With the exception of heart tissues, expressions of different isoforms were too low to be detected in other tissues like brain, liver, lung and kidney (Ching et al., 2003). Since *Bre* was shown to be expressed in the interdigital tissues at E12.5 and E13.5, we wanted to establish which types of *Bre* isoforms were expressed in the interdigital tissues. Beforehand, a multiple alignment of five isoforms of mouse *Bre* gene was performed by ClustalW 1.83 (Figure 6). The result showed that an alternative splicing only occurred at 5' end which was consistent with Ching et al., 2003. In order to find out the expression patterns of different isoforms in interdigital tissues, primers which were specific for each isoform were designed. By semi-quantitative RT-PCR, the expression patterns of different mouse *Bre* isoforms in cultured interdigital cells, interdigital tissues and adult heart tissues were elucidated (Figure 7). The result revealed that the cultured interdigital cells only expressed *Bre* isoform five (Figure 7, left panel). Similar result was also obtained from interdigital tissues isolated from E12.5 hindlimbs (Figure 7, middle panel). Expressions of other *Bre* isoforms were too low to be detected by semi-quantitative RT-PCR

technique. In adult mouse heart tissues, we determined that they expressed *Bre* isoform 2, 4 and 5 (Figure 7, right panel).

Figure 6.

An alignment of five isoforms of mouse *Bre* gene. Isoform 1 (Accession number: NM_181279), Isoform 2 (Accession number: NM_181282), Isoform 3 (Accession number: NM_181281), Isoform 4 (Accession number: NM_181280) and Isoform 5 (Accession number: NM_144541) were aligned by CLUSTALW (1.83). The result showed that an alternative splicing only occurred at 5' end which was consistent with Ching et al., 2003. Conserved nucleotide among all isoforms is indicated with an asterisk.


Isoform 2 CCGGTTACTGATCGGACTTAAGTTCCAG-----ATCCATGAA-------AAAGGGCCGTC 48
Isoform 3 CCGGTTACTGATCGGACTTAAGTTCCAG-----ATCCATGAA-------AAAGGGCCGTC 48
Isoform 4 CCGGTTACTGATCGGACTTAAGTTCCAG-----ATCCATGAA-------AAAGGGCCGTC 48
Isoform 1 CCGGTTACTGATCGGACTTAAGTTCCAGTGGTAACTCATAAATCAAGTTAAAATGTCTCC 60
Isoform 5 CCGGTTACTGATCGGACTTAAGTTCCAGTGGTAACTCATAAATCAAGTTAAAATGTCTCC 60
Isoform 2 ACAGAA-GCTTTCATTCAAGTCC------TGCTCTTATCATCTGC-CGATGTGTG-CCTG 99
Isoform 3 ACAGAA-GCTTTCATTCAAGTCC------TGCTCTTATCATCTGC-CGATGTGTG-CCTG 99
Isoform 4 ACAGAA-GCTTTCATTCAAGTCC------TGCTCTTATCATCTGC-CGATGTGTG-CCTG 99
Isoform 1 AGAAATTGCCTTGAACCGAATTTCTCCAATGCTCTCCCCATTCATATCAAGCGTGGTCCG 120
Isoform 5 AGAAATTGCCTTGAACCGAATTTCTCCAATGCTCTCCCCATTCATATCAAGCGTGGTCCG 120
Isoform 2 TACTG---------- 104
Isoform 3 TA---------- 101
Isoform 4 TAATG---------- 104
Isoform 1 AAATGGGAAGATCCATGAAAAAGGGCCGTCACAGAAGCTTTCATTCAAGTCCTGCTCTTA 180
Isoform 5 AAATGGGAAGGT---------GGGACTG-----GATGCT---------- 145
Isoform 2 ----------
Isoform 3 ----------
Isoform 4 ----------AATGGTATGGTGTGCCAGATCTAGAGAAAGCATC 138
Isoform 1 TCATCTGCCGATGTGTGCCTGTAATGAATGGTATGGTGTGCCAGATCTAGAGAAAGCATC 240
Isoform 5 ----------ACAAACTGTTTG-------AGAATTACGGA------- 168
Isoform 2 ----------TACATC 110
Isoform 3 ----------
Isoform 4 GTACCTTTGGAGAAAGAAAGAAAACCATCTGCCACTAGAAAAAGGCCAAAACTGTACATC 198
Isoform 1 GTACCTTTGGAGAAAGAAAGAAAACCATCTGCCACTAGAAAAAGGCCAAAACTGTACATC 300
Isoform 5 -----CTTGAAG---------------TCTG----------GCTGTACATC 189
Isoform 2 ATTGACTCCTGGACCCAACTGTGACCGCTTCAAACTGCACATCCCGTACGCTGGGGAGAC 170
Isoform 3 ----------
Isoform 4 ATTGACTCCTGGACCCAACTGTGACCGCTTCAAACTGCACATCCCGTACGCTGGGGAGAC 258
Isoform 1 ATTGACTCCTGGACCCAACTGTGACCGCTTCAAACTGCACATCCCGTACGCTGGGGAGAC 360
Isoform 5 ATTGACTCCTGGACCCAACTGTGACCGCTTCAAACTGCACATCCCGTACGCTGGGGAGAC 249
Isoform 2 GTTAAAATGGGACATAATTTTCAATGCTCAGTACCCAGAGCTGCCTCCTGATTTCATCTT 230
Isoform 3 --------GGGACATAATTTTCAATGCTCAGTACCCAGAGCTGCCTCCTGATTTCATCTT 153
Isoform 4 GTTAAAATGGGACATAATTTTCAATGCTCAGTACCCAGAGCTGCCTCCTGATTTCATCTT 318
Isoform 1 GTTAAAATGGGACATAATTTTCAATGCTCAGTACCCAGAGCTGCCTCCTGATTTCATCTT 420
Isoform 5 GTTAAAATGGGACATAATTTTCAATGCTCAGTACCCAGAGCTGCCTCCTGATTTCATCTT 309
Isoform 2 TGGAGAGGATGCTGAGTTTCTGCCAGACCCCTCTGCGCTGCACAACCTTGCCTCCTGGAA 290
Isoform 3 TGGAGAGGATGCTGAGTTTCTGCCAGACCCCTCTGCGCTGCACAACCTTGCCTCCTGGAA 213
Isoform 4 TGGAGAGGATGCTGAGTTTCTGCCAGACCCCTCTGCGCTGCACAACCTTGCCTCCTGGAA 378
Isoform 1 TGGAGAGGATGCTGAGTTTCTGCCAGACCCCTCTGCGCTGCACAACCTTGCCTCCTGGAA 480
Isoform 5 TGGAGAGGATGCTGAGTTTCTGCCAGACCCCTCTGCGCTGCACAACCTTGCCTCCTGGAA 369

```
Isoform 2    CCCTTCAAACCCTGAGTGCCTGTTGCTCGTGGTGAAGGAGCTGGTGCAGCAGTACCACCA 350
Isoform 3    CCCTTCAAACCCTGAGTGCCTGTTGCTCGTGGTGAAGGAGCTGGTGCAGCAGTACCACCA 273
Isoform 4    CCCTTCAAACCCTGAGTGCCTGTTGCTCGTGGTGAAGGAGCTGGTGCAGCAGTACCACCA 438
Isoform 1    CCCTTCAAACCCTGAGTGCCTGTTGCTCGTGGTGAAGGAGCTGGTGCAGCAGTACCACCA 540
Isoform 5    CCCTTCAAACCCTGAGTGCCTGTTGCTCGTGGTGAAGGAGCTGGTGCAGCAGTACCACCA 429
             ************************************************************

Isoform 2    GTTCCAGTGCGGCCGCCTCCGTGAGAGCTCGCGCCTCATGTTTGAGTACCAGACGCTCCT 410
Isoform 3    GTTCCAGTGCGGCCGCCTCCGTGAGAGCTCGCGCCTCATGTTTGAGTACCAGACGCTCCT 333
Isoform 4    GTTCCAGTGCGGCCGCCTCCGTGAGAGCTCGCGCCTCATGTTTGAGTACCAGACGCTCCT 498
Isoform 1    GTTCCAGTGCGGCCGCCTCCGTGAGAGCTCGCGCCTCATGTTTGAGTACCAGACGCTCCT 600
Isoform 5    GTTCCAGTGCGGCCGCCTCCGTGAGAGCTCGCGCCTCATGTTTGAGTACCAGACGCTCCT 489
             ************************************************************

Isoform 2    GGAAGAGCCTCAGTATGGAGAGAACATGGAAATTTATGCTGGAAAGAAAAACAACTGGAC 470
Isoform 3    GGAAGAGCCTCAGTATGGAGAGAACATGGAAATTTATGCTGGAAAGAAAAACAACTGGAC 393
Isoform 4    GGAAGAGCCTCAGTATGGAGAGAACATGGAAATTTATGCTGGAAAGAAAAACAACTGGAC 558
Isoform 1    GGAAGAGCCTCAGTATGGAGAGAACATGGAAATTTATGCTGGAAAGAAAAACAACTGGAC 660
Isoform 5    GGAAGAGCCTCAGTATGGAGAGAACATGGAAATTTATGCTGGAAAGAAAAACAACTGGAC 549
             ************************************************************

Isoform 2    TGGTGAATTTTCAGCTCGTTTTCTATTGAAGTTACCAGTAGATTTCAGCAACATTCCCAC 530
Isoform 3    TGGTGAATTTTCAGCTCGTTTTCTATTGAAGTTACCAGTAGATTTCAGCAACATTCCCAC 453
Isoform 4    TGGTGAATTTTCAGCTCGTTTTCTATTGAAGTTACCAGTAGATTTCAGCAACATTCCCAC 618
Isoform 1    TGGTGAATTTTCAGCTCGTTTTCTATTGAAGTTACCAGTAGATTTCAGCAACATTCCCAC 720
Isoform 5    TGGTGAATTTTCAGCTCGTTTTCTATTGAAGTTACCAGTAGATTTCAGCAACATTCCCAC 609
             ************************************************************

Isoform 2    ATACCTTCTCAAGGATGTAAATGAAGACCCTGGAGAAGATGTGGCCCTTCTTTCTGTCAG 590
Isoform 3    ATACCTTCTCAAGGATGTAAATGAAGACCCTGGAGAAGATGTGGCCCTTCTTTCTGTCAG 513
Isoform 4    ATACCTTCTCAAGGATGTAAATGAAGACCCTGGAGAAGATGTGGCCCTTCTTTCTGTCAG 678
Isoform 1    ATACCTTCTCAAGGATGTAAATGAAGACCCTGGAGAAGATGTGGCCCTTCTTTCTGTCAG 780
Isoform 5    ATACCTTCTCAAGGATGTAAATGAAGACCCTGGAGAAGATGTGGCCCTTCTTTCTGTCAG 669
             ************************************************************

Isoform 2    TTTTGAGGATACTGAAGCTACCCAGGTGTACCCCAAGTTGTACTTGTCACCCCGAATTGA 650
Isoform 3    TTTTGAGGATACTGAAGCTACCCAGGTGTACCCCAAGTTGTACTTGTCACCCCGAATTGA 573
Isoform 4    TTTTGAGGATACTGAAGCTACCCAGGTGTACCCCAAGTTGTACTTGTCACCCCGAATTGA 738
Isoform 1    TTTTGAGGATACTGAAGCTACCCAGGTGTACCCCAAGTTGTACTTGTCACCCCGAATTGA 840
Isoform 5    TTTTGAGGATACTGAAGCTACCCAGGTGTACCCCAAGTTGTACTTGTCACCCCGAATTGA 729
             ************************************************************

Isoform 2    GCATGCACTCGGAGGCTCCTCTGCTCTTCACATCCCTGCTTTCCCCGGAGGAGGATGTCT 710
Isoform 3    GCATGCACTCGGAGGCTCCTCTGCTCTTCACATCCCTGCTTTCCCCGGAGGAGGATGTCT 633
Isoform 4    GCATGCACTCGGAGGCTCCTCTGCTCTTCACATCCCTGCTTTCCCCGGAGGAGGATGTCT 798
Isoform 1    GCATGCACTCGGAGGCTCCTCTGCTCTTCACATCCCTGCTTTCCCCGGAGGAGGATGTCT 900
Isoform 5    GCATGCACTCGGAGGCTCCTCTGCTCTTCACATCCCTGCTTTCCCCGGAGGAGGATGTCT 789
             ************************************************************

Isoform 2    CATTGATTATGTGCCTCAAGTGTGCCACCTGCTCACCAACAAGGTACAGTATGTGATTCA 770
Isoform 3    CATTGATTATGTGCCTCAAGTGTGCCACCTGCTCACCAACAAGGTACAGTATGTGATTCA 693
Isoform 4    CATTGATTATGTGCCTCAAGTGTGCCACCTGCTCACCAACAAGGTACAGTATGTGATTCA 858
Isoform 1    CATTGATTATGTGCCTCAAGTGTGCCACCTGCTCACCAACAAGGTACAGTATGTGATTCA 960
Isoform 5    CATTGATTATGTGCCTCAAGTGTGCCACCTGCTCACCAACAAGGTACAGTATGTGATTCA 849
             ************************************************************
```

```
Isoform 2    AGGCTATCACAAAAGAAGAGAGTACATCGCAGCTTTCCTCAGTCACTTTGGCACAGGTGT 830
Isoform 3    AGGCTATCACAAAAGAAGAGAGTACATCGCAGCTTTCCTCAGTCACTTTGGCACAGGTGT 753
Isoform 4    AGGCTATCACAAAAGAAGAGAGTACATCGCAGCTTTCCTCAGTCACTTTGGCACAGGTGT 918
Isoform 1    AGGCTATCACAAAAGAAGAGAGTACATCGCAGCTTTCCTCAGTCACTTTGGCACAGGTGT 1020
Isoform 5    AGGCTATCACAAAAGAAGAGAGTACATCGCAGCTTTCCTCAGTCACTTTGGCACAGGTGT 909
             ************************************************************

Isoform 2    CGTGGAATATGATGCAGAAGGCTTCACAAAACTTACTCTGCTGCTGATGTGGAAAGACTT 890
Isoform 3    CGTGGAATATGATGCAGAAGGCTTCACAAAACTTACTCTGCTGCTGATGTGGAAAGACTT 813
Isoform 4    CGTGGAATATGATGCAGAAGGCTTCACAAAACTTACTCTGCTGCTGATGTGGAAAGACTT 978
Isoform 1    CGTGGAATATGATGCAGAAGGCTTCACAAAACTTACTCTGCTGCTGATGTGGAAAGACTT 1080
Isoform 5    CGTGGAATATGATGCAGAAGGCTTCACAAAACTTACTCTGCTGCTGATGTGGAAAGACTT 969
             ************************************************************

Isoform 2    TTGTTTTCTTGTCCACATTGACCTGCCCCTGTTTTTCCCTCGAGATCAGCCTACGCTCAC 950
Isoform 3    TTGTTTTCTTGTCCACATTGACCTGCCCCTGTTTTTCCCTCGAGATCAGCCTACGCTCAC 873
Isoform 4    TTGTTTTCTTGTCCACATTGACCTGCCCCTGTTTTTCCCTCGAGATCAGCCTACGCTCAC 1038
Isoform 1    TTGTTTTCTTGTCCACATTGACCTGCCCCTGTTTTTCCCTCGAGATCAGCCTACGCTCAC 1140
Isoform 5    TTGTTTTCTTGTCCACATTGACCTGCCCCTGTTTTTCCCTCGAGATCAGCCTACGCTCAC 1029
             ************************************************************

Isoform 2    ATTTCAGTCAGTCTATCACTTTACCAACAGTGGACAGCTTTACTCCCAAGCACAAAAAAA 1010
Isoform 3    ATTTCAGTCAGTCTATCACTTTACCAACAGTGGACAGCTTTACTCCCAAGCACAAAAAAA 933
Isoform 4    ATTTCAGTCAGTCTATCACTTTACCAACAGTGGACAGCTTTACTCCCAAGCACAAAAAAA 1098
Isoform 1    ATTTCAGTCAGTCTATCACTTTACCAACAGTGGACAGCTTTACTCCCAAGCACAAAAAAA 1200
Isoform 5    ATTTCAGTCAGTCTATCACTTTACCAACAGTGGACAGCTTTACTCCCAAGCACAAAAAAA 1089
             ************************************************************

Isoform 2    CTACCCATACAGCCCCAGATGGGATGGAAATGAAATGGCCAAGAGAGCAAAGGCTTATTT 1070
Isoform 3    CTACCCATACAGCCCCAGATGGGATGGAAATGAAATGGCCAAGAGAGCAAAGGCTTATTT 993
Isoform 4    CTACCCATACAGCCCCAGATGGGATGGAAATGAAATGGCCAAGAGAGCAAAGGCTTATTT 1158
Isoform 1    CTACCCATACAGCCCCAGATGGGATGGAAATGAAATGGCCAAGAGAGCAAAGGCTTATTT 1260
Isoform 5    CTACCCATACAGCCCCAGATGGGATGGAAATGAAATGGCCAAGAGAGCAAAGGCTTATTT 1149
             ************************************************************

Isoform 2    CAAAACCTTTGTCCCTCAGTTCCAGGAGGCCGCATTTGCCAATGGAAAGCTCTAGGAAAC 1130
Isoform 3    CAAAACCTTTGTCCCTCAGTTCCAGGAGGCCGCATTTGCCAATGGAAAGCTCTAGGAAAC 1053
Isoform 4    CAAAACCTTTGTCCCTCAGTTCCAGGAGGCCGCATTTGCCAATGGAAAGCTCTAGGAAAC 1218
Isoform 1    CAAAACCTTTGTCCCTCAGTTCCAGGAGGCCGCATTTGCCAATGGAAAGCTCTAGGAAAC 1320
Isoform 5    CAAAACCTTTGTCCCTCAGTTCCAGGAGGCCGCATTTGCCAATGGAAAGCTCTAGGAAAC 1209
             ************************************************************

Isoform 2    ACCAGTGCTGAGAGGCGGCCAACCAGACTGCTCAGTCCACATGCGTGTCAGCGCTCGGGC 1190
Isoform 3    ACCAGTGCTGAGAGGCGGCCAACCAGACTGCTCAGTCCACATGCGTGTCAGCGCTCGGGC 1113
Isoform 4    ACCAGTGCTGAGAGGCGGCCAACCAGACTGCTCAGTCCACATGCGTGTCAGCGCTCGGGC 1278
Isoform 1    ACCAGTGCTGAGAGGCGGCCAACCAGACTGCTCAGTCCACATGCGTGTCAGCGCTCGGGC 1380
Isoform 5    ACCAGTGCTGAGAGGCGGCCAACCAGACTGCTCAGTCCACATGCGTGTCAGCGCTCGGGC 1269
             ************************************************************

Isoform 2    TGCTTGCTGGAAACTGCTCGGAATGTCTTC 1220
Isoform 3    TGCTTGCTGGAAACTGCTCGGAATGTCTTC 1143
Isoform 4    TGCTTGCTGGAAACTGCTCGGAATGTCTTC 1308
Isoform 1    TGCTTGCTGGAAACTGCTCGGAATGTCTTC 1410
Isoform 5    TGCTTGCTGGAAACTGCTCGGAATGTCTTC 1299
             ******************************
```

Figure 7.

Semi-quantitative RT-PCR analysis determining the types of *Bre* isoforms expressed by cultured interdigital cells (left), interdigital tissues (middle) and adult heart tissues (right). The interdigital cells were digested from interdigital tissues isolated from hindlimbs of E12.5 mouse embryos and further cultured for 24 hours. The interdigital tissues were isolated from hindlimbs of E12.5 mouse embryos. The result showed that *Bre* isoform 5 was the major transcripts expressed by interdigital cells and interdigital tissues. Transcripts of other isoforms remained at undetected level. Transcripts of isoform 2, 4 and 5 were detected in adult mouse heart tissues. *β-actin* served as an internal control.

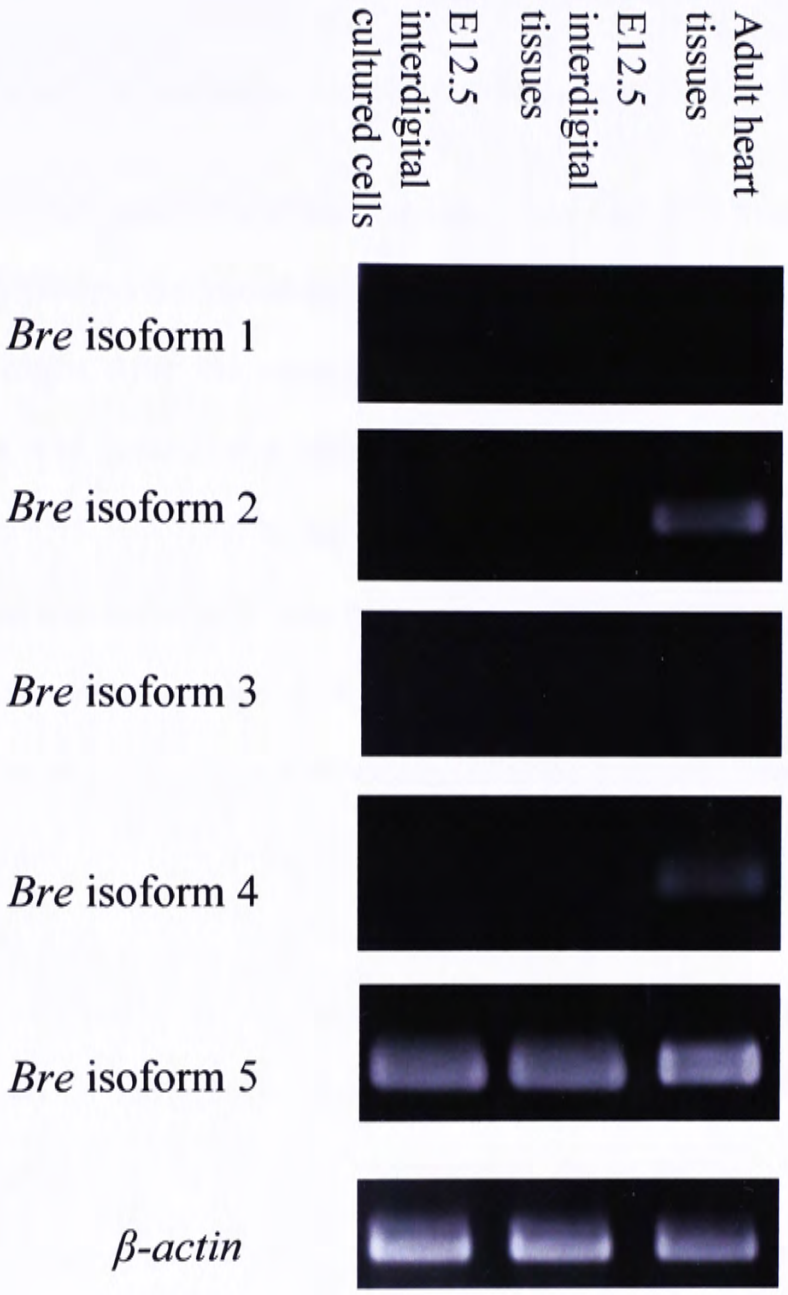
Adult heart tissues
E12.5 interdigital tissues
E12.5 interdigital cultured cells
Bre isoform 1
Bre isoform 2
Bre isoform 3
Bre isoform 4
Bre isoform 5
β-actin

3.3 Silencing of *Bre* expression by siRNA in interdigital cells

Primary interdigital cell culture was established from E12.5 hindlimb interdigital tissues excised between the second and the third digits and from those between the third and the forth digits. After the interdigital cells had been cultured for 24 hours, *Bre*-specific siRNA was transfected to silence *Bre* expression in the interdigital cells while GFP-specific siRNA was used in the control culture. Forty-eight hours after the first transfection, the interdigital cells were harvested and *Bre* expression in experimental and control cultures were established by semi-quantitative RT-PCR (Figure 8). *Bre* expression in the experimental culture was significantly decreased compared with that in the control culture. *β-actin* expression served as an internal control of the experiment. The result was analyzed statistically. *Bre* expression in the GFP-siRNA-transfected culture was normalized to one. *Bre* expression in the *Bre*-siRNA-transfected culture was suppressed to around 30% of that in control culture. As a result, the *Bre*-specific siRNA was able to significantly suppress the expression of *Bre* in our primary culture system. Hence, the *Bre*-siRNA and GFP-siRNA could be used in our comparative proteomic study, where we compared the protein profile of interdigital cells that expressed *Bre* with those that did not.

Figure 8.

Semi-quantitative RT-PCR analysis of *Bre* mRNA level in E12.5 interdigital cells that were transfected with either *Bre*-specific siRNA or GFP-specific siRNA. E12.5 interdigital cells were harvested 48 hours after siRNA transfection. Double transfection was performed in which the second transfection was done at 24 hours after the first transfection. (A) The result of RT-PCR showed that *Bre* expression was significantly down-regulated by the *Bre*-specific siRNA. Expression of *β-actin* served as an internal control. (B) The ratio of *Bre* expression level in GFP-siRNA-treated culture to *Bre* expression level in *Bre*-siRNA-treated culture. For the ease of illustration, the *Bre* expression level in GFP-siRNA-treated group was made up to 1.000. The *Bre* mRNA level in each group was normalized by its corresponding *β-actin* expression level. Value for each group is shown as mean ± SE. Asterisk represents $p<0.05$.

A

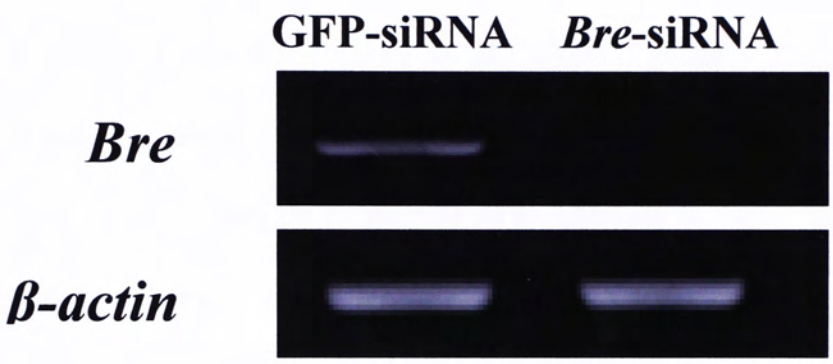
GFP-siRNA
Bre-siRNA
Bre
β-actin

B

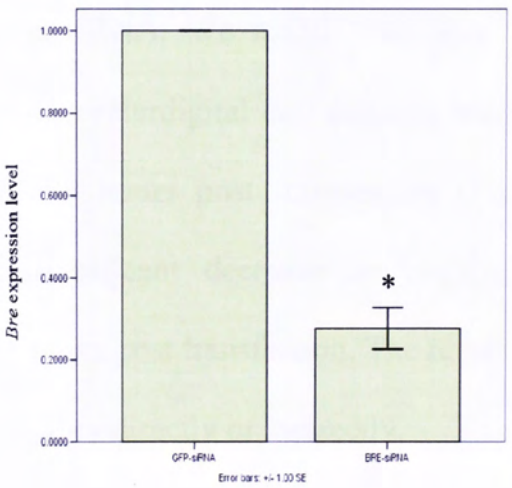
1.0000
0.8000
0.6000
0.4000
0.2000
0.0000
Bre expression level
*
GFP-siRNA
BRE-siRNA
Error bars: +/- 1.00 SE

3.4 Effect on viability of *Bre*-silenced interdigital cells by siRNA

BRE has been demonstrated its anti-apoptotic activity in various cancer cells (Li et al., 2004). Apoptosis in interdigital tissues is the major process of digit separation during development (Mori et al., 1995). In this sense, I proposed that BRE may also play an anti-apoptotic role in interdigital cells during limb development. In chapter 3.1, the result of RT-PCR revealed that *Bre* expression in E12.5 interdigital tissues was higher than that in E13.5 interdigital tissues. Notably, interdigital apoptosis starts at E13.5 and ends at E15.5 (Tang et al., 2000). It is worthy to investigate whether decrease in *Bre* expression along the occurrence of interdigital cell death relates to the anti-apoptotic property of BRE. In my study, I established *Bre* silencing in the interdigital cultured cells. Using this system, I set out MTT assay to investigate the effect on viability of *Bre*-silenced interdigital cells caused by siRNA. We found that there was no significant difference in cell viability between the interdigital cell cultures transfected either with *Bre*-siRNA or GFP-siRNA before 39 hours post transfection (Figure 9). However, comparing with control culture, significant decrease in viability of *Bre*-silenced interdigital cells was observed at 48 hours post transfection. The result suggests that BRE may play a role in regulating cell viability directly or indirectly.

Figure 9.

Effect on viability of *Bre*-silenced interdigital cells by siRNA. Cell viabilities of untransfected cells and cells transfected with either *Bre*-siRNA or GFP-siRNA or RNAiFect Reagent (Control) were measured by MTT assay. MTT was added to the medium at different time points and incubated for four hours at 37°C with 5%CO_2 in the humidified chamber. Culture medium was removed and DMSO solvent was then added to solubilize formazan crystal. Soluble formazan was quantified by a kinetic microplate reader measuring the absorbance at 595nm. Readings of each group at time zero was normalized to 100%. Each group of data consisted of three replicates. The result was analyzed by Kruskal Wallis test. The viability of *Bre*-siRNA treated cells significantly was lower than that of GFP-siRNA treated cells and those of two other groups. Asterisk represents $p<0.05$.

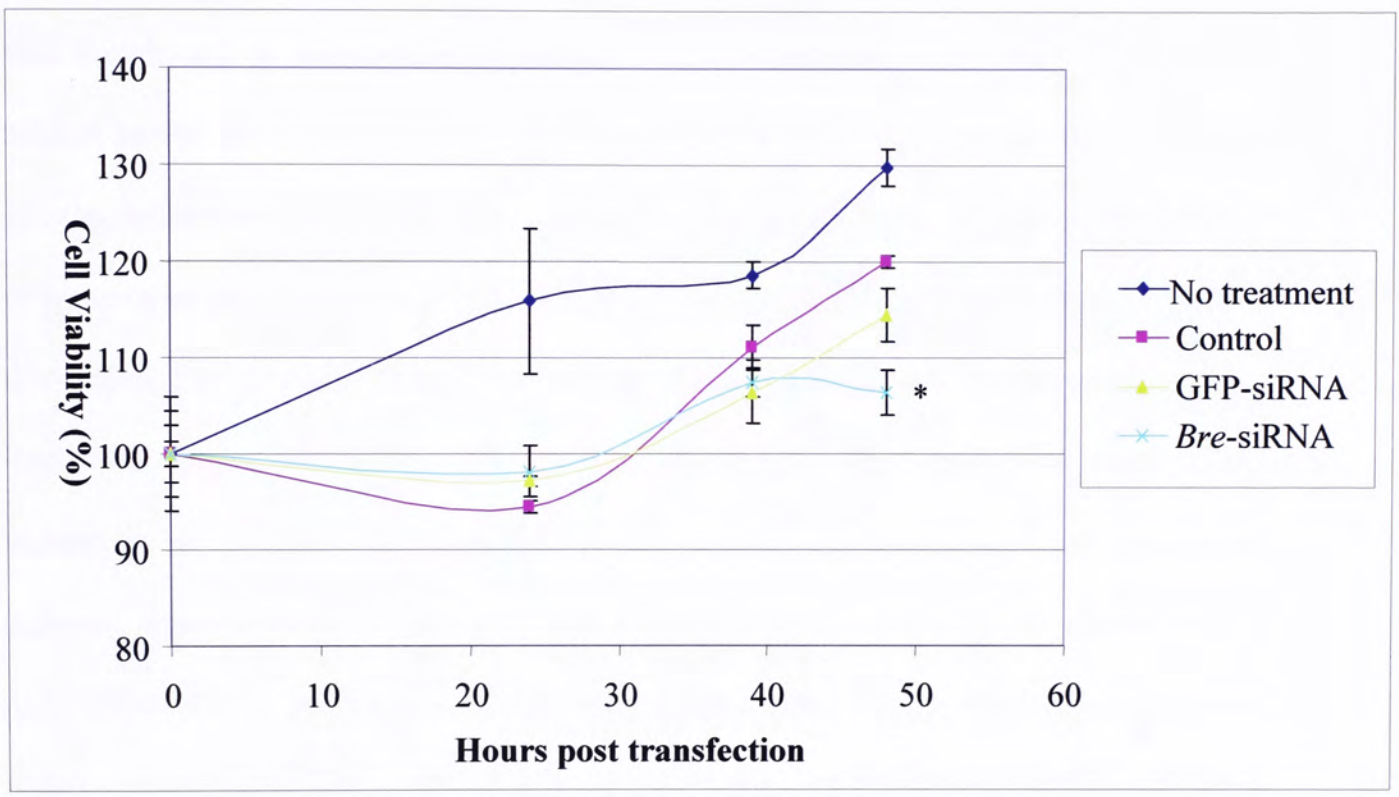
140
130
120
110
100
90
80
Cell Viability (%)
0
10
20
30
40
50
60
Hours post transfection
*
No treatment
Control
GFP-siRNA
Bre-siRNA

3.5 Comparative proteomic profile of *Bre*-silenced interdigital cultured cells

After the GFP-siRNA and *Bre*-siRNA had been shown to work properly on the primary interdigital cultures, we decided to analyze these cultures by comparative proteomic analysis. E12.5 interdigital cells were dissociated from hindlimb interdigital tissues and plated onto culture dishes. After culturing for 24 hours, *Bre*-specific siRNA was transfected to silence *Bre* expression in the interdigital cells while GFP-specific siRNA served as a control. Forty-eight hours after the first transfection, the interdigital cells were harvested and lysed. Protein assay was then performed to quantify the amount of proteins in the cell lysate. Equal amount of proteins in each group was loaded to first-dimension IEF. Proteins were separated by their pI values. After that, proteins were loaded to second-dimension SDS-PAGE, separated by their molecular weights and stained by silver nitrate solution. The protein profiles of *Bre*-silenced and unsilenced cultures were revealed in the 2-D gels (Figure 10, 11). Each figure shown was a representative 2-D gel from two independent experiments. The expression patterns were highly reproducible. The protein profiles between the two groups were compared using The Discovery series, PDQuest 2D Analysis Software (Bio Rad) Version 7.13 PC. Grids were added onto the image of the control gel to enhance identification of protein spots (Figure 12). The location and SSP number of the protein spots analyzed are shown in magnified gel images with the grids (Figures 13 – 21). The intensity measurement of each protein spot was compared between experimental and control group. A quantitative graph report across the groups was generated and sorted by SPP number (Figure 22 – 25).

The protein spots that were differential expressed across the experimental and control groups were picked and identified by MALDI-TOF mass spectrometry.

Figure 10.

Representative two-dimensional electrophoresis of proteins extracted from E12.5 interdigital cells that had been transfected with *Bre*-specific siRNA. The proteins were separated on the basis of pI (x-axis) and molecular weight (y-axis).

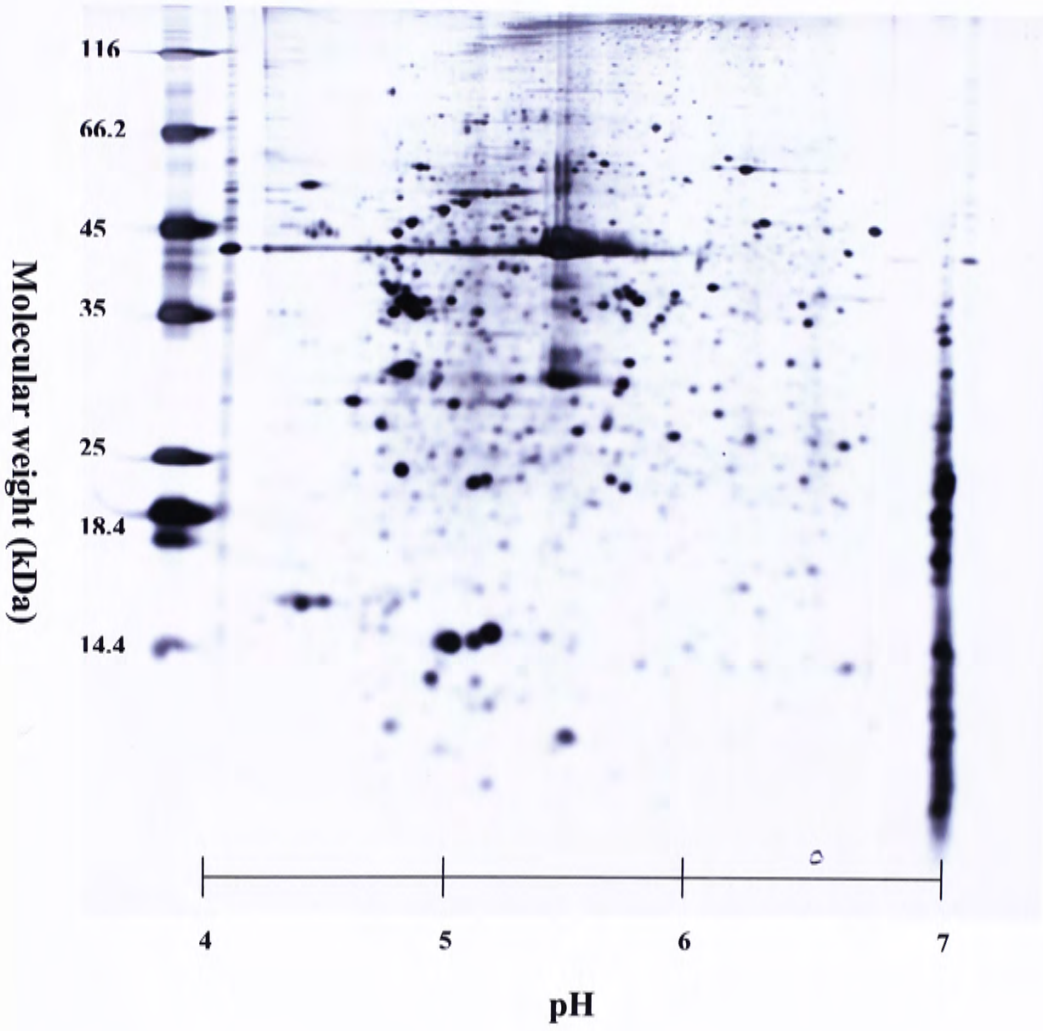
116
66.2
45
35
25
18.4
14.4
Molecular weight (kDa)
4
5
6
7
pH

Figure 11.

Representative two-dimensional electrophoresis of proteins extracted from E12.5 interdigital cells that had been transfected with GFP-specific siRNA. The proteins were separated on the basis of pI (x-axis) and molecular weight (y-axis).

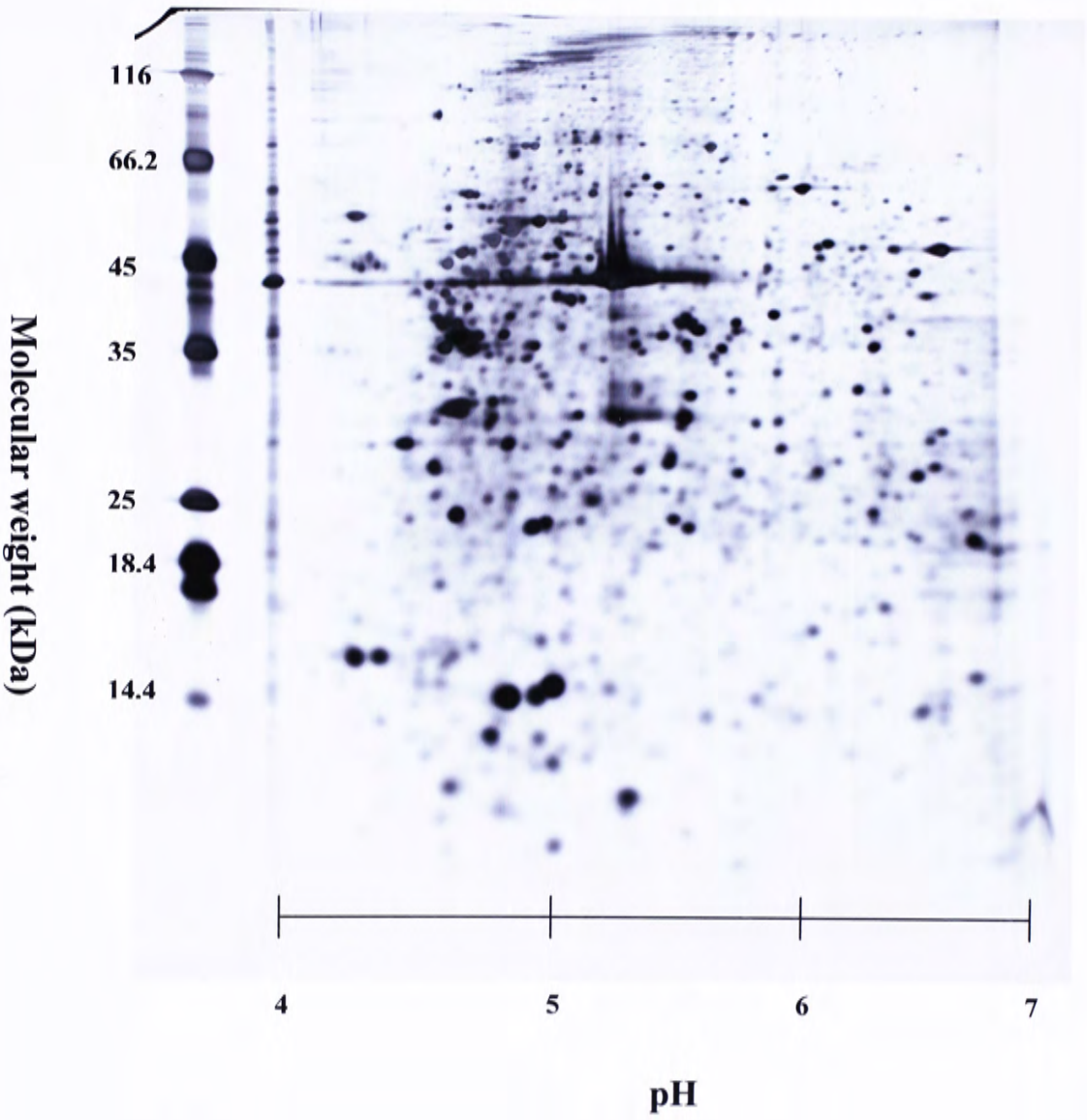
116
66.2
45
35
25
18.4
14.4
Molecular weight (kDa)
4
5
6
7
pH

Figure 12.

Representative two-dimensional electrophoresis of proteins extracted from E12.5 interdigital cells that had been transfected with GFP-specific siRNA. Grids were added onto the gel image for the ease of localizing and identifying protein spots.

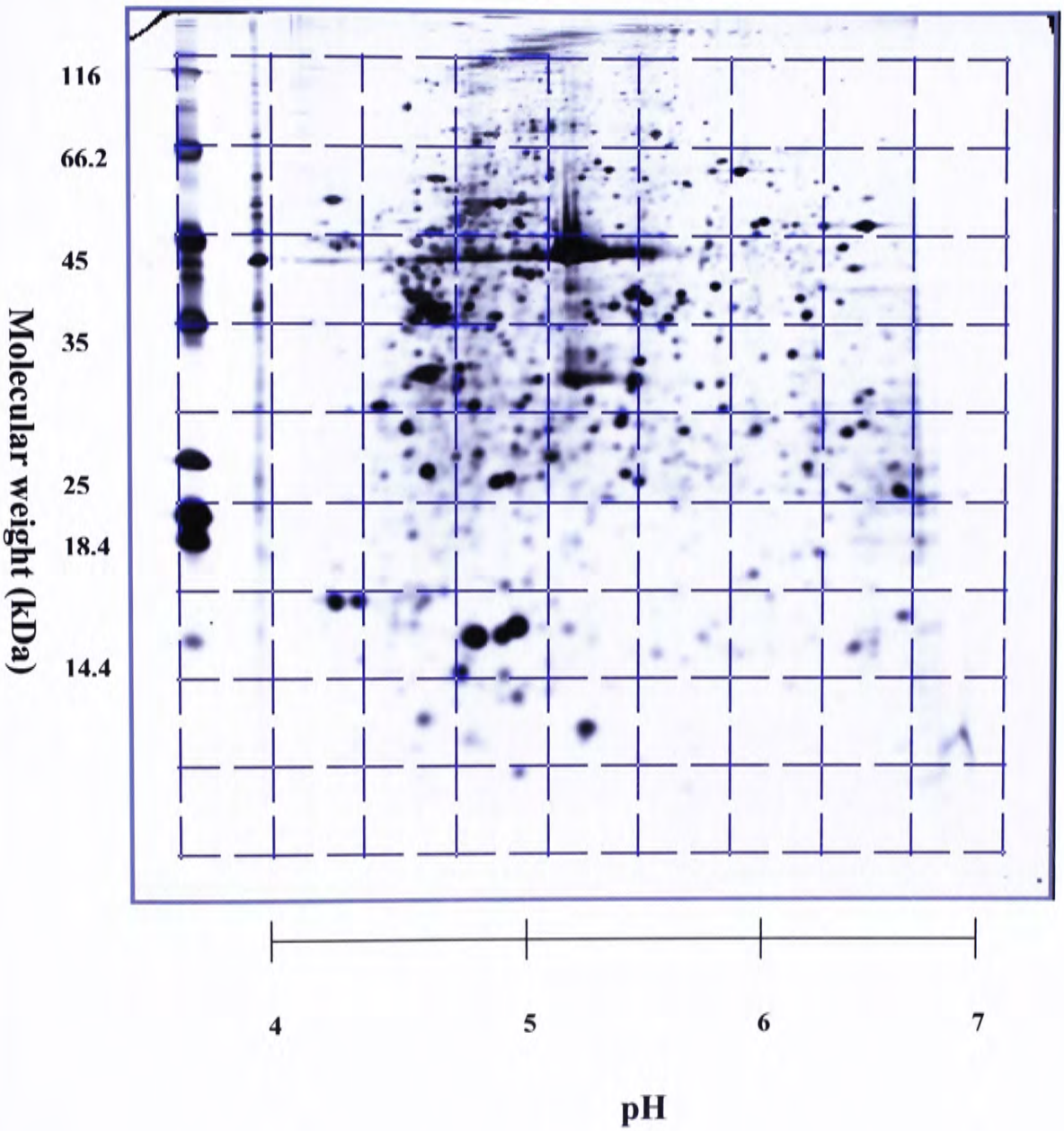
116
66.2
45
35
25
18.4
14.4
Molecular weight (kDa)
4
5
6
7
pH

Figure 13.

Upper left portion of magnified gel image of representative two-dimensional electrophoresis of proteins extracted from E12.5 interdigital cells that had been transfected with GFP-specific siRNA. Each analyzed protein spot was assigned with a spot SSP number for identification.

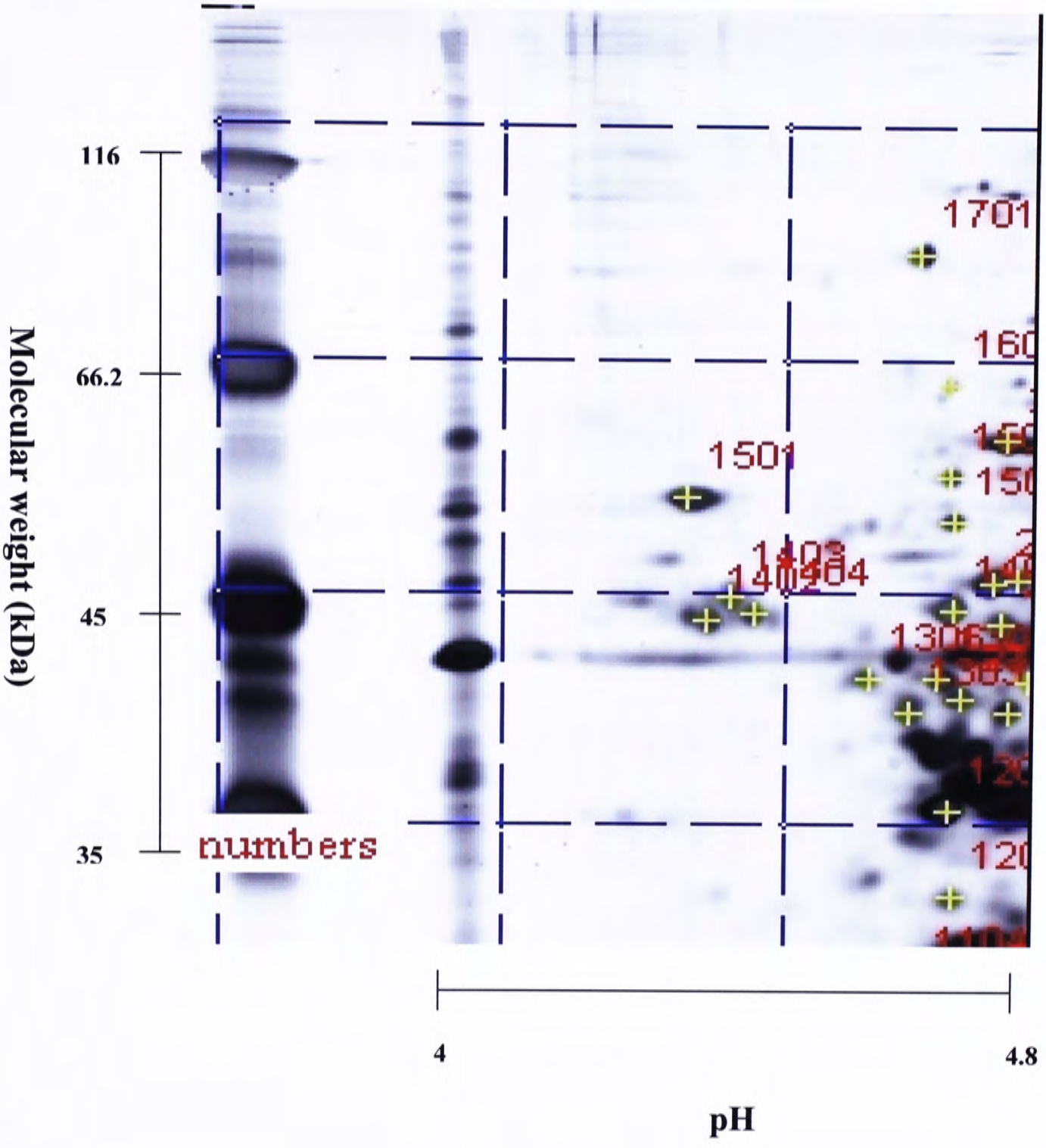
116
66.2
45
35
Molecular weight (kDa)
numbers
1701
1501
4
4.8
pH

Figure 14.

Upper middle portion of magnified gel image of representative two-dimensional electrophoresis of proteins extracted from E12.5 interdigital cells that had been transfected with GFP-specific siRNA. Each analyzed protein spot was assigned with a spot SSP number for identification.

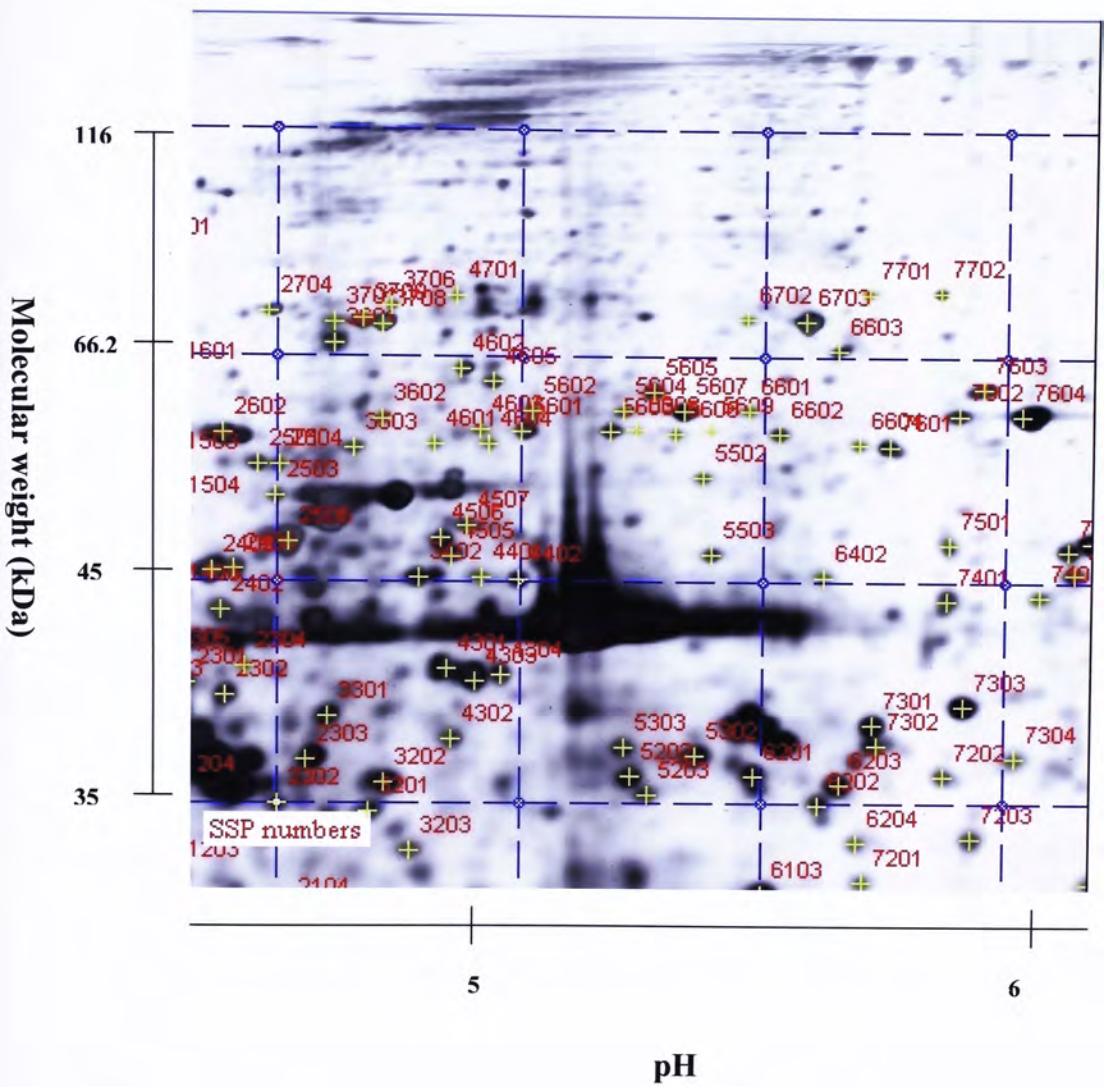
116
66.2
45
35
Molecular weight (kDa)
SSP numbers
5
6
pH

Figure 15.

Upper right portion of magnified gel image of representative two-dimensional electrophoresis of proteins extracted from E12.5 interdigital cells that had been transfected with GFP-specific siRNA. Each analyzed protein spot was assigned with a spot SSP number for identification.

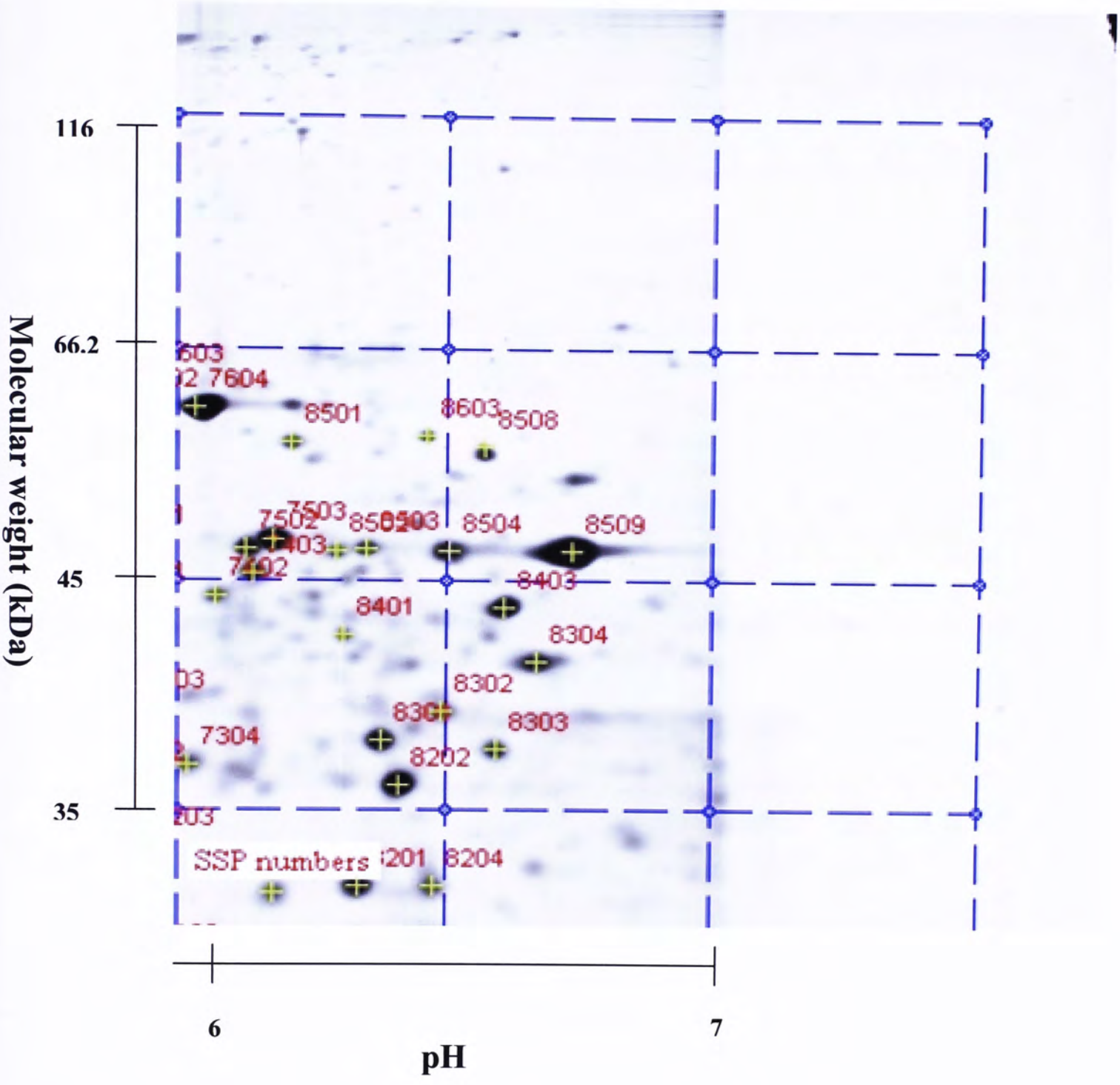
116
66.2
45
35
Molecular weight (kDa)
8501
8603
8508
8504
8509
8403
8401
8304
8302
8303
7304
8202
SSP numbers
6
7
pH

Figure 16.

Middle left portion of magnified gel image of representative two-dimensional electrophoresis of proteins extracted from E12.5 interdigital cells that had been transfected with GFP-specific siRNA. Each analyzed protein spot was assigned with a spot SSP number for identification.

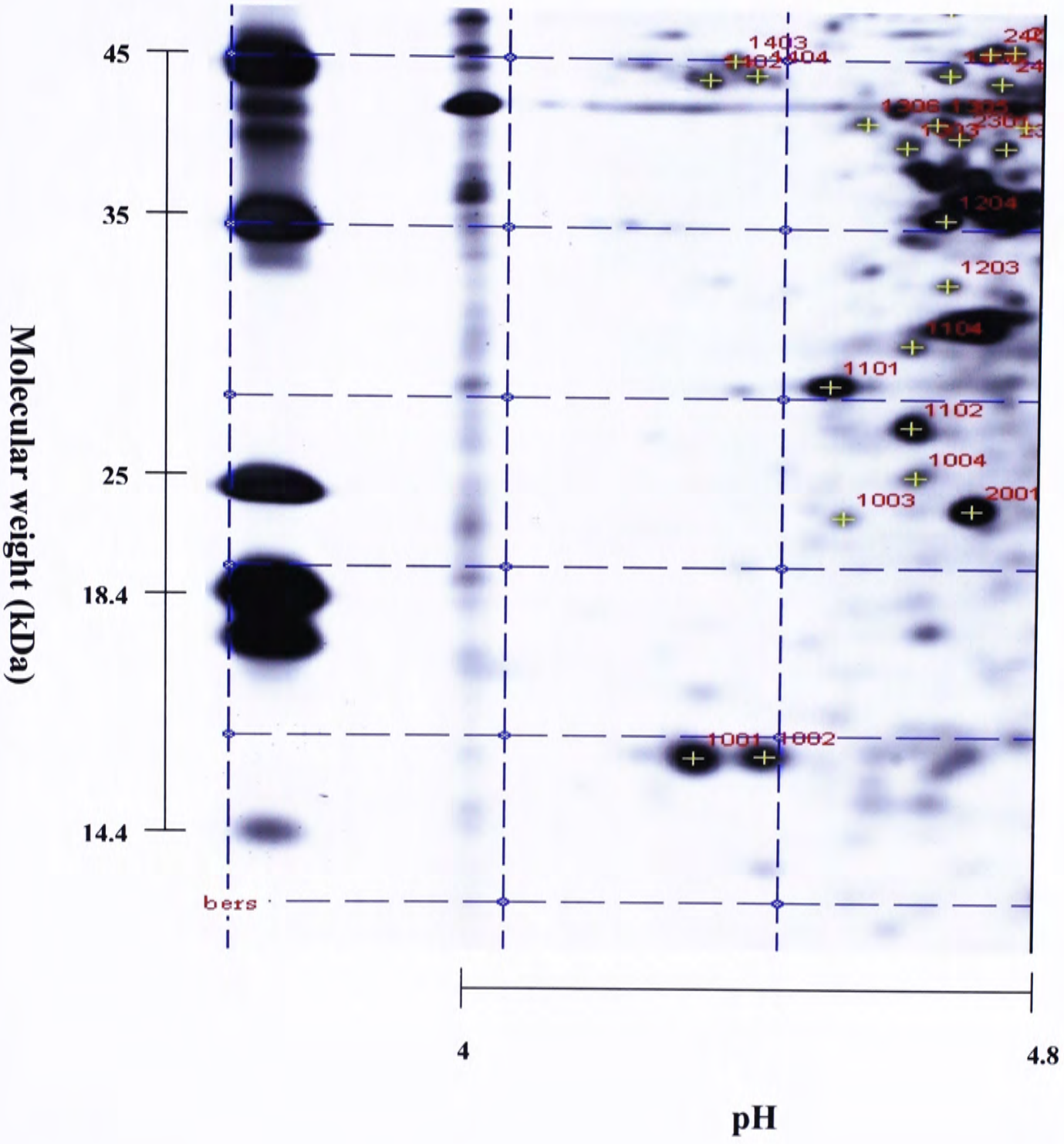
45
35
25
18.4
14.4
Molecular weight (kDa)
1403
1204
1203
1104
1101
1102
1004
1003
2001
1001
1002
4
4.8
pH

Figure 17.

Middle portion of magnified gel image of representative two-dimensional electrophoresis of proteins extracted from E12.5 interdigital cells that had been transfected with GFP-specific siRNA. Each analyzed protein spot was assigned with a spot SSP number for identification.

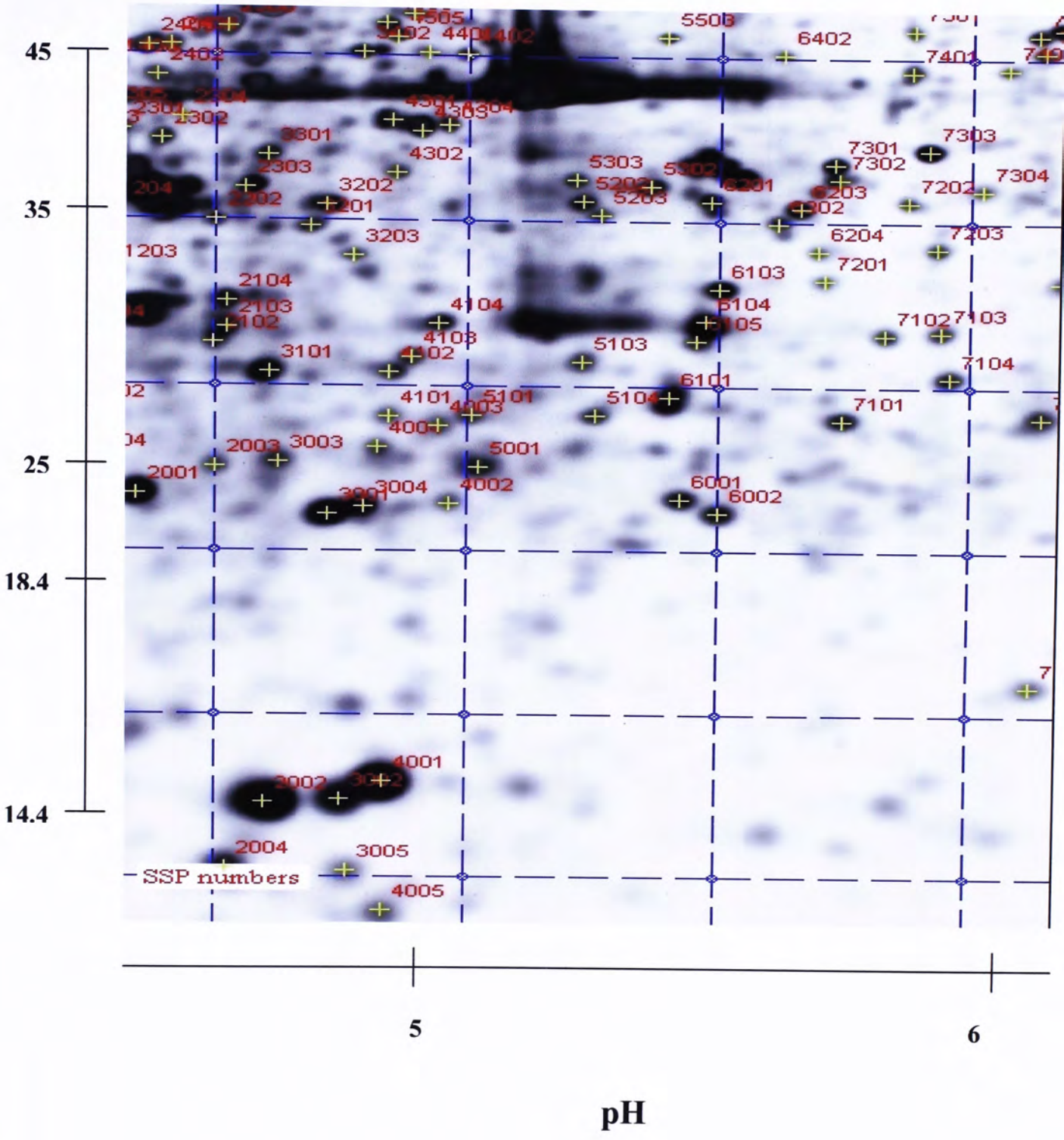
45
35
25
18.4
14.4
Molecular weight (kDa)
5
6
pH
SSP numbers
2001
2002
2003
2004
3001
3002
3003
3004
3005
4001
4002
4003
4004
4005
5001
6001
6002
6103
6104
6204
7101
7102
7103
7104
7201
7202
7203
7301
7302
7303
7304
7401

Figure 18.

Middle right portion of magnified gel image of representative two-dimensional electrophoresis of proteins extracted from E12.5 interdigital cells that had been transfected with GFP-specific siRNA. Each analyzed protein spots was assigned with a spot SSP number for identification.

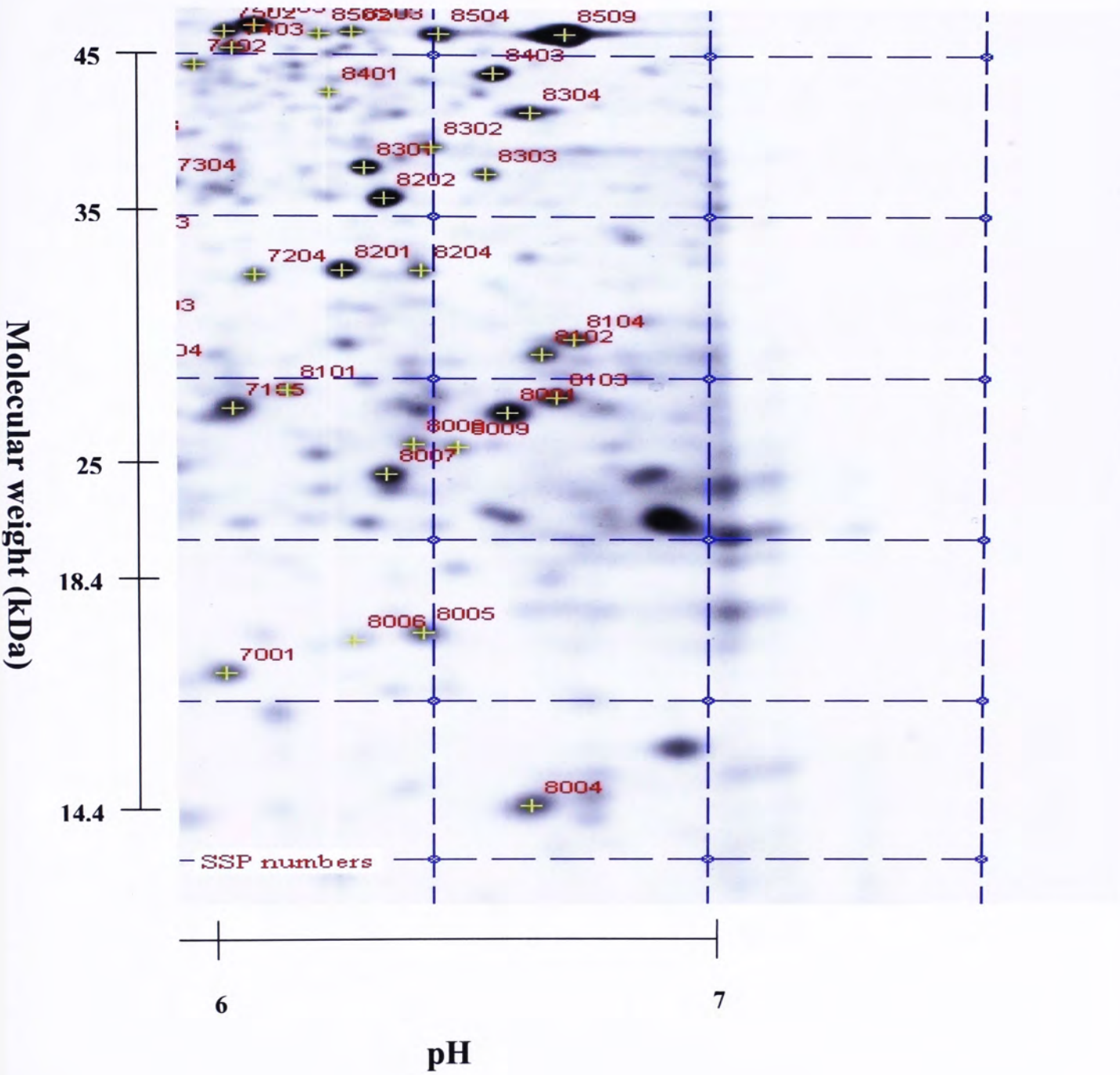
Molecular weight (kDa)
45
35
25
18.4
14.4
8504
8509
8403
8401
8304
8302
8303
8202
7304
7204
8201
8204
8104
8101
8103
8009
8007
8006
8005
7001
8004
SSP numbers
6
7
pH

Figure 19.

Lower left portion of magnified gel image of representative two-dimensional electrophoresis of proteins extracted from E12.5 interdigital cells that had been transfected with GFP-specific siRNA. Each analyzed protein spot was assigned with a spot SSP number for identification.

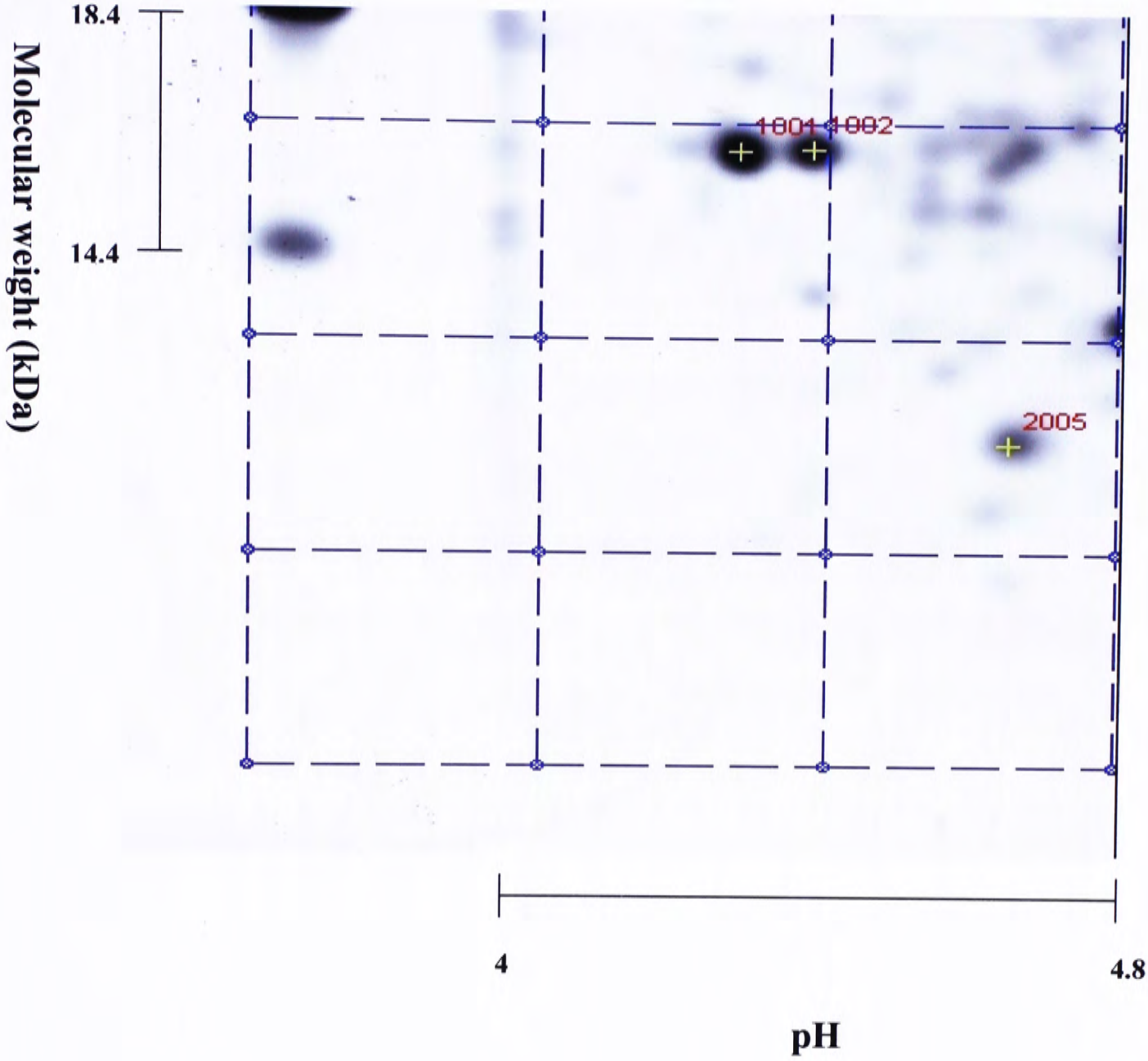
18.4
14.4
Molecular weight (kDa)
1001
1002
2005
4
4.8
pH

Figure 20.

Lower middle portion of magnified gel image of representative two-dimensional electrophoresis of proteins extracted from E12.5 interdigital cells that had been transfected with GFP-specific siRNA. Each analyzed protein spot was assigned with a spot SSP number for identification.

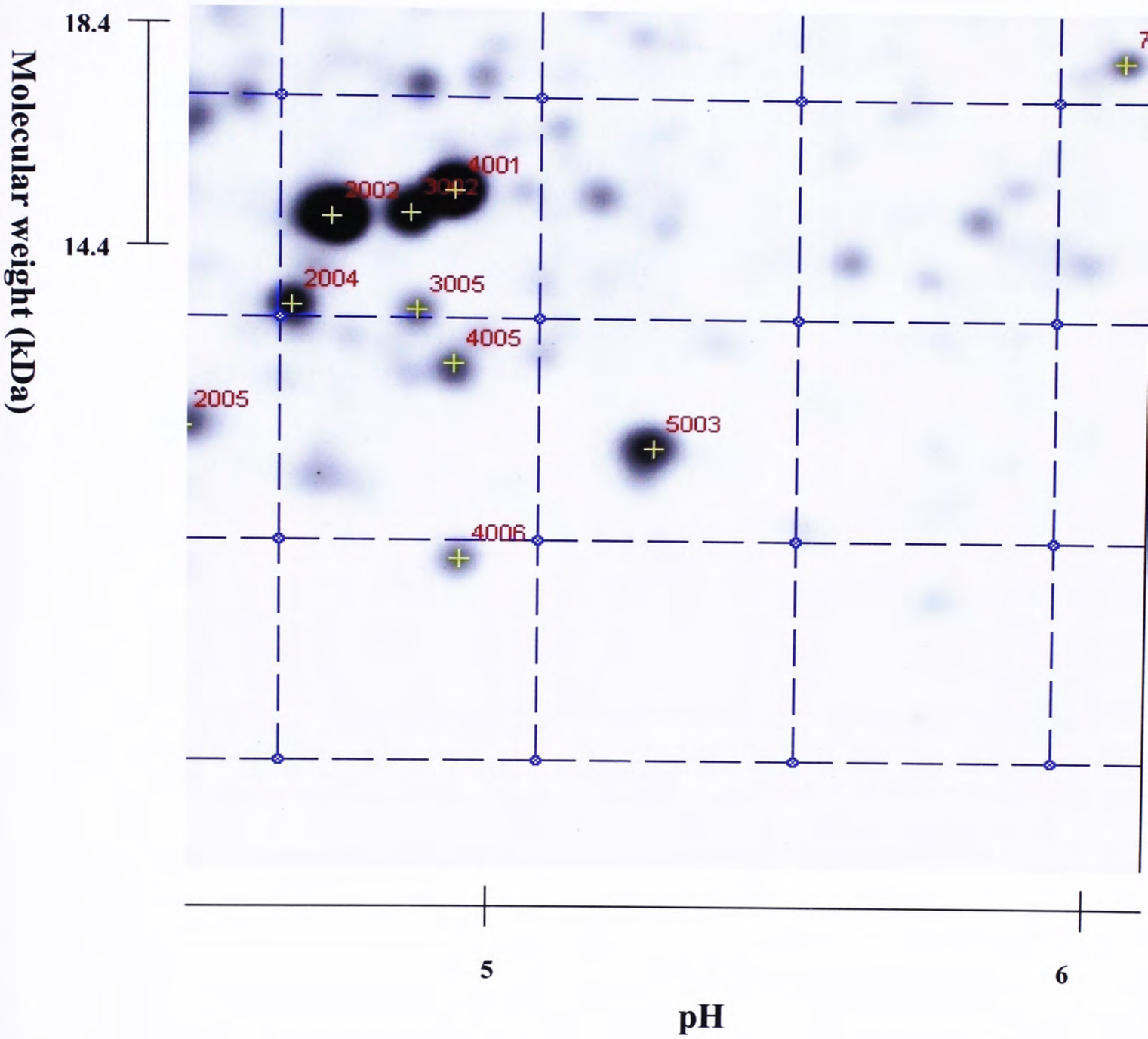
18.4
14.4
Molecular weight (kDa)
4001
2002
3002
2004
3005
4005
2005
5003
4006
5
6
pH

Figure 21.

Lower right portion of magnified gel image of representative two-dimensional electrophoresis of proteins extracted from E12.5 interdigital cells that had been transfected with GFP-specific siRNA. Each analyzed protein spot was assigned with a spot SSP number for identification.

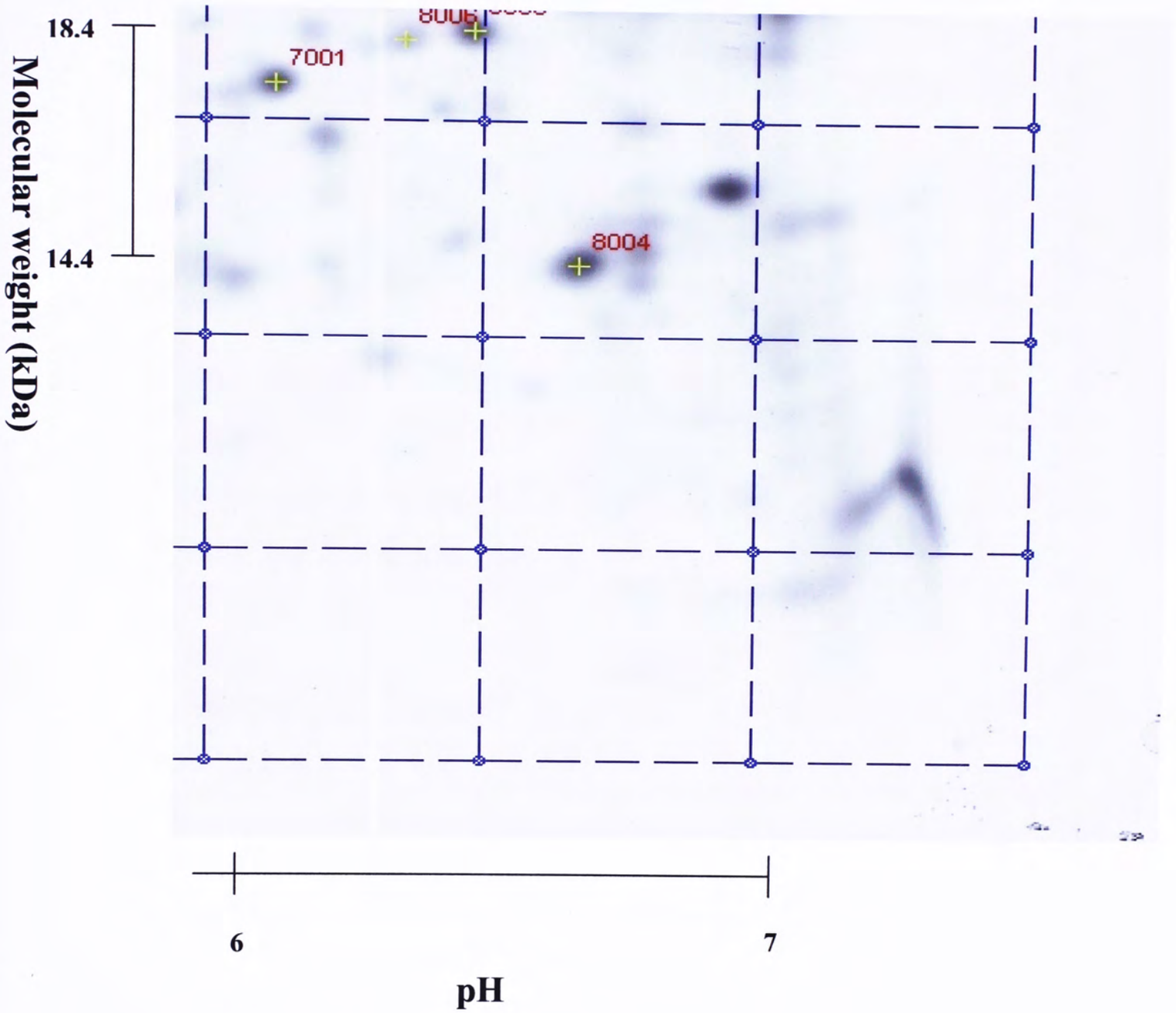
18.4
14.4
Molecular weight (kDa)
7001
8004
6
7
pH

Figure 22.

A quantity graph report showing the comparison of spot intensity of each analyzed spot across group (SSP 1001 – SSP3201). The SSP number is the number assigned to each analyzed protein spot for identification purpose. In each graph, the height of the bar represents the relative expression level of the protein spots analyzed in GFP-siRNA- and *Bre*-siRNA-treated group (from left to right).

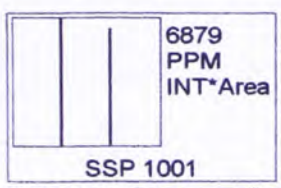

SSP 1001

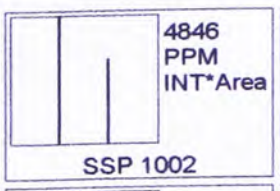

SSP 1002

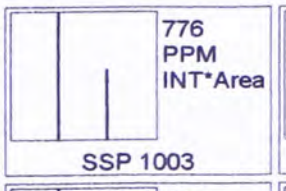

SSP 1003

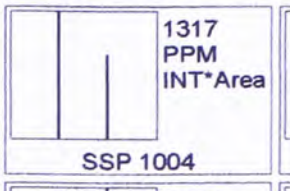

SSP 1004

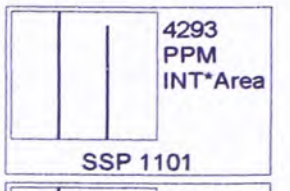

SSP 1101

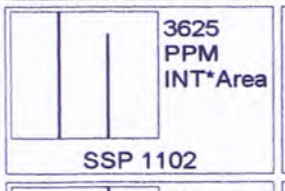

SSP 1102

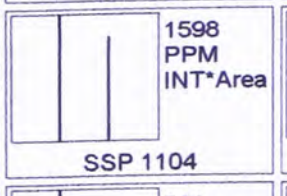

SSP 1104

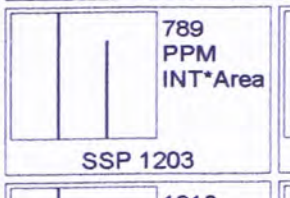

SSP 1203

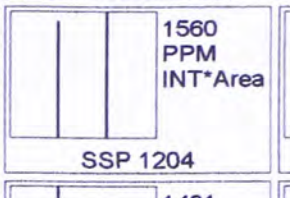

SSP 1204

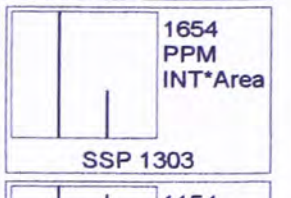

SSP 1303

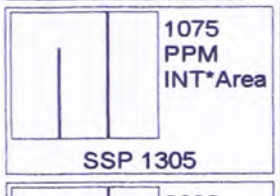

SSP 1305

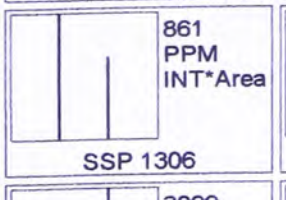

SSP 1306

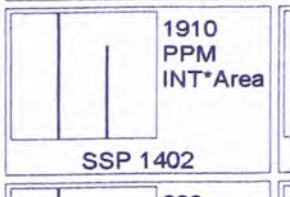

SSP 1402

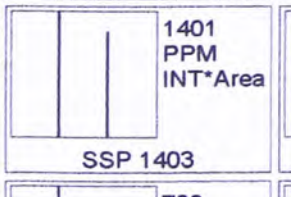

SSP 1403

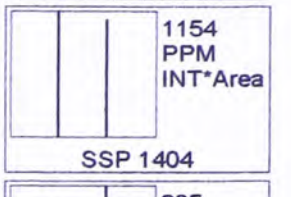

SSP 1404

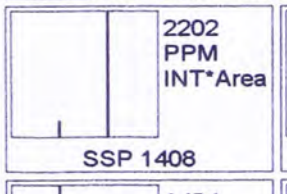

SSP 1408

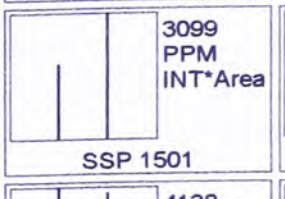

SSP 1501

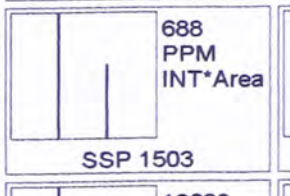

SSP 1503

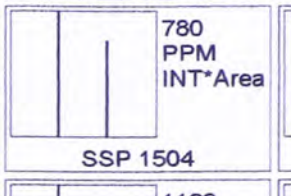

SSP 1504

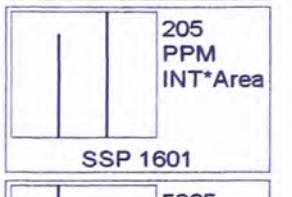

SSP 1601

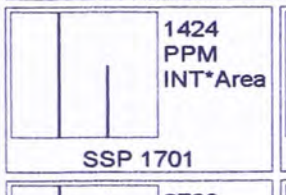

SSP 1701

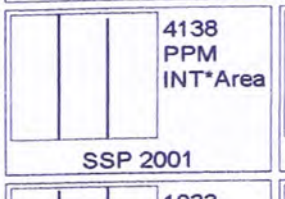

SSP 2001

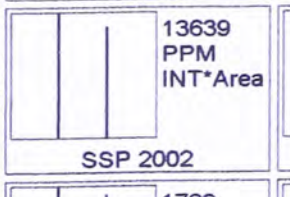

SSP 2002

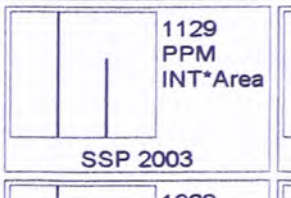

SSP 2003

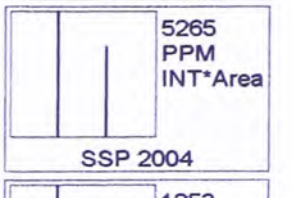

SSP 2004

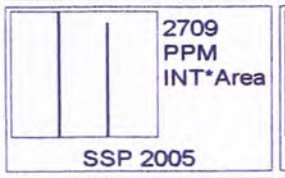

SSP 2005

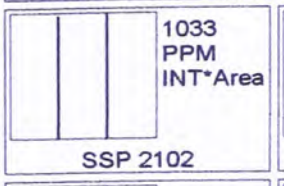

SSP 2102

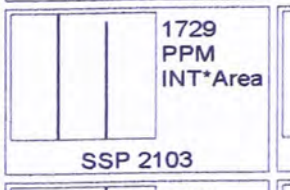

SSP 2103

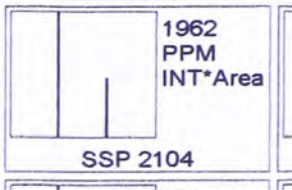

SSP 2104

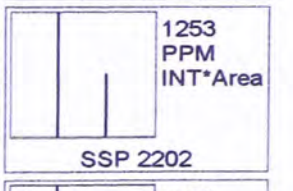

SSP 2202

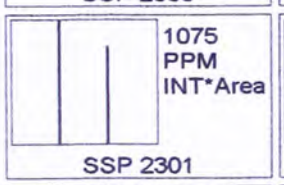

SSP 2301

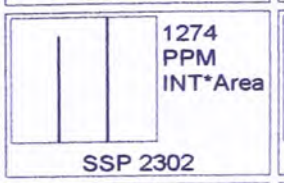

SSP 2302

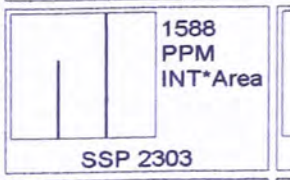

SSP 2303

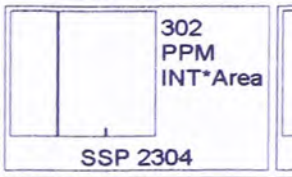

SSP 2304

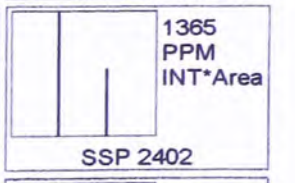

SSP 2402

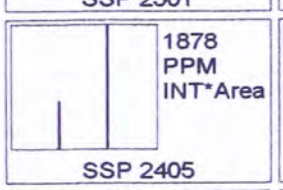

SSP 2405

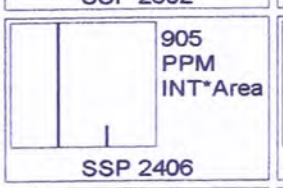

SSP 2406

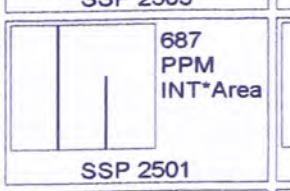

SSP 2501

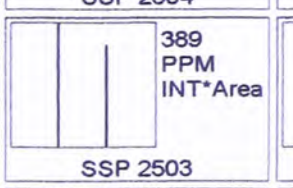

SSP 2503

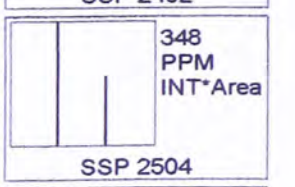

SSP 2504

SSP 2506

SSP 2602

SSP 2704

SSP 3001

SSP 3002

SSP 3003

SSP 3004

SSP 3005

SSP 3101

SSP 3201

Figure 23.

A quantity graph report showing the comparison of spot intensity of each analyzed spot across group (SSP 3202 – SSP5603). The SSP number is the number assigned to each analyzed protein spot for identification purpose. In each graph, the height of the bar represents the relative expression level of the protein spots analyzed in GFP-siRNA- and *Bre*-siRNA-treated group (from left to right).

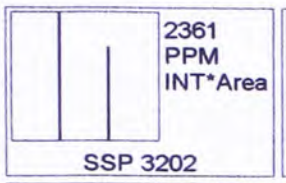

SSP 3202

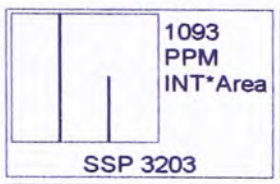

SSP 3203

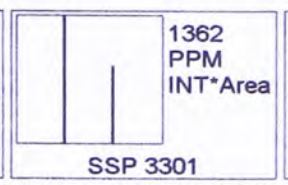

SSP 3301

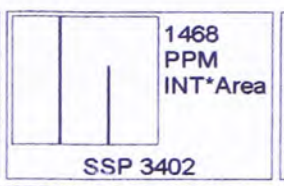

SSP 3402

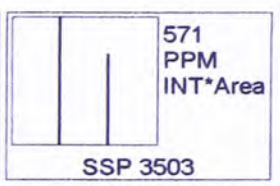

SSP 3503

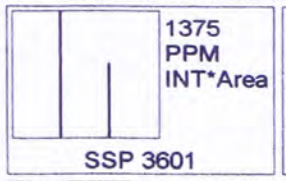

SSP 3601

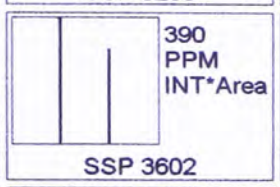

SSP 3602

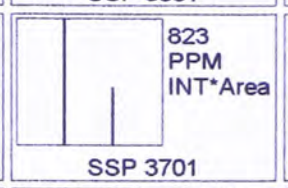

SSP 3701

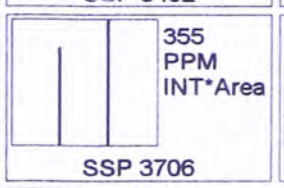

SSP 3706

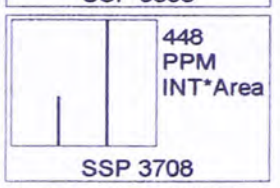

SSP 3708

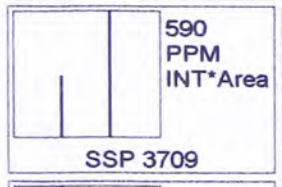

SSP 3709

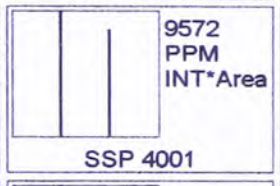

SSP 4001

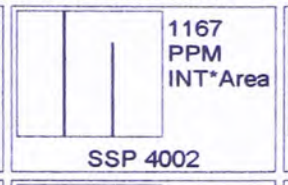

SSP 4002

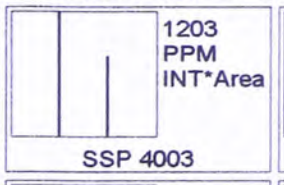

SSP 4003

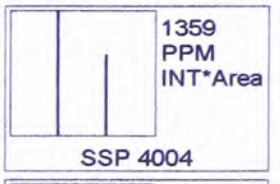

SSP 4004

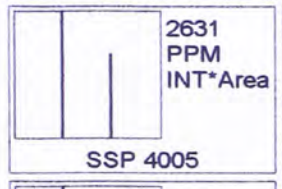

SSP 4005

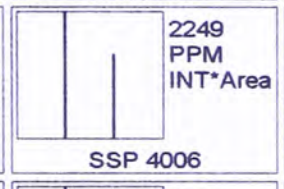

SSP 4006

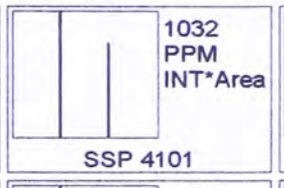

SSP 4101

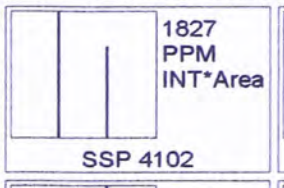

SSP 4102

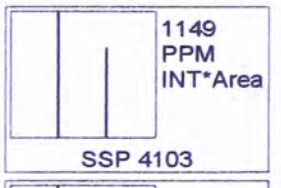

SSP 4103

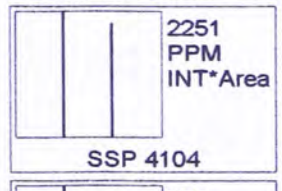

SSP 4104

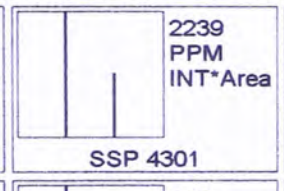

SSP 4301

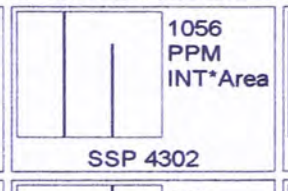

SSP 4302

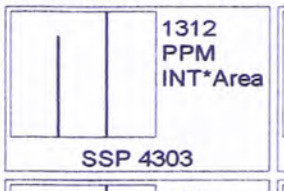

SSP 4303

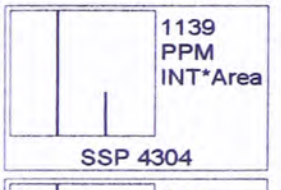

SSP 4304

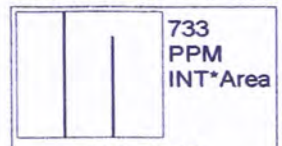

SSP 4401

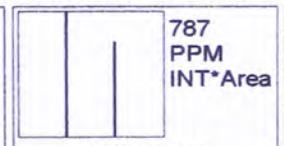

SSP 4402

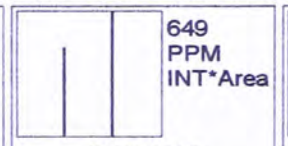

SSP 4505

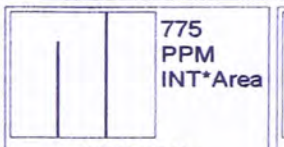

SSP 4506

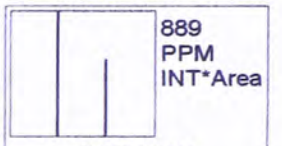

SSP 4507

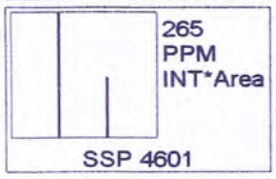

SSP 4601

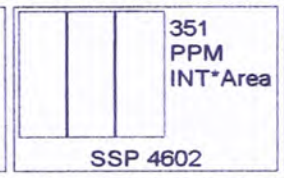

SSP 4602

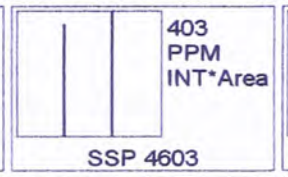

SSP 4603

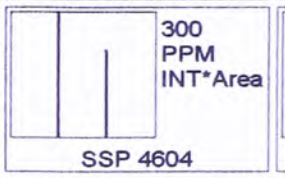

SSP 4604

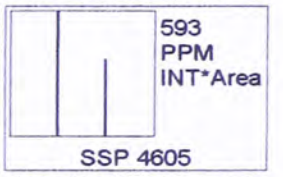

SSP 4605

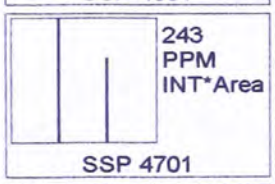

SSP 4701

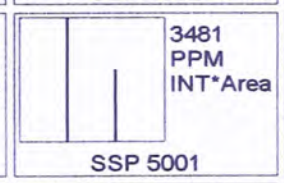

SSP 5001

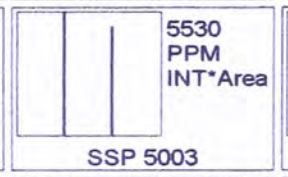

SSP 5003

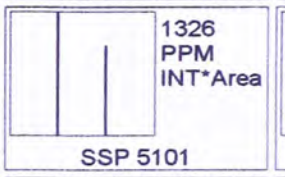

SSP 5101

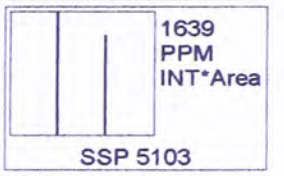

SSP 5103

SSP 5104

SSP 5202

SSP 5203

SSP 5302

SSP 5303

SSP 5502

SSP 5503

SSP 5601

SSP 5602

SSP 5603

Figure 24.

A quantity graph report showing the comparison of spot intensity of each analyzed spot across group (SSP 5604 – SSP8001). The SSP number is the number assigned to each analyzed protein spot for identification purpose. In each graph, the height of the bar represents the relative expression level of the protein spots analyzed in GFP-siRNA- and *Bre*-siRNA-treated group (from left to right).

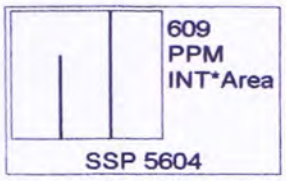

SSP 5604

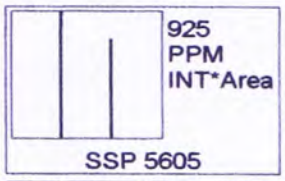

SSP 5605

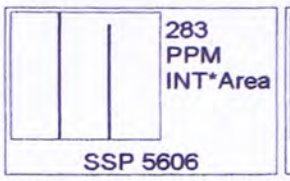

SSP 5606

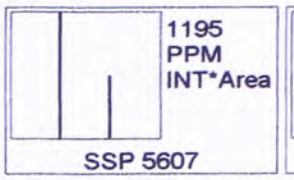

SSP 5607

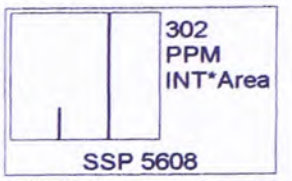

SSP 5608

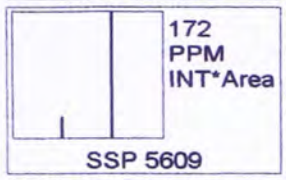

SSP 5609

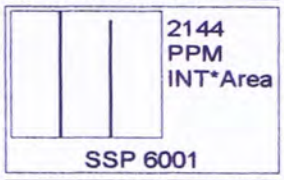

SSP 6001

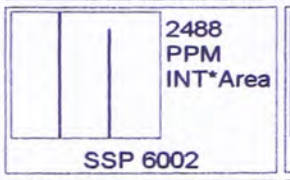

SSP 6002

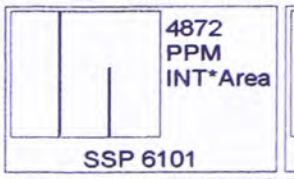

SSP 6101

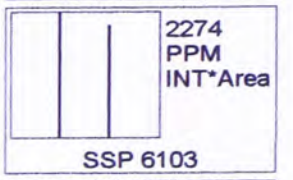

SSP 6103

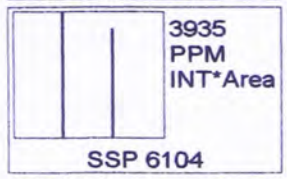

SSP 6104

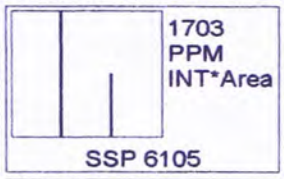

SSP 6105

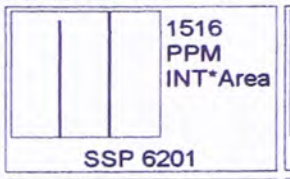

SSP 6201

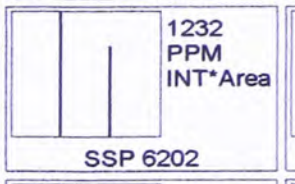

SSP 6202

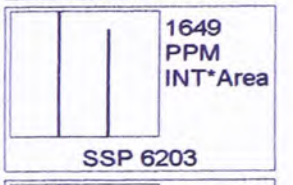

SSP 6203

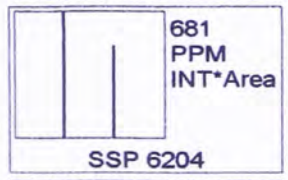

SSP 6204

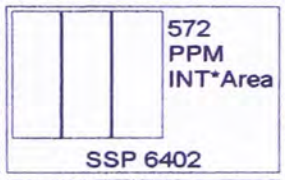

SSP 6402

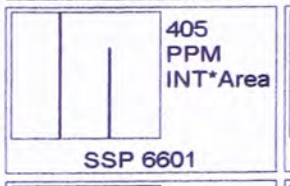

SSP 6601

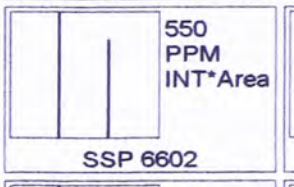

SSP 6602

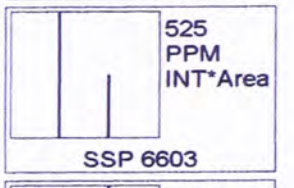

SSP 6603

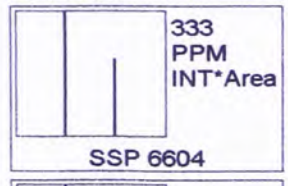

SSP 6604

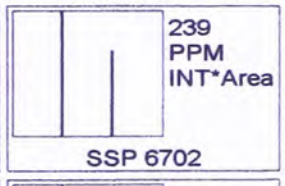

SSP 6702

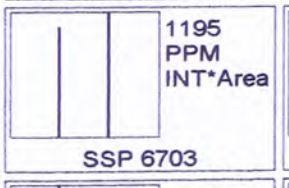

SSP 6703

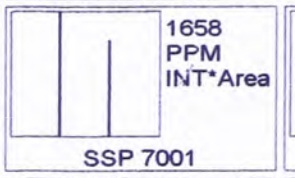

SSP 7001

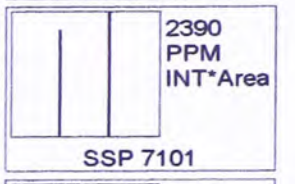

SSP 7101

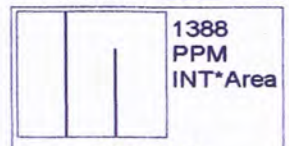

SSP 7102

SSP 7103

SSP 7104

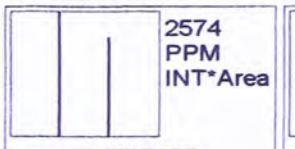

SSP 7105

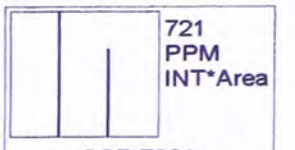

SSP 7201

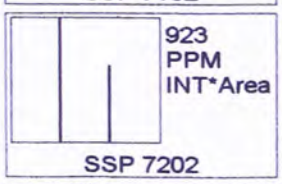

SSP 7202

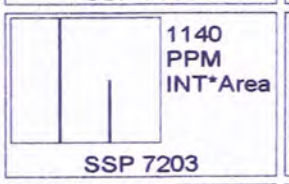

SSP 7203

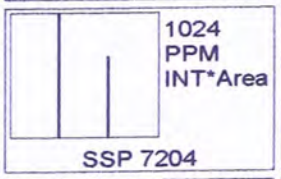

SSP 7204

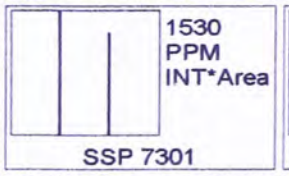

SSP 7301

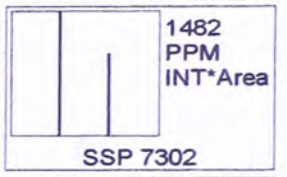

SSP 7302

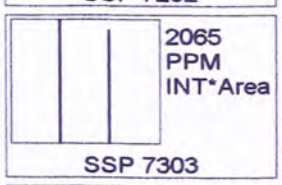

SSP 7303

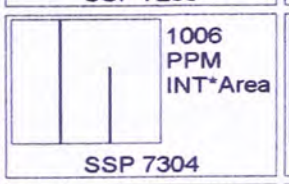

SSP 7304

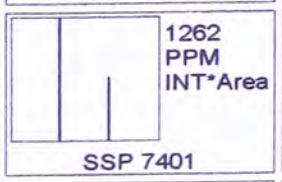

SSP 7401

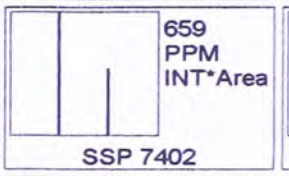

SSP 7402

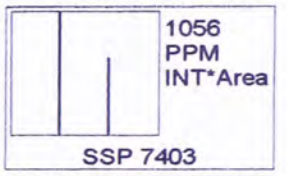

SSP 7403

SSP 7501

SSP 7502

SSP 7503

SSP 7601

SSP 7602

SSP 7603

SSP 7604

SSP 7701

SSP 7702

SSP 8001

Figure 25.

A quantity graph report showing the comparison of spot intensity of each analyzed spot across group (SSP 8004 – SSP8603). The SSP number is the number assigned to each analyzed protein spot for identification purpose. In each graph, the height of the bar represents the relative expression level of the protein spots analyzed in GFP-siRNA- and *Bre*-siRNA-treated group (from left to right).

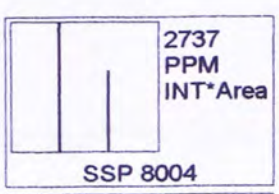

SSP 8004

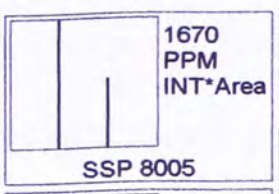

SSP 8005

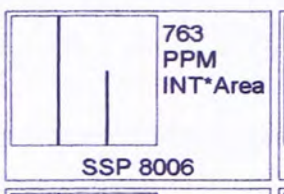

SSP 8006

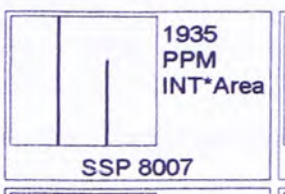

SSP 8007

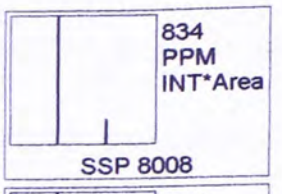

SSP 8008

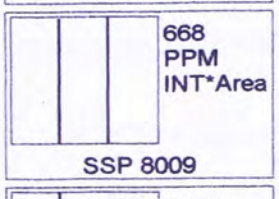

SSP 8009

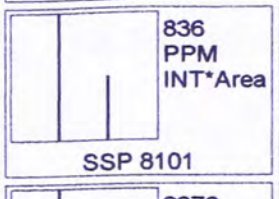

SSP 8101

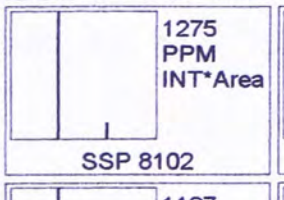

SSP 8102

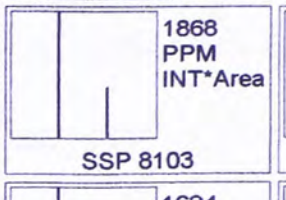

SSP 8103

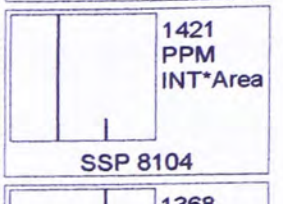

SSP 8104

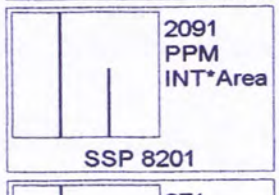

SSP 8201

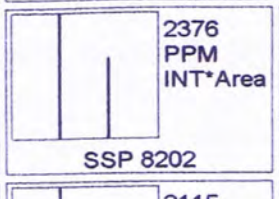

SSP 8202

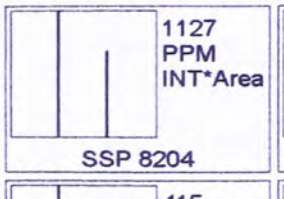

SSP 8204

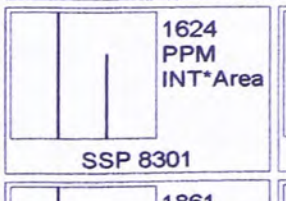

SSP 8301

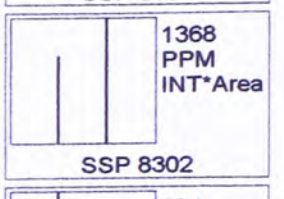

SSP 8302

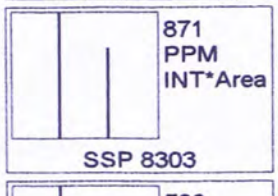

SSP 8303

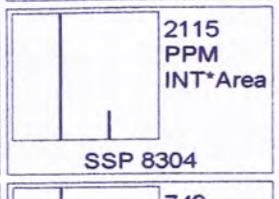

SSP 8304

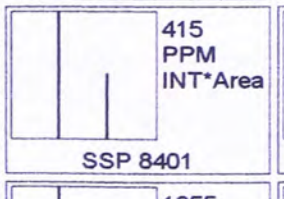

SSP 8401

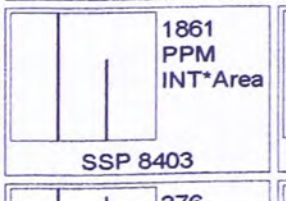

SSP 8403

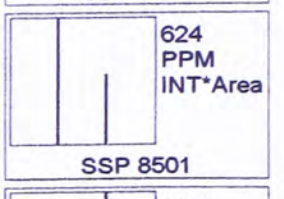

SSP 8501

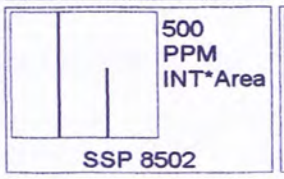

SSP 8502

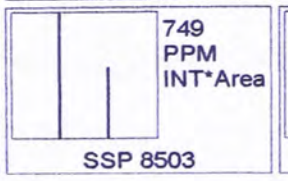

SSP 8503

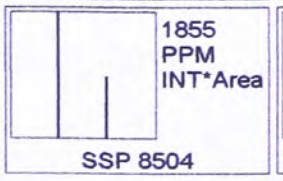

SSP 8504

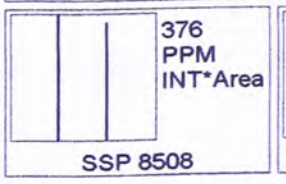

SSP 8508

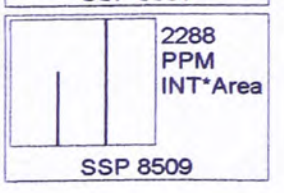

SSP 8509

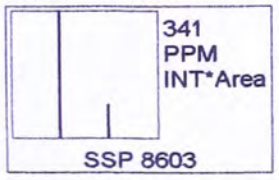

SSP 8603

3.6 Identification of proteins that were differentially expressed by MALDI-TOF

Protein expression profiles of *Bre*-siRNA- and GFP-siRNA-transfected interdigital cells were established by two-dimensional electrophoresis and analyzed by gel-imaging software. The protein spots that were differentially expressed were picked from the two-dimensional gels using a spot picker. They were destained to remove the silver nitrate inside the spots followed by in-gel digestion. The colorless protein spots were then soaked in trypsin solution overnight to obtain cleaved peptides which were in turn extracted. Extracted peptides followed by matrix solution were spotted onto MALDI-TOF sample plate which was in turn loaded into the mass spectrometer. The mass to charge ratio of each peptide of a protein was elucidated and revealed as a mass spectrum (Refer to appendices). By submitting the result obtained to database search, several protein candidates with basic information such as pI value, molecular weight and peptide mass fingerprint were ascertained. The rank was also provided which indicated the like-hood that the protein identified correlated with the mass spectrum. By considering the rank and discrepancy between the experimental and theoretical information of protein candidates, the protein identities were confidentially predicted. In this experiment, a total of eight proteins were identified to be differentially expressed in the *Bre*-silenced interdigital cells (Figure 26). Beside SSP number, each protein spot was named with a spot number for simpler illustration in the figure. The identities of the eight protein spots are listed in Table 5. In the Table, the corresponding SSP number, the ratio of protein spot intensity measurement in *Bre*-siRNA-treated cells to that of GFP-siRNA-treated cells are provided. Also the ranks obtained in the database search are listed.

Figure 26.

Representative two-dimensional electrophoresis of proteins extracted from E12.5 interdigital cells that had been transfected with GFP- or *Bre*- specific siRNA. Eight proteins that were differentially expressed were identified. Each protein spot was provided with a number to assist in the identification process.

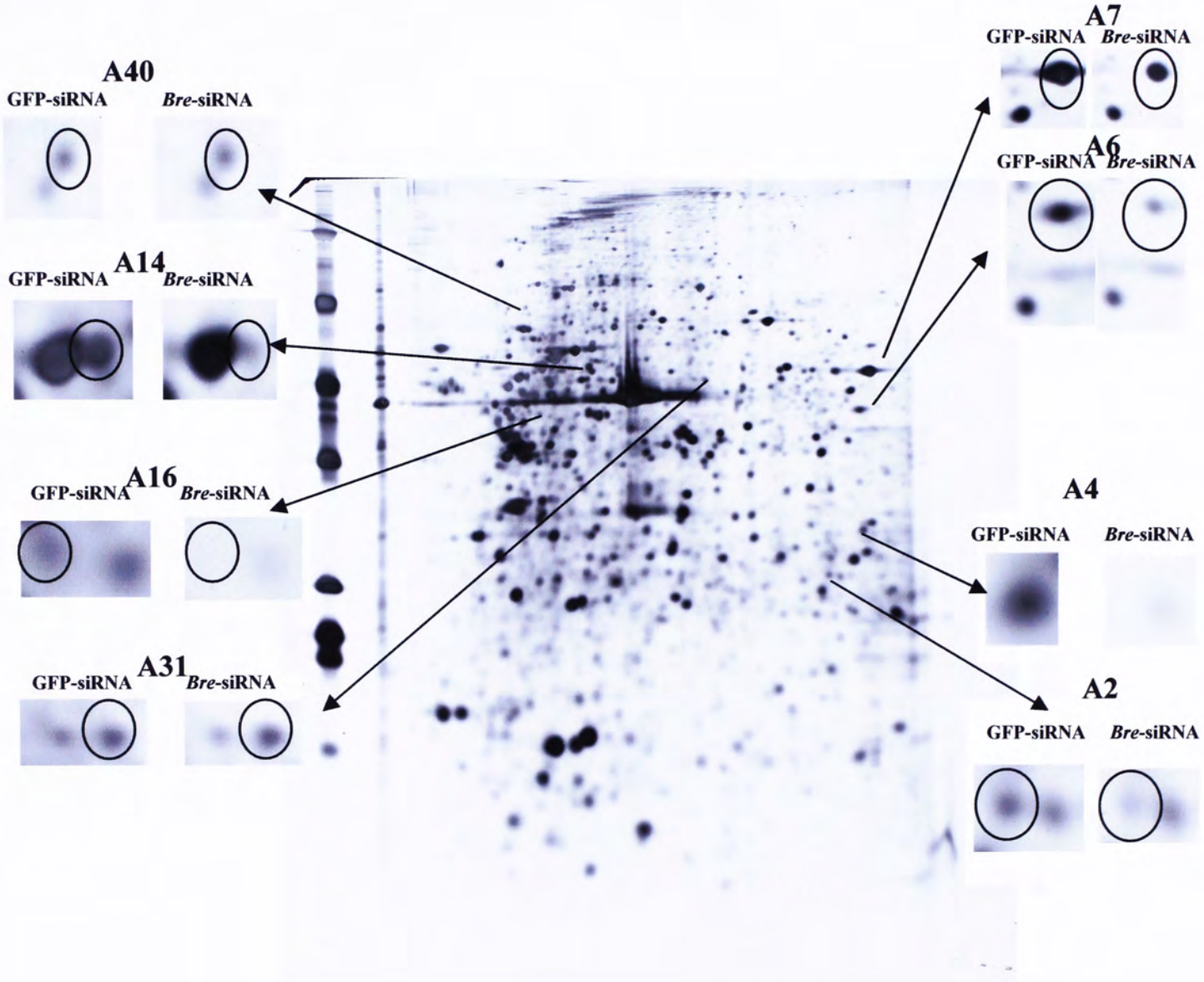
A40
GFP-siRNA
Bre-siRNA
A14
GFP-siRNA
Bre-siRNA
A16
GFP-siRNA
Bre-siRNA
A31
GFP-siRNA
Bre-siRNA
A7
GFP-siRNA
Bre-siRNA
A6
GFP-siRNA
Bre-siRNA
A4
GFP-siRNA
Bre-siRNA
A2
GFP-siRNA
Bre-siRNA

Table 5.

Proteins that are differentially expressed in *Bre*-silenced E12.5 interdigital cells. The ratio of spot intensity was estimated by the The Discovery series, PDQuest 2D Analysis Software. The protein identities are shown with ranks of the search.

Spot Number	SSP Number	Proteins identified	Ratio of spot intensity measurements (bre-siRNA/GFP-siRNA)	Rank of search
A2	8008	Proteasome beta 3	0.001	9
A4	8102	Proteasome (prosome, macropain) subunit, alpha type 6	0.01	26
A6	8304	Txndc7/PDIA6	0.17	1
A7	8509	Enolase 1, alpha non-neuron	0.41	2
A14	2406	Vimentin	0.0006	1
A16	2304	Drebrin A2	0.01	18
A31	6402	Gpc6 Protein	1.08	40
A40	1601	Ubiquilin-1	1.24	2

3.7 The mRNA levels of proteins identified that were differentially expressed

Since the comparative proteomic technique only demonstrated genes that were differentially expressed at the protein level, we also decided to examine the mRNA levels of the genes identified by semi-quantitative RT-PCR. Among eight protein candidates, *Pdia6* and *vimentin* were selected for further analysis because their ranks from the database search were extremely convincing. Our semi-quantitative RT-PCR result revealed that *Pdia6* was down-regulated by *Bre*-specific siRNA at the mRNA level. Expression of *β-actin* demonstrated the suppressed *Pdia6* expression was not a non-specific effect resulted from the siRNA transfection (Figure 27). However, this was not the case for *vimentin*. The mRNA level of *vimentin* was unaffected by *Bre*-silencing as compared with control group (Figure 28). The expression level of *β-actin* served as an internal control for the experiment.

Figure 27.

Semi-quantitative RT-PCR analysis of *Pdia6* mRNA level in E12.5 interdigital cells that were transfected with either *Bre*-specific siRNA or GFP-specific siRNA. E12.5 interdigital cells were harvested 48 hours after transfection. (A) The result showed that *Pdia6* expression was down-regulated by *Bre*-specific siRNA. Expression of *β-actin* served as an internal control. (B) The ratio of *Pdia6* expression level in GFP-siRNA and *Bre*-siRNA treated E12.5 interdigital cells. For the ease of illustration, the *Pdia6* expression level in GFP-siRNA treated E12.5 interdigital cells was made up to 1.0. The *Pdia6* mRNA level in each group was normalized by its corresponding *β-actin* expression level.

A

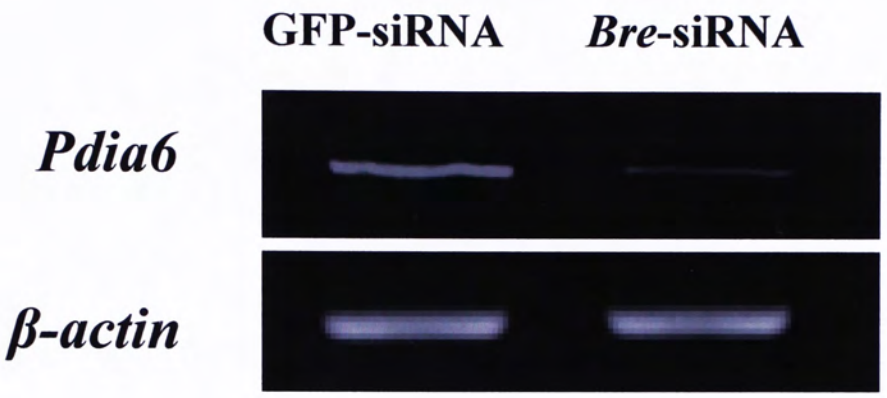
GFP-siRNA
Bre-siRNA
Pdia6
β-actin

B

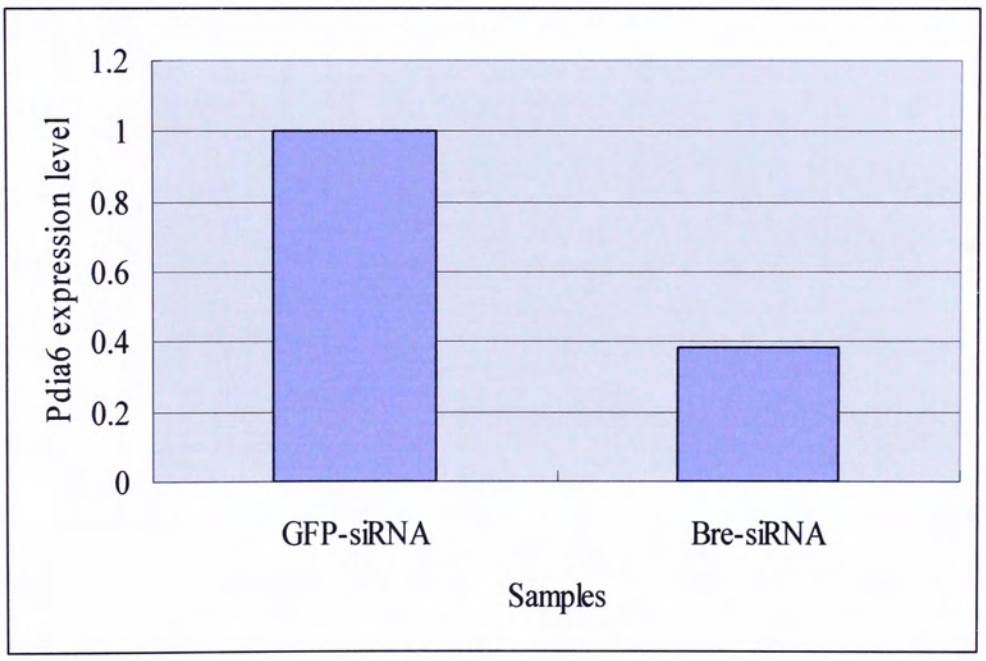
1.2
1
0.8
0.6
0.4
0.2
0
Pdia6 expression level
GFP-siRNA
Bre-siRNA
Samples

Figure 28.

Semi-quantitative RT-PCR analysis of *vimentin* mRNA level in E12.5 interdigital cells that were transfected with either *Bre*-specific siRNA or GFP-specific siRNA. E12.5 interdigital cells were harvested 48 hours after transfection. (A) The result revealed that *vimentin* mRNA expression was not affected by *Bre*-silencing even though *vimentin* was down-regulated at protein level, as determined by comparative proteomic analysis. Expression of *β-actin* served as an internal control. (B) The ratio of *vimentin* expression level in GFP-siRNA and *Bre*-siRNA treated E12.5 interdigital cells. For the ease of illustration, the *vimentin* expression level in GFP-siRNA treated E12.5 interdigital cells was made up to 1.0. The *vimentin* mRNA level in each group was normalized by its corresponding *β-actin* expression level.

A

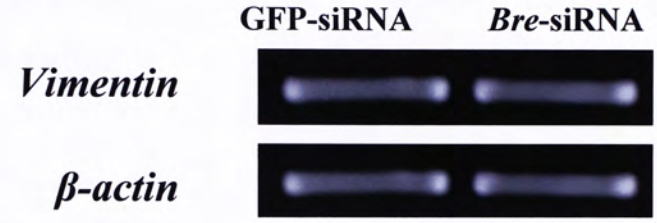
GFP-siRNA
Bre-siRNA
Vimentin
β-actin

B

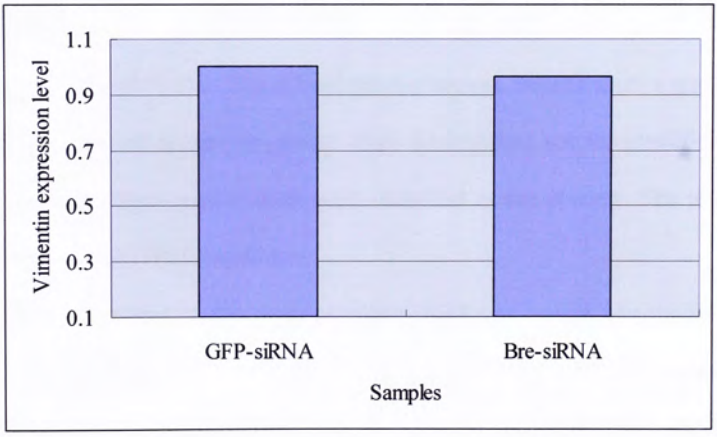
Vimentin expression level
1.1
0.9
0.7
0.5
0.3
0.1
GFP-siRNA
Bre-siRNA
Samples

Chapter IV

Discussion

In the first part of my study, I have established the spatial-temporal expression pattern of *Bre* gene in E12.5 and E13.5 hindlimbs by in-situ hybridization. The expression level of *Bre* transcripts in the interdigital tissues of E12.5 and E13.5 hindlimbs was determined by semi-quantitative RT-PCR technique. The presence of different isoforms of *Bre* transcripts in interdigital tissues of E12.5 hindlimbs was determined by RT-PCR and using different isoform-specific primers. In the second part of my study, I have used *Bre*-specific siRNA to silence *Bre* expression in the interdigital cells. The viability of interdigital cultured cells was assayed after siRNA transfection. Afterwards, the protein profiles of interdigital cells that could and could not express *Bre* were produced and compared by two-dimensional electrophoresis. Several spots were found to be differential expressed across the groups. They were picked out for identification by mass fingerprinting. Eight protein spots were identified in this process. The result was further confirmed by RT-PCR technique.

The result obtained in this study provides significant insight into the biological function of the *Bre* gene. Human *Bre* gene has been shown to be highly expressed in brain, testis, ovary, adrenal gland and heart (Li et al., 1995; Miao et al., 2001). The hamster *Bre* gene has been shown to be highly expressed in neurons and luminal epithelia of urogenital, digestive and respiratory organs (Poon et al., 2004). In this project, I used *in-situ* hybridization to demonstrate that the *Bre* gene was expressed in the interdigital

tissues. In addition, using RT-PCR revealed that only *Bre* isoform 5 was expressed in the interdigital tissues and cells but not the other four isoforms.

I have determined the spatial expression pattern of the *Bre* gene in E12.5 and E13.5 mouse hindlimbs by *in-situ* hybridization. *Bre* was preferentially expressed in the interdigital tissues than in the digits, in both E12.5 and E13.5 hindlimbs. In addition using semi-quantitative RT-PCR, I determined that *Bre* was expressed at a significantly higher level in E12.5 interdigital tissues than E13.5. Previously, it has been reported that *Bre* may behave like an anti-apoptotic protein by mediating through the TNF-α-induced apoptotic pathway (Li et al., 2004). In addition, TNF-α is highly expressed in the interdigital tissues when the digits start to separate at E13.5 (Martin, 1990). Therefore, *Bre* may be involved in the regulation of interdigital cell death because its expression pattern overlapped the interdigital tissues and also because of its ability to modulate the actions of TNF-α.

The mouse *Bre* gene has been reported to exist as different isoforms resulting from alternative splicing (Ching et al., 2003). According to the NCBI database, mouse *Bre* gene has five isoforms. I have aligned all of them using multiple alignment software Clustal W 1.83. The result indicated that all of the *Bre* isoforms were produced by alternative splicing at the 5'end. Using the result, I designed five pairs of isoform-specific primers. Using the primers, I detected only *Bre* isoform 5 in the E12.5 and E13.5 interdigital tissues and cells by semi-quantitative RT-PCR. The expressions of other *Bre* isoforms were undetectable. In adult heart tissues, *Bre* isoform 2, 4 and 5 could be detected by RT-PCR. This result is consistent with Ching et al., 2003 that most of the mouse organs expressed *Bre* isoform 5 as the major transcript with the expressions of

other isoforms at undetectable levels, except for the adult mouse heart which expressed all *Bre* isoforms. However, my result only revealed that *Bre* isoform 2, 4 and 5 were expressed in the adult heart. This discrepancy could be attributed to using ICR in our study while Ching et al., 2003 used F1 mice (produced by mating C57BL/6 with CBA mice). The use of different mouse models may yield a variation of *Bre* isoform expression in the heart tissues. Previously, our laboratory has determined that the interdigital tissues were not committed to program cell death until E13.5 (Tang et al., 2000). In addition, interdigital tissues isolated from E12.5 hindlimbs were capable of surviving and developing into cartilage and soft connective tissues (Lee et al., 1994). I have found that *Bre* isoform 5 was expressed at a higher level in E12.5 than E13.5 interdigital tissues. This would suggest that the product of *Bre* may be acting as a survival factor preventing the interdigital cells from entering into the death program until the appropriate time, at E13.5.

In this study, I have used siRNA technique to silence *Bre* expression in order to understand the function of *Bre* in the interdigital cells. I found that it was more difficult to transfect siRNAs into primary cell cultures than transformed cell lines and so, I have used special reagents and protocols to overcome the problem. The optimal condition for transfecting siRNAs into the interdigital cultured cells was precisely determined and established. siRNA is a powerful tool in the loss of function study and I have used it to silence *Bre* expression in primary interdigital cells. Semi-quantitative RT-PCR revealed that my *Bre*-specific siRNA could suppress *Bre* expression by 70% in the interdigital cells.

Although BRE has been previously proposed as an anti-apoptotic factor in cancer cell lines (Li et al., 2004), whether it has the same role in the interdigital cultured cells has still not been clarified. In my study, we are able to knockdown endogenous *Bre* expression. In order to investigate the anti-apoptotic role of BRE as previously described, we set out MTT assay to quantitate the viability of cells with or without *Bre* expression. As expected, knockdown of endogenous *Bre* reduced cell viability after 39 hours post transfection of *Bre*-siRNA. Longer period of siRNA treatment (e.g. 60 hours post transfection) should be carried out to strengthen the existing data. In addition, further experiments such as cell proliferation assay and apoptosis assay by flow cytometry may help identifying the causes of reduction in cell viability by *Bre*-siRNA, for example, decrease in cell proliferation, increase in apoptosis, or involvement in other signaling pathways.

The preliminary result of the reduction in cell viability by *Bre*-siRNA suggests that BRE may also play an anti-apoptotic role in interdigital cultured cells. In order to further investigate the downstream effect of *Bre* silencing, I used two-dimensional electrophoresis technique to compare the protein expression profiles of interdigital cells silenced by *Bre*-siRNA with that of control culture transfected with GFP-siRNA. I discovered many proteins which were differentially expressed and managed to identify eight of them by mass fingerprinting. The accession numbers and the known functions of these eight identified proteins are summarized in Table 6. None of the identified proteins were found to be directly associated with apoptosis or cell proliferation. However, this does not imply that the *Bre* gene do not have a role in apoptosis because my successful rate in identifying the differentially expressed protein by MALDI-TOF mass

spectrometry was very low. This weakness does greatly affect the interpretation of the results and the conclusion of *Bre* gene function. It would be better to use tandem mass spectrometry (MS-MS) so that not only mass-to-charge ratio but also amino acid sequence of the peptides could be obtained. In fact, a well-established comparative proteomic system can yield fruitful results. Any proteins that were differential expressed across the sample groups can be easily identified. The mechanisms, pathways and even the function of the gene of interest can be extrapolated from the clusters of proteins that were differential expressed. Similar strategy can be applied to the mRNAs using cDNA microarray analysis. The expressions of thousands of genes can be monitored at a time.

Among the eight protein identified, I focus my attention on two of them - protein disulfide isomerase associated 6 (PDIA6) and vimentin. PDIA6 belongs to a family of protein disulfide isomerase (PDI). Recently, PDI has been reported to be expressed in the interdigital tissues and involved in interdigital cell death (Shan et al., 2005). PDIA6 has been reported to have isomerase, chaperone and peptide-binding activities (Kikuchi et al., 2002). The result of semi-quantitative RT-PCR revealed and confirmed that *Pdia6* expression was down-regulated by *Bre* silencing in the interdigital cells. This implies that *Bre* may be involved in the regulation of interdigital cell death through PDIA6 – since it has been reported that PDI plays an important role in the induction of interdigital cell death (Shan et al., 2005).

Vimentin is known to play a pivotal role in supporting and anchoring organelles to their positions in the cytosol (Takemura et al., 2002). Besides acting as a structural constituent of the cytoskeleton, it also regulates the transportation of low density lipoprotein-derived cholesterol for esterification (Sarria et al., 1992). In addition,

vimentin was found to be a death substrate cleaved by activated Caspase-9 enzyme in apoptotic cells, in the embryonic nervous system and in the interdigital regions (Nakanishi et al., 2001). My RT-PCR result showed that *Bre* silencing did not affect *vimentin* expression even though vimentin protein expression was down-regulated. This implies that the reduced level of vimentin protein in the cytoplasm was the result of post-transcriptional modification. It is possible that the reduction was the result of vimentin being cleaved by the Caspase-9 enzyme leading to their degradation. In addition, *Bre* has been reported to play an anti-apoptotic role in cells by modulating the signals through the TNF-α-induced apoptotic pathway and inhibition of the mitochondrial apoptotic machinery (Li et al., 2004). Caspase-9 acts as an initiator of the mitochondrial apoptotic pathway (Cohen, 1997), so suppressing *Bre* expression in interdigital cells may lead to down-regulation of vimentin through a common apoptotic pathway. However, I need to perform more functional analysis to verify this conclusion.

In sum, my study has demonstrated for the first time that the *Bre* gene was expressed in limb interdigital cells. In addition, the interdigital cells only expressed *Bre* isoform 5 and the corresponding expression is higher at E12.5 than E13.5. The *Bre* loss-of-function study combined with comparative proteomics revealed it affected PDIA6 and vimentin expressions. In future, I would like to perform over-expression studies to determine how *Bre* affects major transduction pathways. I would also like to test whether over-expressing *Bre* makes the interdigital cells more resistant to experimentally induced cell death. Furthermore, comparative microarray analysis on *Bre*-silenced interdigital cells can be used to determine the clusters of genes affected by *Bre* silencing. These

experiments will provide definitive information on the functional role of the *Bre* gene in limb interdigital tissues.

Table 6.

The table listing the accession number and summary of some known functions of each identified and differential expressed protein obtained in the comparative proteomic analysis.

Protein Identified	Accession number	Known functions
Proteasome beta 3	NM_011971	Threonine endopeptidase activity
Proteosome (prosome, macropain) subunit, alpha type 6	NM_011968	RNA binding, protein binding, threonine endopeptidase activity
Txndc7/PDIA6	NM_027959	Isomerase activity, chaperone activity and peptide-binding activity
Enolase 1, alpha non-neuron	NM_023119	Lyase activity, magnesium ion binding, metal ion binding, phosphopyruvate hydratase activity
Vimentin	NM_011701	Structural constituent of cytoskeleton, structural molecule activity, involvement in the metabolism of lipoprotein derived cholesterol
Drebrin A2	AB064321	Actin binding, profiling binding
Gpc6 Protein	BC023448	GPI anchor binding
Ubiquilin-1	BC026847	Intermediate filament binding, kinase binding, oxidoreductase activity, receptor binding

References

Ali-Khan, S.E. and Hales, B.F. (2003). Caspase-3 mediates retinoid-induced apoptosis in the organogenesis-stage mouse limb. *Birth Defects Res. Part A Clin. Mol. Teratol.* **67**, 848-860

Alles, A.J. and Sulik, K.K. (1989). Retinoic-acid-induced limb-reduction defects: perturbation of zones of programmed cell death as a pathogenetic mechanism. *Teratology* **40**, 163-171

Alnemri, E.S., Livingston, D.J., Nicholson, D.W., Salvesen, G., Thornberry, N.A., Wong, W.W. and Yuan, J. (1996). Human ICE/CED-3 protease nomenclature. *Cell* **87**, 171

Beg, A.A. and Baltimore, D. (1996). An essential role for NF-kappa B in preventing TNF-alpha-induced cell death. *Science* **274**, 782-784

Boldin, M.P., Goncharov, T.M., Goltsev, Y.V. and Wallach, D. (1996). Involvement of MACH, a novel MORT1/FADD-interacting protease, in Fas/APO-1- and TNF-receptor-induced cell death. *Cell* **85**, 803-815

Capdevila, J. and Izpisua Belmonte, J.C. (2001). Patterning mechanisms controlling vertebrate limb development. *Annu. Rev. Cell Dev. Biol.* **17**, 87-132.

Cecconi, F., Alvarez-Bolado, G., Meyer, B.I., Roth, K.A. and Gruss, P. (1998). Apaf-1 (CED-4 homolog) regulates programmed cell death in mammalian development. *Cell* **94**, 727-737

Chan, B.C., Li, Q., Chow, S.K., Ching, A.K., Liew, C.T., Lim, P.L., Lee, K.K., Chan, J.Y. and Chui, Y.L. (2005). BRE enhances in vivo growth of tumor cells. *Biochem. Biophys. Res. Commun.* **326**, 268-273

Chaudhary, P.M., Eby, M., Jasmin, A., Bookwalter, A., Murray, J. and Hood, L. (1997). Death receptor 5, a new member of the TNFR family, and DR4 induce FADD-dependent apoptosis and activate the NF-kappaB pathway. *Immunity* **7**, 821-830

Chautan, M., Chazal, G., Cecconi, F., Gruss, P. and Golstein, P. (1999). Interdigital cell death can occur through a necrotic and caspase-independent pathway. *Curr. Biol.* **9**, 967-970

Cheng, E.H., Levine, B., Boise, L.H., Thompson, C.B. and Hardwick, J.M. (1996). Bax-independent inhibition of apoptosis by Bcl-XL. *Nature* **379**, 554-556

Ching, A.K., Li, P.S., Li, Q., Chan, B.S., Chan, J.Y., Lim, P.L., Pang, J.C. and Chui, Y.L. (2001). Expression of human BRE in multiple isoforms. *Biochem. Biophys. Res. Commun.* **288**, 535-545

Ching, A.K., Li, Q., Lim, P.L., Chan, J.Y. and Chui, Y.L. (2003). Expression of a conserved mouse stress-modulating gene, *Bre*: Comparison with the human ortholog. *DNA Cell Biol.* **22**, 497-504

Chinnaiyan, A.M., O'Rourke, K., Tewari, M. and Dixit, V.M. (1995). FADD, a novel death domain-containing protein, interacts with the death domain of Fas and initiates apoptosis. *Cell* **81**, 505-512

Chinnaiyan, A.M., O'Rourke, K., Yu, G.L., Lyons, R.H., Garg, M., Duan, D.R., Xing, L., Gentz, R., Ni, J. and Dixit, V.M. (1996a). Signal transduction by DR3, a death domain-containing receptor related to TNFR-1 and CD95. *Science* **274**, 990-992

Chinnaiyan, A.M., Tepper, C.G., Seldin, M.F., O'Rourke, K., Kischkel, F.C., Helbardt, S., Krammer, P.H., Peter, M.E. and Dixit, V.M. (1996b). FADD/MORT1 is a common mediator of CD95 (Fas/APO-1) and tumor necrosis factor receptor-induced apoptosis. *J. Biol. Chem.* **271**, 4961-4965

Chittenden, T., Flemington, C., Houghton, A.B., Ebb, R.G., Gallo, G.J., Elangovan, B., Chinnadurai, G. and Lutz, R.J. (1995). A conserved domain in Bak, distinct from BH1 and BH2, mediates cell death and protein binding functions. *EMBO J.* **14**, 5589-5596

Cohen, G.M. (1997). Caspases: the executioners of apoptosis. *Biochem. J.* **326**, 1-16

Cohn, M.J., Izpisúa-Belmonte, J.C., Abud, H., Heath, J.K. and Tickle, C. (1995). Fibroblast growth factors induce additional limb development from the flank of chick embryos. *Cell* **80**, 739-746

Dawd, D.S. and Hinchliffe, J.R. (1971). Cell death in the "opaque patch" in the central mesenchyme of the developing chick limb: a cytological, cytochemical and electron microscopic analysis. *J. Embryol. Exp. Morphol.* **26**, 401-424

Dealy, C.N., Roth, A., Ferrari, D., Brown, A.M.C. and Kosher, R.A. (1993). *Wnt-5a* and *Wnt 7a* are expressed in the developing chick limb bud in a manner that suggests role in pattern formation along the proximodistal and dorsoventral axes. *Mech. Dev.* **43,** 175-186

Dhein, J., Walczak, H., Baumler, C., Debatin, K.M. and Krammer, P.H. (1995). Autocrine T-cell suicide mediated by APO-1 (Fas/CD95). *Nature* **373**, 438-441

Dong, Y., Hakimi, M.A., Chen, X., Kumaraswamy, E., Cooch, N.S., Godwin, A.K. and Shiekhattar, R. (2003). Regulation of BRCC, a holoenzyme complex containing BRCA1 and BRCA2, by a signalosome-like subunit and its role in DNA repair. *Mol. Cell.* **12**, 1087-1099

Du, C., Fang, M., Li, Y., Li, L. and Wang, X. (2000). Smac, a mitochondrial protein that promotes cytochrome c-dependent caspase activation by eliminating IAP inhibition. *Cell* **102**, 33-42

Dupé, V., Ghyselinck, N.B., Thomazy, V., Nagy, L., Davies, P.J., Chambon, P. and Mark, M. (1999). Essential roles of retinoic acid signaling in interdigital apoptosis and control of BMP-7 expression in mouse autopods. *Dev. Biol.* **208**, 30-43

Dynlacht, J.R., Earles, M., Henthorn, J. and Seno, J.D. (2000). Different patterns of DNA fragmentation and degradation of nuclear matrix proteins during apoptosis induced by radiation, hyperthermia or etoposide. *Radiat. Res.* **154**, 515-530

Ferrari, D., Lichtler, A.C., Pan, Z., Dealy, C.N., Upholt, W.B. and Kosher, R.A. (1998). Ectopic expression of *Msx2* in posterior limb bud mesoderm impairs limb morphogenesis while inducing *Bmp4* expression, inhibiting cell proliferation, and promoting apoptosis. *Dev. Biol.* **197**, 12-24

Gañan, Y., Macias, D., Basco, R.D., Merino, R. and Hurlé, J.M. (1998). Morphological diversity of the avian foot is related with the pattern of Msx gene expression in the developing autopod. *Dev. Biol.* **196**, 33-41

Gañan, Y., Macias, D., Duterque-Coquillaud, M., Ros, M.A. and Hurlé, J.M. (1996). Role of TGFβs and BMPs as signals controlling the position of the digits and the areas of interdigital cell death in the developing chick limb autopod. *Development* **122**, 2349-2357

Garcia-Martinez, V., Macias, D., Gañan, Y., Garcia-Lobo, J.M., Francia, M.V., Fernandez-Teran, M.A. and Hurlé, J.M. (1993). Internucleosomal DNA fragmentation and programmed cell death (apoptosis) in the interdigital tissue of the embryonic chick leg bud. *J. Cell Sci.* **106**, 201-208

Geduspan, J.S. and MacCabe, J.A. (1987). The ectodermal control of mesodermal patterns of differentiation in the developing chick wing. *Dev. Biol.* **124**, 398-408

Grotewold, L. and Rüther, U. (2002a). Bmp, Fgf and Wnt signaling in programmed cell death and chondrogenesis during vertebrate limb development: the role of Dickkopf-1. *Int. J. Dev. Biol.* **46**, 943-947

Grotewold, L. and Rüther, U. (2002b). The Wnt antagonist Dickkopf-1 is regulated by BMP signaling and c-jun and modulates programmed cell death. *EMBO* **21**, 966-975

Gu, C., Castellino, A., Chan, J.Y. and Chao, M.V. (1998). BRE: a modulator of TNF-alpha action. *FASEB J.* **12**, 1101-1108

Guha, U., Gomes, W.A., Kobayashi, T., Pestell, R.G. and Kessler, J.A. (2002). In vivo evidence that BMP signaling is necessary for apopotsis in the developing limb. *Dev. Biol.* **249**, 108-120

Hayashi, K. and Ozawa, E. (1995). Myogenic cell migration from somites is induced by tissue contact with medial region of the presumptive limb mesoderm in chick embryos. *Development* **121**, 661–669.

Hockenbery, D., Nunez, G., Milliman, C., Schreiber, R.D. and Korsmeyer, S.J. (1990). Bcl-2 is an inner mitochondrial membrane protein that blocks programmed cell death. *Nature* **348**, 334-336

Hsu, H., Huang, J., Shu, H.B., Baichwal, V. and Goeddel, D.V. (1996a). TNF-dependent recruitment of the protein kinase RIP to the TNF receptor-1 signaling complex. *Immunity* **4**, 387-396

Hsu, H., Shu, H.B., Pan, M.G. and Goeddel, D.V. (1996b). TRADD-TRAF2 and TRADD-FADD interactions define two distinct TNF receptor 1 signal transduction pathways. *Cell* **84**, 299-308

Hsu, H., Xiong, J. and Goeddel, D.V. (1995). The TNF receptor 1-associated protein TRADD signals cell death and NF-kappa B activation. *Cell* **81**, 495-504

Hu, S., Snipas, S.J., Vincenz, C., Salvesen, G. and Dixit, V.M. (1998a). Caspase-14 is a novel developmentally regulated protease. *J. Biol. Chem.* **273**, 29648-29653

Hu, Y., Benedict, M.A., Wu, D., Inohara, N. and Nunez, G. (1998b). Bcl-XL interacts with Apaf-1 and inhibits Apaf-1-dependent caspase-9 activation. *Proc. Natl. Acad. Sci. U. S. A.* **95**, 4386-4391

Huang, C. and Hales, B.F. (2002). Role of caspases in murine limb bud cell death induced by 4-hydroperoxycyclophosphamide, an activated analog of cyclophosphamide. *Teratology* **66**, 288-299

Hunter, J.J. and Parslow, T.G. (1996). A peptide sequence from Bax that converts Bcl-2 into an activator of apoptosis. *J. Biol. Chem.* **271**, 8521-8524

Johnson, R.L. and Tabin, C.J. (1997). Molecular models for vertebrate limb development. *Cell* **90**, 979 -990

Jurgensmeier, J.M., Xie, Z., Deveraux, Q., Ellerby, L., Bredesen, D. and Reed, J.C. (1998). Bax directly induces release of cytochrome c from isolated mitochondria. *Proc. Natl. Acad. Sci. U. S. A.* **95**, 4997-5002

Kawakami, Y., Capdevila, J., Buscher, D., Itoh, T., Rodriguez Esteban, C. and Izpisua Belmonte, J.C. (2001). WNT signals control FGF-dependent limb initiation and AER induction in the chick embryo. *Cell* **104**, 891-900

Kawakami, Y., Ishikawa, T., Shimabara, M., Tanda, N., Enomoto-Iwamoto, M., Iwamoto, M., Kuwana, T., Ueki, A., Noji, S. and Nohno, T. (1996). BMP signaling during bone pattern determination in the developing limb. *Development* **122**, 3557-3566

Kikuchi, M., Doi, E., Tsujimoto, I., Horibe, T. and Tsujimoto, Y. (2002). Functional analysis of human P5, a protein disulfide isomerase homologue. *J. Biochem (Tokyo)* **132**, 451-455

Kimura, N., Matsuo, R., Shibuya, H., Nakashima, K. and Taga, T. (2000). BMP-2 induced apoptosis is mediated by activation of the TAK1-p38 kinase pathway that is negatively regulated by Smad 6. *J. Biol. Chem.* **275**, 17647-17652

Klein, K.L., Scott, W.J. and Wilson, J.G. (1981). Aspirin-induced teratogenesis: a unique pattern of cell death and subsequent polydactyly in the rat. *J. Exp. Zool.* **216**, 107-112

Kluck, R.M., Bossy-Wetzel, E., Green, D.R. and Newmeyer, D.D. (1997). The release of cytochrome c from mitochondria: a primary site for Bcl-2 regulation of apoptosis. *Science* **275**, 1132-1136

Knudson, C.M. and Korsmeyer, S.J. (1997). Bcl-2 and Bax function independently to regulate cell death. *Nat. Genet.* **16**, 358-363

Kuida, K., Haydar, T.F., Kuan, C.Y., Gu, Y., Taya, C., Karasuyama, H., Su, M.S., Rakic, P. and Flavell, R.A. (1998). Reduced apoptosis and cytochrome c-mediated caspase activation in mice lacking caspase 9. *Cell* **94**, 325-337

Kuida, K., Zheng, T.S., Na, S., Kuan, C., Yang, D., Karasuyama, H., Rakic, P. and Flavell, R.A. (1996). Decreased apoptosis in the brain and premature lethality in CPP32-deficient mice. *Nature* **384**, 368-372

Lacronique, V., Mignon, A., Fabre, M., Viollet, B., Rouquet, N., Molina, T., Porteu, A., Henrion, A., Bouscary, D., Varlet, P., Joulin, V. and Kahn, A. (1996). Bcl-2 protects from lethal hepatic apoptosis induced by an anti-Fas antibody in mice. *Nat. Med.* **2**, 80-86

Laufer, E., Pizette, S., Zou, H., Orozco, O.E. and Niswander, L. (1997). BMP expression in duck interdigital webbing: a reanalysis. *Science* **278**, 305

Lee, K.K., Li, F.C., Yung, W.T., Kung, J.L., Ng, J.L., Cheah, K.S. (1994). Influence of digits, ectoderm, and retinoic acid on chondrogenesis by mouse interdigital mesoderm in culture. *Dev. Dyn.* **201**, 297-309

Lee, K.K.H, Leung, A.K.C., Tang, M.K., Cai, D.Q., Schneider, C., Brancolini, C. and Chow, P.H. (2001). Functions of the growth arrest specific 1 gene in the development of the mouse embryo. *Dev. Biol.* **234**, 188-203

Lee, K.K.H., Tang, M.K., Yew, D.T.W., Chow, P.H., Yee, S.P., Schneider, C. and Brancolini, C. (1999). *gas2* is a multifunctional gene involved in the regulation of apoptosis and chondrogenesis in the developing mouse limb. *Dev. Biol.* **207**, 14-25

Lee, N. (2002). Interplay between the molecular signals that control vertebrate limb development. *Int. J. Dev. Biol.* **46**, 877-881

Letai, A., Bassik, M.C., Walensky, L.D., Sorcinelli, M.D., Weiler, S. and Korsmeyer, S.J. (2002). Distinct BH3 domains either sensitize or activate mitochondrial apoptosis, serving as prototype cancer therapeutics. *Cancer Cell* **2**, 183-192

Li, H., Zhu, H., Xu, C.J. and Yuan, J. (1998). Cleavage of BID by caspase 8 mediates the mitochondrial damage in the Fas pathway of apoptosis. *Cell* **94**, 491-501

Li, L., Yoo, H., Becker, F.F., Ali-Osman, F. and Chan, J.Y. (1995). Identification of a brain- and reproductive-organs-specific gene responsive to DNA damage and retinoic acid. *Biochem. Biophys. Res. Commun.* **206**, 764-774

Li, Q., Ching, A.K., Chan, B.C., Chow, S.K., Lim, P.L., Ho, T.C., Ip, W.K., Wong, C.K., Lam, C.W., Lee, K.K., Chan, J.Y. and Chui, Y.L. (2004). A death receptor-associated anti-apoptotic protein, BRE, inhibits mitochondrial apoptotic pathway. *J.Bio. Chem.* **279**, 52106-52116

Lindahl, T., Satoh, M.S., Poirier, G.G. and Klungland, A. (1995). Post-translational modification of poly(ADP-ribose) polymerase induced by DNA strand breaks. *Trends Biochem. Sci.* **20**, 405-411

Lindsten, T., Ross, A.J., King, A., Zong, W.X., Rathmell, J.C., Shiels, H.A., Ulrich, E., Waymire, H.G., Mahar, P., Frauwirth, K., Chen, Y., Wei, M., Eng, V.M., Adelman, D.M., Simon, M.C., Ma, A., Golden, J.A., Evan, G., Korsmeyer, S.J., MacGregor, G.R. and Thompson, C.B. (2000). The combined functions of proapoptotic Bcl-2 family members bak and bax are essential for normal development of multiple tissues. *Mol. Cell.* **6**, 1389-1399

Liu, X., Kim, C.N., Yang, J., Jemmerson, R. and Wang, X. (1996). Induction of apoptotic program in cell-free extracts: requirement for dATP and cytochrome c. *Cell* **86**, 147-157

Logan, C., Hornbruch, A., Campbell, I. and Lumsden, A. (1997). The role of Engrailed in establishing the dorsoventral axis of the chick limb. *Development* **124**, 2317-2324

Logan, M. (2003). Finger or toe: the molecular basis of limb identity. *Development* **130**, 6401-6410

Loomis, C.A., Harris, E., Michaud, J., Wurst, W., Hanks, M. and Joyner, A.L. (1996). The mouse Engrailed-1 gene and ventral limb patterning. *Nature* **382**, 360-363

Luo, X., Budihardjo, I., Zou, H., Slaughter, C. and Wang, X. (1998). Bid, a Bcl2 interacting protein, mediates cytochrome c release from mitochondria in response to activation of cell surface death receptor. *Cell* **94**, 481-490

MacCabe, J.A., Errick, J. and Saunders, J.W. (1974). Ectodermal control of the dorsoventral axis in the leg bud of the chick embryo. *Dev. Biol.* **39**, 69-82

Macias, D., Gañon, Y., Sampath, T.K., Piedra, M.E., Ros, M.A. and Hurlé, J.M. (1997). Role of BMP2 and OP-1 (BMP7) in programmed cell death and skeletogenesis during chick limb development. *Development* **124**, 1109-1117

Martin, P. (1990). Tissue patterning in the developing mouse limb. *Int. J. Dev. Biol.* **34**, 323-336

Medema, J.P., Scaffidi, C., Kischkel, F.C., Shevchenko, A., Mann, M., Krammer, P.H. and Peter, M.E. (1997). FLICE is activated by association with the CD95 death-inducing signaling complex (DISC). *EMBO J.* **16**, 2794-2804

Merino, R., Rodriquez-Leon, J., Macias, D., Gañan, Y., Economides, A.N. and Hurlé, J.M. (1999). The BMP antagonist Gremlin regulates outgrowth, chondrogenesis and programmed cell death in the developing limb. *Development* **126**, 5515-5522

Miao, J., Chan, K.W., Chen, G.G., Chun, S.Y., Xia, N.S., Chan, J.Y. and Panesar, N.S. (2005). Blocking BRE expression in Leydig cells inhibits steroidogenesis by down-regulating 3β-hydroxysteriod dehydrogenase. *J. Endocrinol.* **185**, 507-517

Miao, J., Panesar, N.S., Chan, K.T., Lai, F.M., Xia, N., Wang, Y., Johnson, P.J. and Chan, J.Y. (2001). Differential expression of a stress-modulating gene, BRE, in the adrenal gland, in adrenal neoplasia, and in abnormal adrenal tissues. *J. Histochem. Cytochem.* **49**, 491-500

Mirkes, P.E., Little, S.A. and Umpierre, C.C. (2001). Co-localization of active caspase 3 and DNA fragmentation (TUNEL) in normal and hyperthermia-induced abnormal mouse development. *Teratology* **63**, 134-143

Mori, C., Nakamura, N., Kimura, S., Irie, H., Takigawa, T. and Shiota, K. (1995). Programmed cell death in the interdigital tissue of the fetal mouse limb is apoptosis with DNA fragmentation. *Anat. Rec.* **242**, 103-110

Muzio, M., Chinnaiyan, A.M., Kischkel, F.C., O'Rourke, K., Shevchenko, A., Ni, J., Scaffidi, C., Bretz, J.D., Zhang, M., Gentz, R., Mann, M., Krammer, P.H., Peter, M.E. and Dixit, V.M. (1996). FLICE, a novel FADD-homologous ICE/CED-3-like protease, is recruited to the CD95 (Fas/APO-1) death –inducing signaling complex. *Cell* **85**, 817-827

Nakanishi, K., Maruyamia, M., Shibata, T. and Morishima, N. (2001). Identification of a caspase 9 substrate and detection of its cleavage in programmed cell death during mouse development. *J. Biol. Chem.* **276**, 41237-41244

Naruse, I. and Kameyama, Y. (1986). Prevention of polydactyly manifestation in *Polydactyly nagoya* (Pdn) mice by administration of cytosine arabinoside during pregnancy. *Teratology* **34**, 283-289

Ohuchi, H., Nakagawa, T., Yamamoto, A., Araga, A., Ohata, T., Ishimaru, Y., Yoshioka, H., Kuwana, T., Nohno, T., Yamasaki, M., Itoh, N. and Noji, S. (1997). The mesenchymal factor, FGF10, initiates and maintains the outgrowth of the chick limb bud through interaction with FGF8, an apical ectodermal factor. *Development* **124**, 2235-2244

Ohuchi, H., Nakagawa, T., Yamauchi, M., Ohata, T., Yoshioka, H., Kuwana, T., Mima, T., Mikawa, T., Nohno, T. and Noji, S. (1995). An additional limb can be induced from the flank of the chick embryo by FGF4. *Biochem. Biophys. Res. Commun.* **209**, 809- 816

Pan, G., Bauer, J.H., Haridas, V., Wang, S., Liu, D., Yu, G., Vincenz, C., Aggarwal, B.B., Ni, J. and Dixit, V.M. (1998). Identification and functional characterization of DR6, a novel death domain-containing TNF receptor. *FEBS Lett.* **431**, 351-356

Pan, G., O'Rourke, K., Chinnaiyan, A.M., Gentz, R., Ebner, R., Ni, J. and Dixit, V.M. (1997). The receptor for the cytotoxic ligand TRIAL. *Science* **276**, 111-113

Panman, L. and Zeller, R. (2003). Patterning the limb before and after SHH signaling. *J. Anat.* **202**, 3-12

Parr, B.A. and McMahon, A.P. (1995). Dorsalizing signal *Wnt-7a* required for normal polarity of D-V and A-P axes of the mouse limb. *Nature* **374**, 350-353

Parr, B.A., Shea, M.J., Vassileva, G. and McMahon., A.P. (1993). Mouse *Wnt* genes exhibit discrete domains of expression in early embryonic CNS and limb buds. *Development* **119**, 247-261

Patel, T., Gores, G.J. and Kaufmann, S.H. (1996). The role of proteases during apoptosis. *FASEB J.* **10**, 587-597

Pautou, M.P. (1977). Dorso-ventral axis determination of chick limb bud development. In *Vertebrate Limb and Somite Morphogenesis*, D.A. Ede, J.R. Hinchliffe and M. Balls, eds.: Cambridge Univ. Press, 257-266

Pizette, S., Abate-Shen, C. and Niswander, L. (2001). BMP controls proximodistal outgrowth, via induction of the apical ectodermal ridge, and dorsoventral patterning in the vertebrate limb. *Development* **128**, 4463-4474

Poon, H.K., Chan, J.Y., Lee, K.H. and Chow, P.H. (2004). Tissue specific expression and sequence analysis of a stress responsive gene *Bre* in adult golden hamster (*Mesocricetus auratus*). *Cell Tissue Res.* **316**, 305-313

Quillet-Mary, A., Jaffrezou, J.P., Mansat, V., Bordier, C., Naval, J. and Laurent, G. (1997). Implication of mitochondrial hydrogen peroxide generation in ceramide-induced apoptosis. *J. Biol. Chem.* **272**, 21388-21395

Ratan, R.R., Murphy, T.H. and Baraban, J.M. (1994). Oxidative stress induces apoptosis in embryonic cortical neurons. *J. Neurochem.* **62**, 376-379

Riddle, R.D., Johnson, R.L., Laufer, E. and Tabin, C. (1993). Sonic hedgehog mediates the polarizing activity of the ZPA. *Cell* **75**, 1401-1416

Rosse, T., Olivier, R., Monney, L., Rager, M., Conus, S., Fellay, I., Jansen, B. and Borner, C. (1998). Bcl-2 prolongs cell survival after Bax-induced release of cytochrome c. *Nature* **391**, 496-499

Rothe, M., Wong, S.C., Henzel, W.J. and Goeddel, D.V. (1994). A novel family of putative signal transducers associated with the cytoplasmic domain of the 75 kDa tumor necrosis factor receptor. *Cell* **78**, 681-692

Salas-Vidal, E., Lomelí, H., Castro-Obregón, S., Cuervo, R., Escalante-Alcalde, D. and Covarrubias, L. (1998). Reactive oxygen species participates in the control of mouse embryonic cell death. *Exp. Cell Res.* **238**, 136-147

Sanz-Ezquerro, J.J. and Tickle, C. (2001). "Fingering" the vertebrate limb. *Differentiation* **69**, 91-99

Sanz-Ezquerro, J.J. and Tickle, C. (2003). Digital development and morphogenesis. *J. Anat.* **202**, 51-58

Sarria, A.J., Panini, S.R. and Evans, R.M. (1992). A functional role for vimentin intermediate filaments in the metabolism of lipoprotein-derived cholesterol in human SW-13 cells. *J. Biol. Chem.* **267**, 19455-19463

Saunders, J.W. (1948). The proximo-distal sequence of origin of the parts of the chick wing and role of the ectoderm. *J. Exp. Zool.* **108**, 363-404

Saunders, J.W. (1966). Death in embryonic systems. *Science* **154**, 604-612

Saunders, J.W. and Fallon, J. (1967). Cell death in morphogenesis. In M. Locke (ed.), *Major Problems in Developmental Biology*. Academic Press, New York, 289-314

Saunders, J.W. and Gasseling, M.T. (1968). Ectodermal-mesenchymal interactions in the origin of limb symmetry. In R. Fleischmeyer and R.E. Billingham (eds.), *Epithelial-mesenchymal interactions*. Williams and Wilkins, Baltimore, 78-97.

Schnabel, D., Salas-Vidal, E., Narváez, V., Sánchez-Varbente, M., Hernández-García, D., Cuervo, R. and Covarrubias, L. (2006). Expression and regulation of antioxidant enzymes in the developing limb support a function of ROS in interdigital cell death. *Dev. Biol.* **291**, 291-299

Sentman, C.L., Shutter, J.R., Hockenbery, D., Kanagawa, O. and Korsmeyer, S.J. (1991). Bcl-2 inhibits multiple forms of apoptosis but not negative selection in thymocytes. *Cell* **67**, 879-888

Shan, S.W., Tang, M.K., Cai, D.Q., Chui, Y.L., Chow, P.H., Grotewold, L. and Lee, K.K. (2005). Comparative proteomic analysis identifies protein disulfide isomerase and peroxiredoxin 1 as new players involved in embryonic interdigital cell death. *Dev. Dyn.* **233**, 266-281

Shimizu, S., Narita, M. and Tsuhimoto, Y. (1999). Bcl-2 family proteins regulate the release of apoptogenic cytochrome c by the mitochondrial channel VDAC. *Nature* **399**, 483-487

Solursh, M., Drake, C. and Meier, S. (1987). The migration of myogenic cells from the somites at the wing level in avian embryos. *Dev. Biol.* **121**, 389-396

Srinivasula, S.M., Ahmad, M., Fernandes-Alnemri, T. and Alnemri, E.S. (1998). Autoactivation of procaspase-9 by Apaf-1-mediated oligomerization. *Mol. Cell.* **1**, 949-957

Stanger, B.Z., Leder, P., Lee, T.H., Kim, E. and Seed, B. (1995). RIP: a novel protein containing a death domain that interacts with Fas/APO-1 (CD95) in yeast and causes cell death. *Cell* **81**, 513-523

Strasser, A., Harris, A.W. and Cory, S. (1991). Bcl-2 transgene inhibits T cell death and perturbs thymic self-censorship. *Cell* **67**, 889-899

Susin, S.A., Lorenzo, H.K., Zamzami, N., Marzo, I., Brenner, C., Larochette, N., Prevost, M.C., Alzari, P.M. and Kroemer, G. (1999). Mitochondrial release of caspase-2 and -9 during the apoptotic process. *J. Exp. Med.* **189**, 381-394

Susin, S.A., Zamzami, N., Castedo, M., Daugas, E., Wang, H.G., Geley, S., Fassy, F., Reed, J.C. and Kroemer, G. (1997). The central executioner of apoptosis: multiple connections between protease activation and mitochondria in Fas/APO-1/CD95- and ceramide-induced apoptosis. *J. Exp. Med.* **186**, 25-37

Takemura, M., Comi, H., Colucci-Guyon, E. and Itohara, S. (2002). Protective role of phosphorylation in turnover of glial fibrillary acidic protein in mice. *J. Neurosci.* **22**, 6972-6979

Tang, M.K., Leung, A.K., Kwong, W.H., Chow, P.H., Chan, J.Y., Ngo-Muller, V., Li, M. and Lee, K.K. (2000). BMP-4 requires the presence of the digits to initiate programmed cell death in limb interdigital tissues. *Dev. Biol.* **218**, 89-98

Tang, M.K., Wang, C.M., Shan, S.W., Chui, Y.L., Ching, A.K., Chow, P.H., Grotewold, L., Chan, J.Y. and Lee, K.K. (2006). Comparative proteomic analysis reveals a function of the novel death receptor-associated protein BRE in the regulation of prohibitin and p53 expression and proliferation. *Proteomics* **6**, 2376-2385

Tartaglia, L.A., Ayres, T.M., Wong, G.H. and Goeddel, D.V. (1993). A novel domain within the 55kd TNF receptor signals cell death. *Cell* **74**, 845-853

Tewari, M., Quan, L.T., O'Rourke, K., Desnoyers, S., Zeng, Z., Beidler, D.R., Poirier, G.G., Salvesen, G.S. and Dixit, V.M. (1995). Yama/CPP32 beta, a mammalian homolog of CED-3, is a CrmA-inhibitable protease that cleaves the death substrate poly-(ADP-ribose) polymerase. *Cell* **81**, 801-809

Tickle, C. (1995). Vertebrate limb development. *Curr. Opin. Genet. Dev.* **5**, 478-484

Tickle, C. (2006). Making digit patterns in the vertebrate limb. *Nature Rev. Mol. Cell Biol.* **7**, 45-53

Tickle, C. and Münsterberg A. (2001). Vertebrate limb development – the early stages in chick and mouse. *Curr. Opin. Genet. Dev.* **11**, 476-481

Tickle, C., Summerbell, D. and Wolpert, L. (1975). Positional signaling and specification of digits in chick limb morphogenesis. *Nature* **254**, 199-202

Todt, W.L. and Fallon, J.F. (1984). Development of the apical ectodermal ridge in the chick wing bud. *J. Embryol. Exp. Morphol.* **80**, 21-41

Verhagen, A.M., Ekert, P.G., Pakusch, M., Silke, J., Connolly, L.M., Reid, G.E., Moritz, R.L., Simpson, R.J. and Vaux, D.J. (2000). Identification of DIABLO, a mammalian protein that promotes apoptosis by binding to and antagonizing IAP proteins. *Cell* **102**, 43-53

Villunger, A., Huang, D.C., Holler, N., Tschopp, J. and Strasser, A. (2000). Fas ligand-induced c-Jun kinase activation in lymphoid cells requires extensive receptor aggregation but is independent of DAXX, and Fas-mediated cell death does not involve DAXX, RIP and RAIDD. *J. Immunol.* **165**, 1337-1343

Wanek, N., Muneoka, K., Holler-Dinsmore, G., Burton, R. and Bryant, S.V. (1989). A staging system for mouse limb development. *J Exp Zool.* **249**, 41-49

Wang, C.K., Omi, M., Ferrari, D., Cheng, H.C., Lizarraga, G., Chin, H.J., Upholt, W.B., Dealy, C.N. and Kosher, R.A. (2004). Function of BMPs in the apical ectoderm of the developing mouse limb. *Dev. Biol.* **269**, 109-122

Wang, K., Yin, X.M., Chao, D.T., Millimam, C.L. and Korsmeyer, S.J. (1996). BID: a novel BH3 domain-only death agonist. *Genes Dev.* **10**, 2859-2869

Woo, M., Hakem, R., Soengas, M.S., Duncan, G.S., Shahinian, A., Kagi, D., Hakem, A., McCurrach, M., Khoo, W., Kaufman, S.A., Senaldi, G., Howard, T., Lowe, S.W. and Mak, T.W. (1998). Essential contribution of caspase 3/CPP32 to apoptosis and its associated nuclear changes. *Genes Dev.* **12**, 806-819

Wride, M.A., Lapchak, P.H. and Saunders, E.J. (1994). Distribution of TNF-α-like protein correlates with some regions of programmed cell death in the chick embryo. *Int. J. Dev. Biol.* **38**, 673-682

Wyllie, A.H., Kerr, J.F.R. and Currie, A.R. (1980). Cell death: The significance of apoptosis. *Int. Rev. Cytol.* **68**, 251-306

Xu, X., Weinstein, M., Li, C., Naski, M., Cohen, R.I., Ornitz, D.M., Leder, P. and Deng, C. (1998). Fibroblast growth factor receptor 2 (FGFR2)-mediated reciprocal regulation loop between FGF8 and FGF10 is essential for limb induction. *Development* **125**, 753-765

Yang, E., Zha, J., Jockel, J., Boise, L.H., Thompson, C.B. and Korsmeyer, S.J. (1995). Bad, a heterodimeric partner for Bcl-XL and Bcl-2, displaces Bax and promotes cell death. *Cell* **80**, 285-291

Yang, J., Liu, X., Bhalla, K., Kim, C.N., Ibrado, A.M., Cai, J., Peng, T.I., Jones, D.P. and Wang, X. (1997a). Prevention of apoptosis by Bcl-2: release of cytochrome c from mitochondria blocked. *Science* **275**, 1129-1132

Yang, X., Khosravi-Far, R., Chang, H.Y. and Baltimore, D. (1997b). Daxx, a novel Fas-binding protein that activates JNK and apoptosis. *Cell* **89**, 1067-1076

Yokouchi, Y., Sakiyama, T., Kameda, T., Iba, H., Suzuki, A., Ueno, N. and Kuroiwa, A. (1996). BMP-2/-4 mediate programmed cell death in chicken limb buds. *Development* **122**, 3725-3734

Yonei-Tamura, S.T., Endo, H., Yajima, H., Ohuichi, H., Ide, H. and Tamura, K. (1999). FGF7 and FGF10 directly induce apical ectodermal ridge in chick embryos. *Dev. Biol.* **211**, 133-143

Zamzami, N., Marchetti, P., Castedo, M., Zanin, C., Vayssiere, J.L., Petit, P.X. and Kroemer, G. (1995). Reduction in mitochondrial potential constitutes an early irreversible step of programmed lymphocyte death *in vivo*. *J. Exp. Med.* **181**, 1661-1672

Zamzami, N., Susin, S.A., Marchetti, P., Hirsch, T., Gomez-Monterrey, I., Castedo, M. and Kroemer, G. (1996). Mitochondrial control of nuclear apoptosis. *J. Exp. Med.* **183**, 1533-1544

Zou, H., Henzel, W.J., Liu, X., Lutschg, A. and Wang, X. (1997). Apaf-1, a human protein homologous to C. elegans CED-4, participates in cytochrome c-dependent activation of caspase 3. *Cell* **90**, 405-413

Zou, H., Li, Y., Liu, X., and Wang, X. (1999). An APAF-1. cytochrome c multimeric complex is a functional apoptosome that activates procaspase-9. *J. Biol. Chem.* **274**, 11549-11556

Zou, H. and Niswander, L. (1996). Requirement for BMP signaling in interdigital apoptosis and scale formation. *Science* **272**, 738-741

Zuzarte-Luís, V. and Hurlé, J.M. (2002). Programmed cell death in the developing limb. *Int. J. Dev. Biol.* **46**, 871-876

Zuzarte-Luís, V. and Hurlé, J.M. (2005). Programmed cell death in the embryonic vertebrate limb. *Semin. Cell Dev. Biol.* **16**, 261-269

Zuzarte-Luís, V., Montero, J.A., Rodriguez-Léon, J., Merino, R., Rodríguez-Rey, J.C. and Hurlé, J.M. (2004). A new role for BMP during limb development acting through the synergic activation of Smad and MAPK pathways. *Dev. Biol.* **272**, 39-52

Appendices

Composition of Gel Buffer (3M Tris, pH8.45, 0.3% SDS)

Tris (USB, United States)	181.7g
Ajust to pH 8.45	
SDS (USD, United States)	1.5g
MilliQ water	Up to 500ml

Composition of 40% Acylamide Solution

Acrylamide (USB, United States)	195g
1,4-Bis(acryloyl)piperazine (Sigma, United States)	5g
MilliQ water	Up to 500ml

Composition of 12% SDS-acrylamide separating gel solution

(For two-dimensional electrophoresis)

50% Glycerol (v/v, USB, United States)	8ml
40% Acrylamide solution (w/v)	33ml
Gel buffer (3M Tris, pH8.45, 0.3% SDS)	24ml
MilliQ water	Up to 100ml
10% AP solution (v/v, Bio-Rad Laboratories, United States)	360µl
TEMED (Bio-Rad Laboratories, United States)	36µl

Composition of Anode Buffer

Tris (USB, United States)	12.11g
MilliQ water	Up to 500ml
Adjust to pH 8.9	

Composition of Cathode Buffer

Tris (USB, United States)	6g
Tricine (USB, United States)	8.96g
SDS (USB, United States)	0.5g
MilliQ water	Up to 500ml

Composition of Solution A

Tris (USB, United States)	30.3g
Glycine (USB, United States)	144g
SDS (USB, United States)	1.25g
MilliQ water	Up to 1000ml

Composition of Transfer Buffer

Solution A	100ml
Methanol (Lab Scan, Ireland)	200ml
MilliQ water	Up to 1000ml

Composition of 1.5M Tris solution (pH 8.8)

Tris (USB, United States)	181.71g
MilliQ water	Up to 1000ml
Adjust to pH 8.8	

Composition of Equilibration Buffer

1.5M Tris solution (pH8.8)	16.7ml
Urea (USB, United States)	180.2g
Glycerol (USB, United States)	150ml
SDS (USB, United States)	10g
Bromophenol blue (Sigma-Aldrich, United States)	0.5g
MilliQ water	Up to 500ml

Composition of Fixing Solution

Methanol (Lab Scan, Ireland)	250ml
Acetic acid (BDH Chemicals Ltd., United Kingdom)	60ml
37% Formaldehyde (v/v, Sigma-Aldrich, United States)	250ml
MilliQ water	Up to 500ml

Composition of Silver Reaction Solution

Silver nitrate	0.75g
37% Formaldehyde (v/v, Sigma-Aldrich, United States)	375µl
MilliQ water	Up to 500ml

Composition of Developing Solution

37% Formaldehyde (v/v, Sigma-Aldrich, United States)	125ul
Sodium carbonate	15g
Sodium thiosulphate	0.001g
MilliQ water	Up to 500ml

Composition of 100X Denhardt's Reagent

Ficoll 400	10g
Polyvinylprrolidone	10g
BSA	10g
DEPC-treated water	500ml

Filter and store at -20°C in 25ml aliquots

DEPC (diethylpyrocarbonate) treatment of solution

Add 1ml of DEPC to 1000ml of double-distilled water. Shake vigorously and place overnight in a fume hood. The water is then autoclaved to inactivate the DEPC.

CAUTION: Wear gloves and use a fume hood when using DEPC, as it is a suspected carcinogen.

Preparation of TESPA coated slides

1. Wash the pre-coated slide with detergent in ultrasonic cleaner for 15 minutes.
2. Rinse the slides in tap water for 30 minutes and then in distilled water for a few minutes.
3. Heat-treated the slides at 150°C for 3 hours.
4. Mix 10ml of the TESPA with 500ml acetone (This makes a 2% solution, which is stable for 8 hours, after which the color will change).
5. Dip the cleaned slides in TESPA solution for 2 minutes.
6. Wash the slides in 2 changes of distilled water.
7. Dry the slides completely in oven and cool.
8. Store the TESPA coated slides in boxes at room temperature.

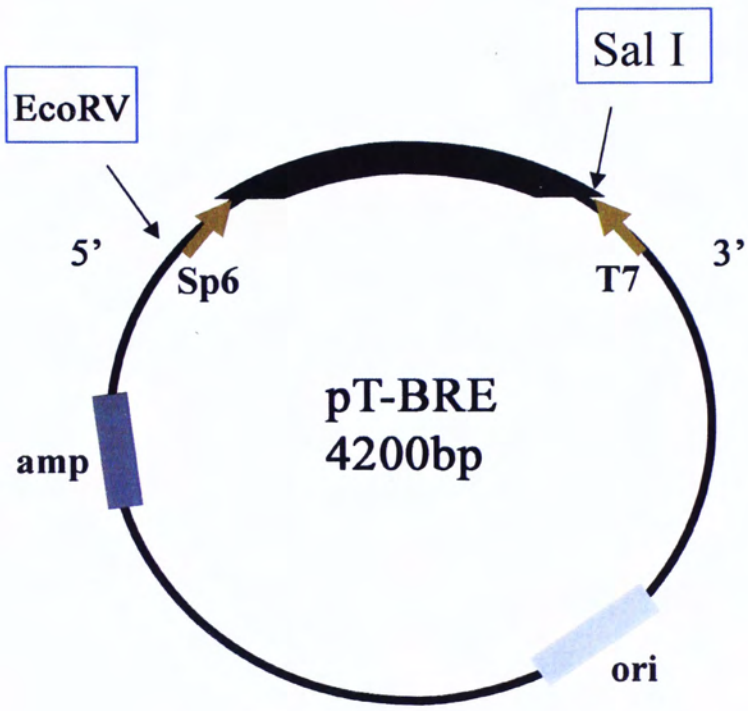

Plasmid name: pT-BRE

Plasmid size: 4200bp

Proteasome beta 3 Peptide Spectrum

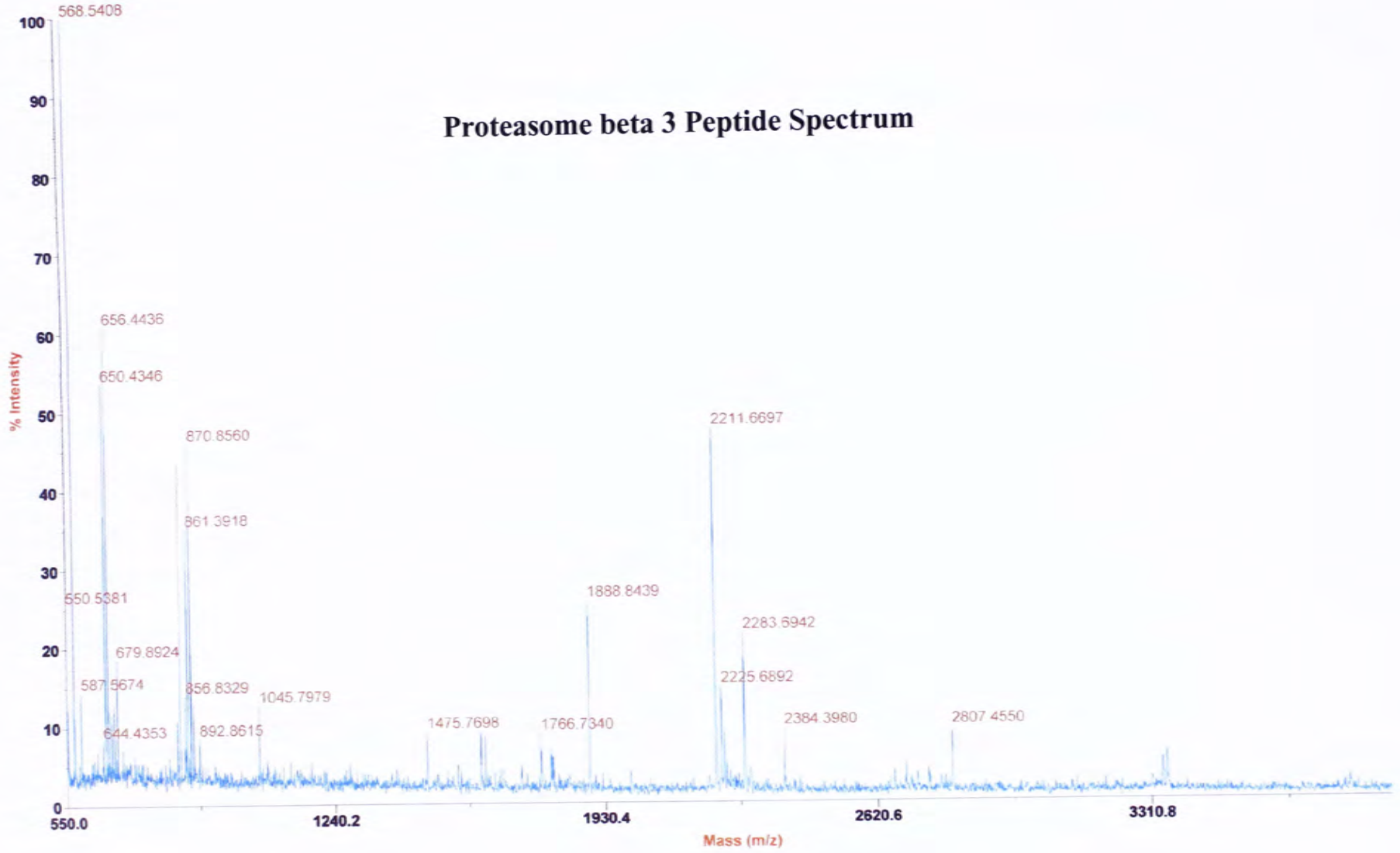

Proteasome (prosome, macropain) subunit, alpha type 6 Peptide Spectrum

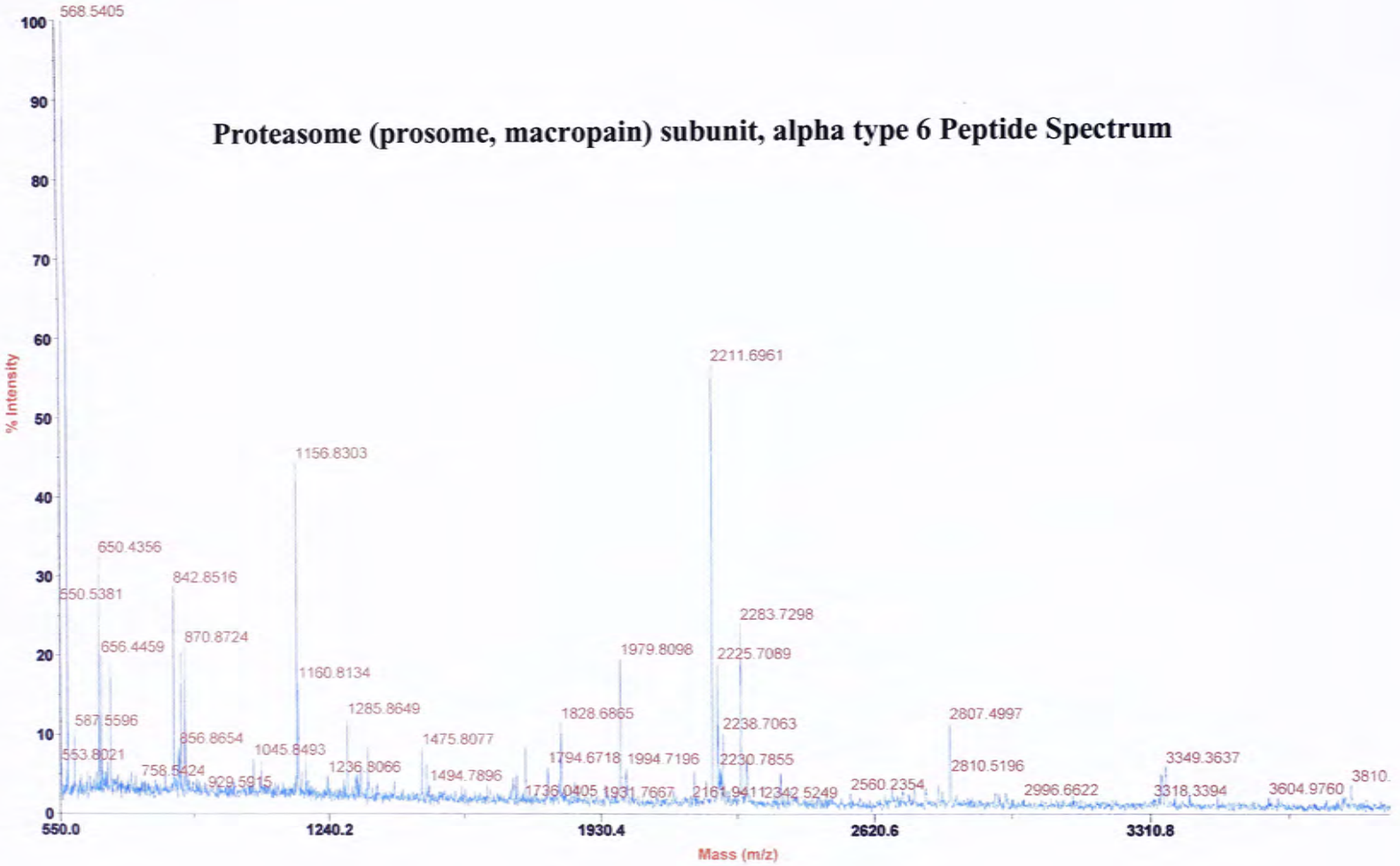

PDIA6 Peptide Spectrum

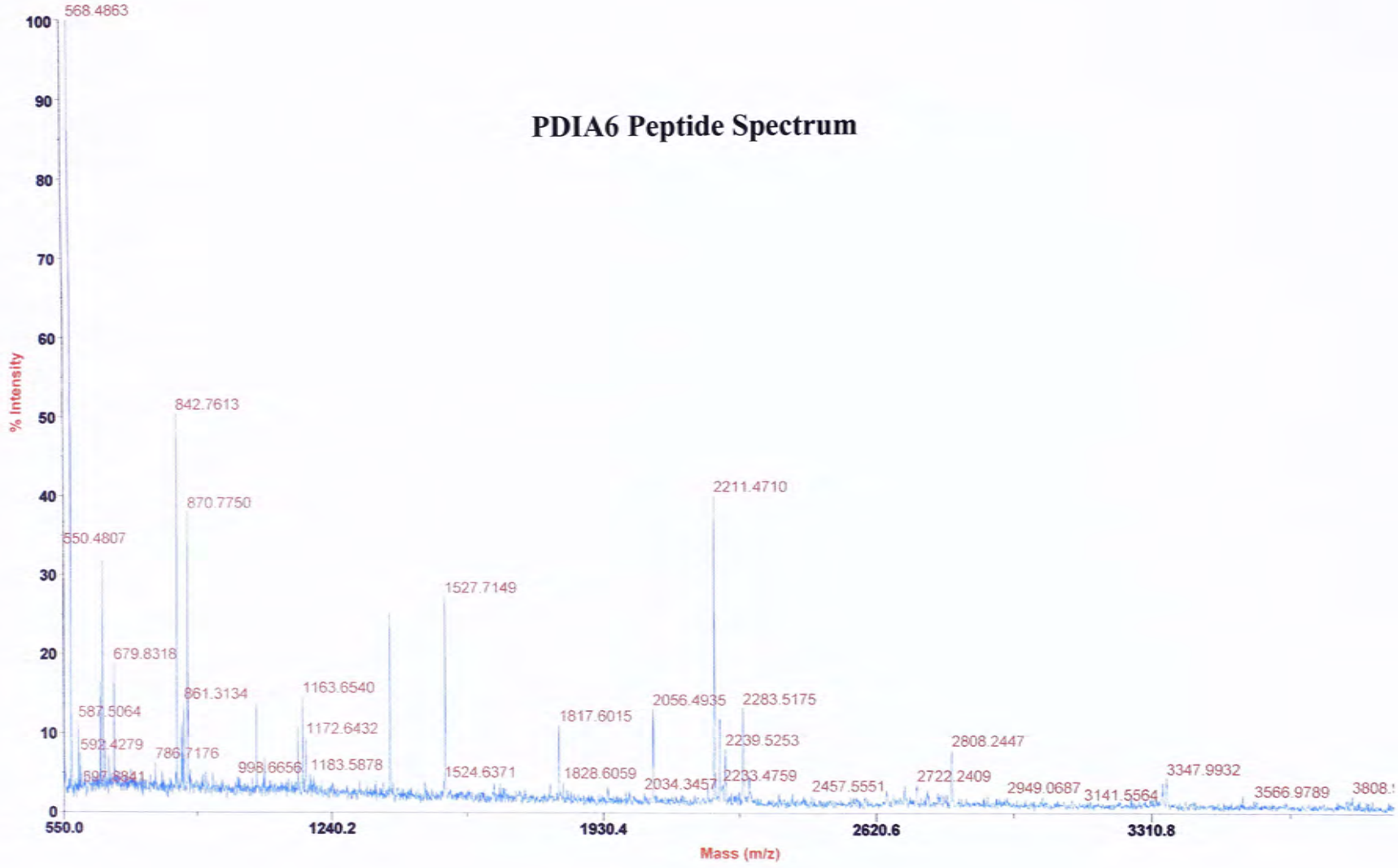

Enolase Peptide Spectrum

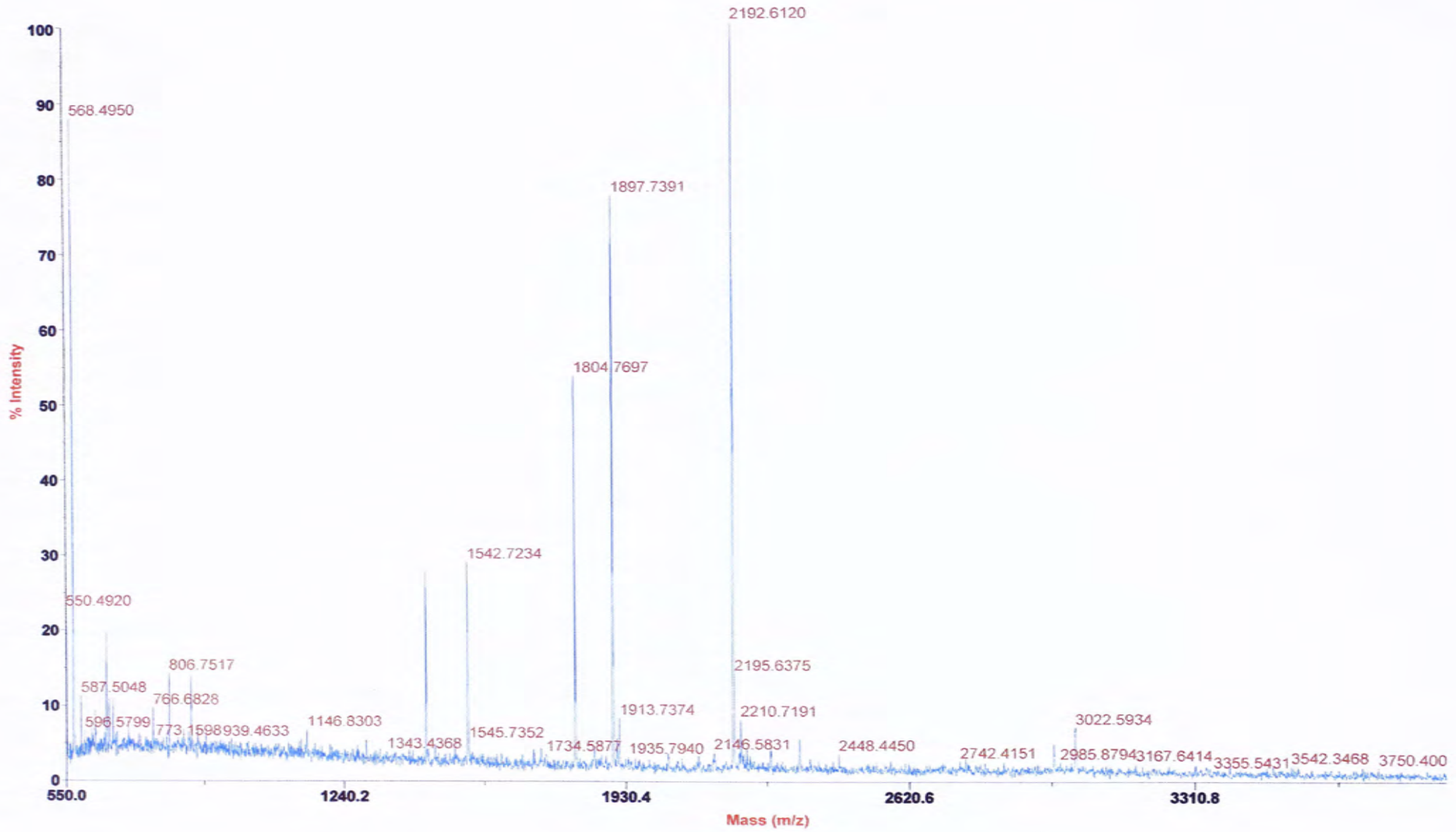

Vimentin Peptide Spectrum

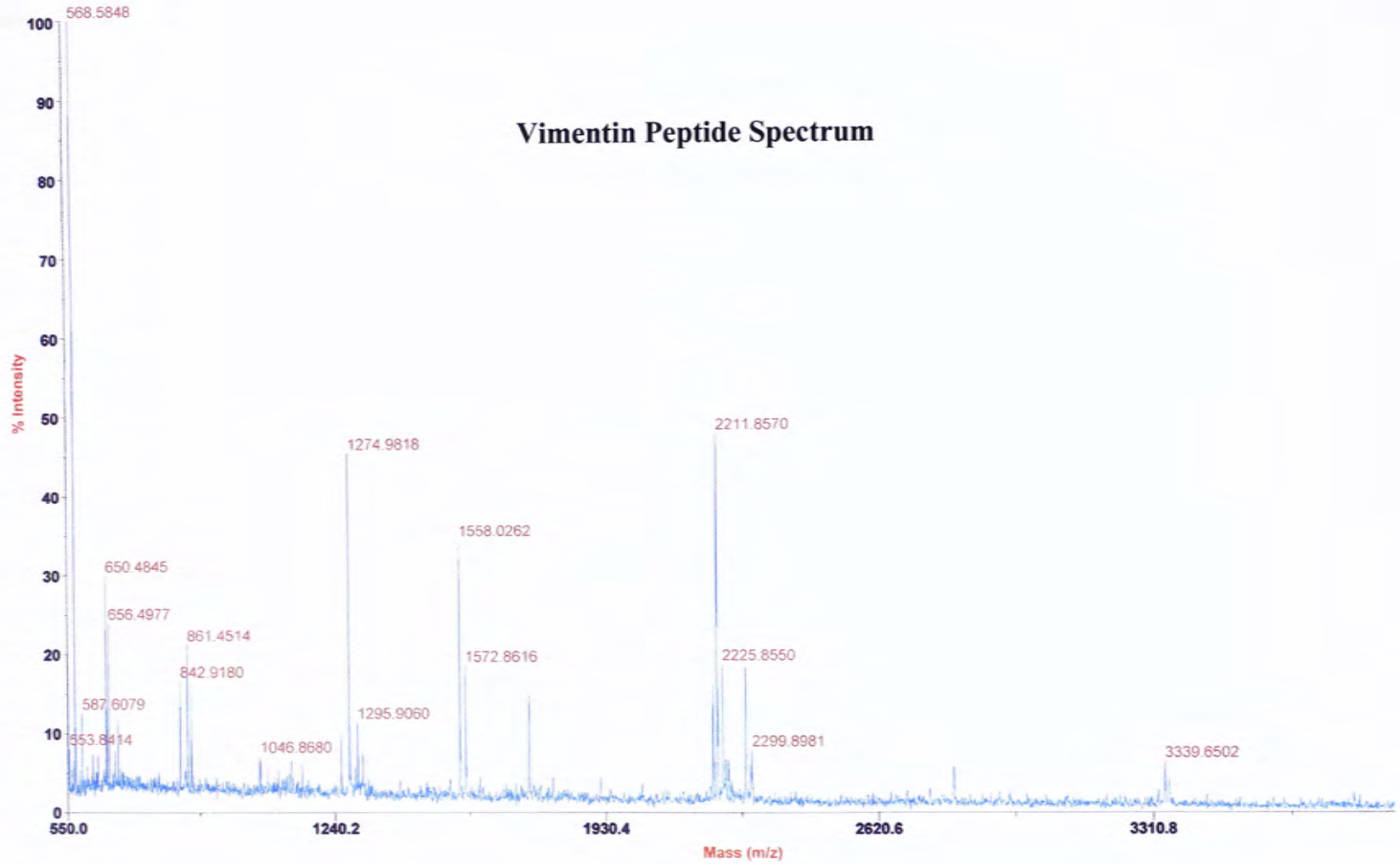

Drebrin A2 Peptide Spectrum

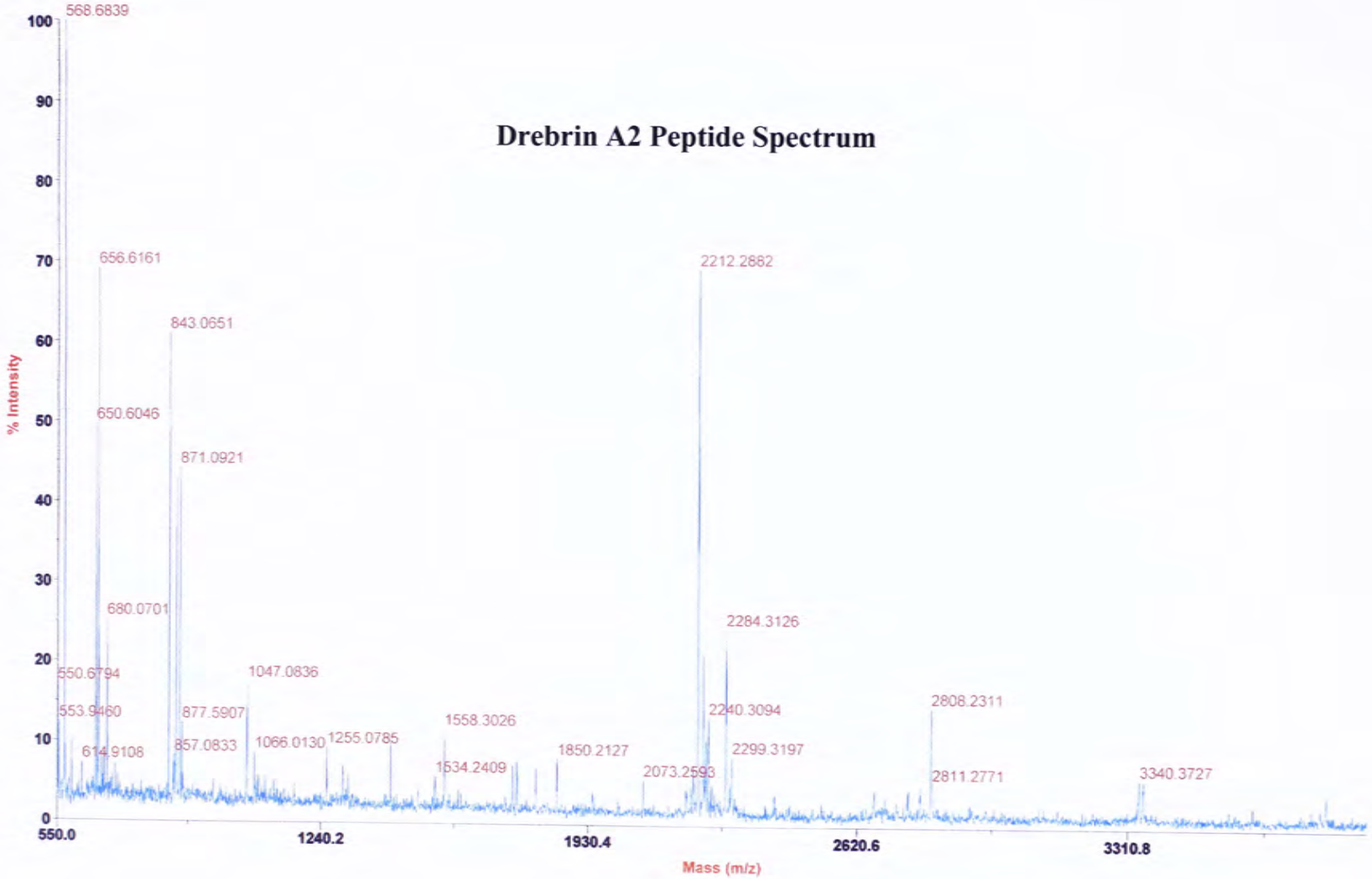

Gpc6 protein Peptide Spectrum

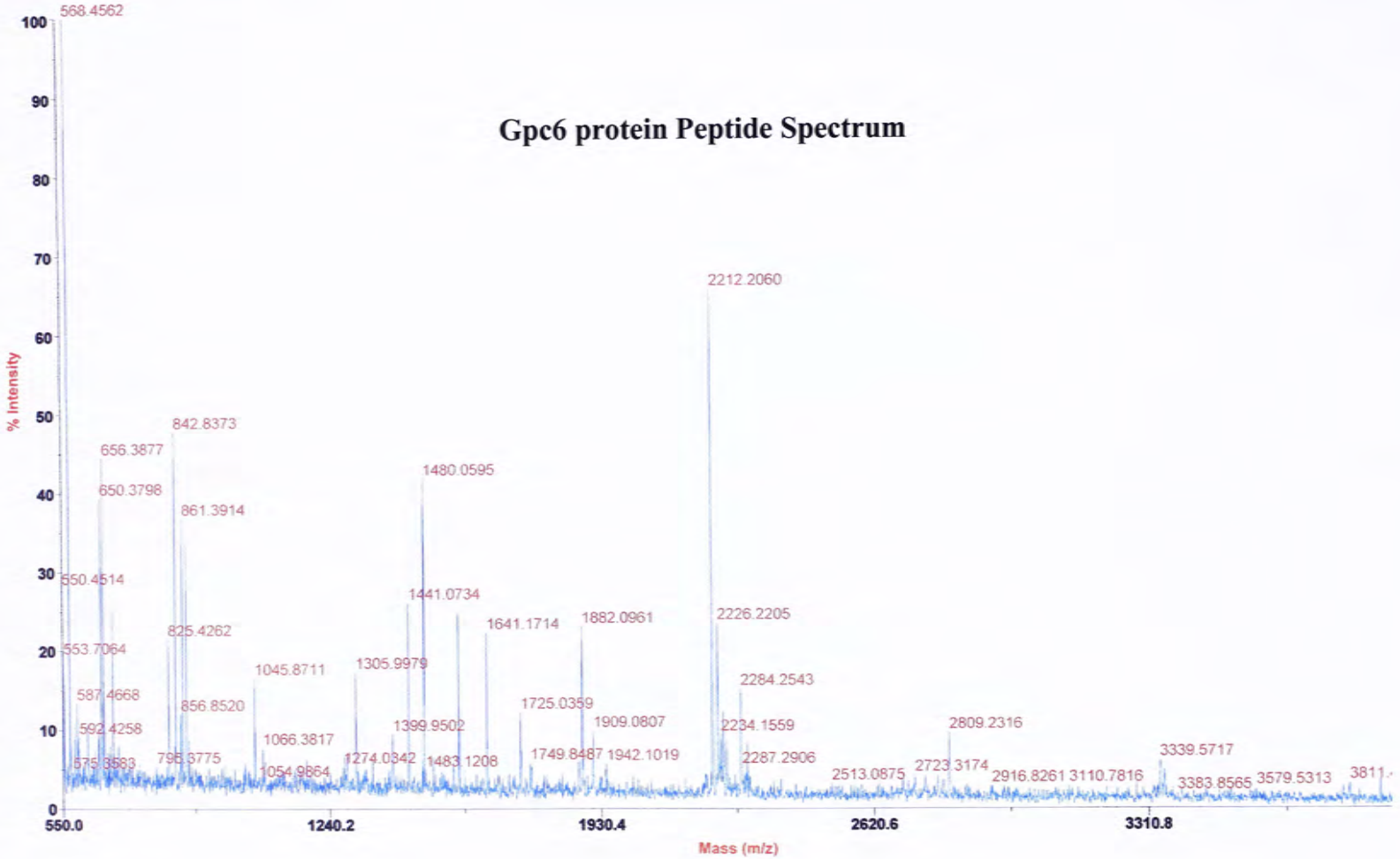

Ubiquilin-1 Peptide Spectrum

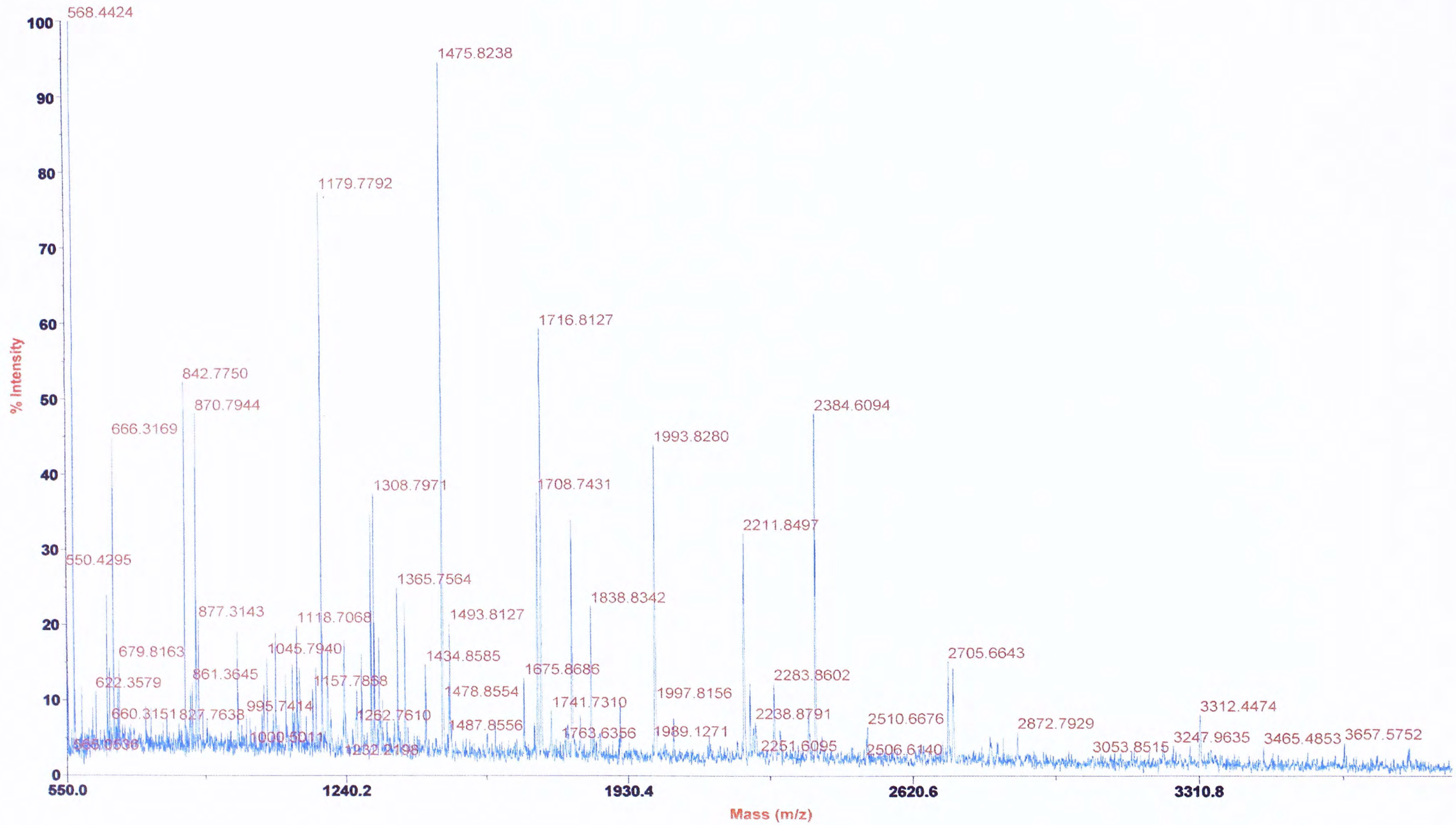

1. **Liu, Y., Tang, M.K., Cai, D.Q., Wong, L.W.M., Chow, P.H. and Lee, K.K.H.** (2006). Cyclin I and p53 are differentially expressed during the terminal differentiation of the postnatal mouse heart. *Proteomics* (in press).